INAUGURAL-DISSERTATION

Submitted to the
Combined Faculties for the Natural Sciences and for Mathemathics
Of the Ruprecht-Karls University of Heidelberg
For the degree of
Doctor of Natural Sciences

Presented by
Sarah Zahedi Hamedani
born in Tehran

Date of oral examination:
15.12. 2010

Common fragile site genes, *CNTLN* and *LINGO2*, are associated with increased genome instability in different tumors

Referees: **Prof. Dr. Gert Fricker**

Prof. Dr. Manfred Schwab

To my parents, for their love
and to my brother, Sahab

Since I've been…

Table of Contents

Acknowledgements

I am indebted to many people without whom I could not have finishd this thesis and to whom I would like to express my gratitude.
First, I would like to thank Professor Dr. Manfred Schwab for giving me the opportunity to do my PhD thesis at his department and for his useful comments that were a great help in carrying out this thesis.
I am also grateful for the willingness of Professor Dr. Gert Fricker to be a referee for this thesis.
Professor Dr. Stefan Wölfl and PD. Dr. Martin Müller I would like to thank for their readiness to be examiners for my oral defence.
I owe my deepest gratitude to my supervisor, Dr. Larissa Savelyeva, whose supervision, encouragement, support and stimulating discussions enabled me to develop an understanding of the subject and to accomplish my PhD project to the end.
I would like to thank my friend Ann Na Tan for proofreading and correcting the English of the manuscript.
Thanks to Steffen Bannert and Young-Gyu Park for their help in the lab work and also special thanks to Elisa Hess for her great assistance in the experiments. My colleagues, whose generosity in providing materials and also helping and giving tips in performing the experiments was a great value to me, Fabiola Hormozian, Seda Ghazarian, Elena Afanasyeva, Vitalya Sagulenko, Lena Brückner (super thanks for the German abstract), Daniel Dreidax, Kai Henrich, Anne Blumrich, Diana Ibragimova, Filip Pattyn, Malgorzata Sawinska, and Ralitsa Arnaudova.
I would also like to name Christina Pöler, Sina Gogolin, Frank Wesetermann, Daniel Muth and all the members from Prof. Olaf Witt's department. It is a pleasure to thank them all for the nice atmosphere that was impposible to experience without them.

Finally, I would like to express my heartful gratitude to my parents for their continual support, understanding and patience during the years of my study in Heidelberg.

Abstract

Genomic instability is a characteristic of almost all human cancers. Most commonly, it may result from gross chromosomal changes, such as translocations, deletions and amplifications, which lead to chromosomal instability. Such chromosomal abnormalities are the consequence of DNA double-strand breaks (DSBs) which result from stalled replication forks formed within common fragile sites (CFSs). Based on several studies it is proposed that CFSs are prone to deletions and translocations in cancer cells and also instability-induced alterations in some CFS genes contribute to cancer development.

The short arm of chromosome 9 has been found to be involved in several types of tumors. Translocations and loss of heterozygosity (LOH) on 9p have been frequently reported in various cancers. In this thesis the overall rearrangement events on entire 9p and the impact of two 9p-located CFSs and their associated genes (*FRA9G/CNTLN* and *FRA9C/LINGO2*) on instability of the region were investigated. The analysis was performed on four tumor model types using high resolution array-based comparative genomic hybridization (CGH).

A high percentage of the cell lines showed rearrangements on their 9p arm. Overall, three regions of breakpoint clusters were identified on 9p including the two CFSs (*FRA9G/CNTLN*, *FRA9C/LINGO2*) and the *CDKN2A* locus. Different patterns of alterations and distribution of breakpoints were observed in each tumor type. *FRA9G/CNTLN* and *FRA9C/LINGO2* were frequently involved in genomic alterations of 9p, particulary in glioma/glioblastoma and neuroblastoma cells. Additionally, in three tumor types (glioma/glioblastoma, neuroblastoma and colon cancers) a significant number of breakages occurred in a region flanked by the two CFSs. Moreover, having the advantage of high-resolution aCGH, other genes of frequently damage were observed, leading to suggest them as novel candidates for tumor-susceptibility loci.

All these results strongly indicate the association of *FRA9G/CNTLN* and *FRA9C/LINGO2* to increased genomic instability of 9p in different tumor types. One important task to be explored in the future will be the causes and effects of dysfunction of these newly identified genes in tumor development.

Zusammenfassung

Genomische Instabilität tritt charakteristischerweise bei fast allen Krebsarten des Menschen auf. In den meisten Fällen liegen ihr wahrscheinlich schwerwiegende chromosomale Veränderungen, wie beispielsweise Translokationen, Deletionen und Amplifikationen zugrunde. Solche chromosomalen Anomalitäten entstehen aufgrund von DNA Doppelstrangbrüchen (DSBs), die wiederum während einer abnormen Zellteilung durch Verzögerung der Replikationsgabel innerhalb von bestimmten chromosomalen Regionen, den sogenannten "Common Fragile Sites" (CFSs), entstehen. Studien haben gezeigt, dass CFSs in Krebszellen zu Deletionen und Translokationen neigen und außerdem Veränderungen in CFS Genen, die durch genomische Instabilität ausgelöst worden sind, zur Krebsentstehung beitragen.

Der kurze Arm von Chromosom 9 ist bei einigen Tumorarten von solchen Abweichungen betroffen, beispielsweise wird bei vielen verschiedenen Krebsarten häufig von Translokationen und Verlust der Heterozygosität (Loss of Heterozygosity, LOH) auf 9p berichtet.

Diese Dissertation untersucht genetische Abweichungen, die auf dem gesamten Chromosomenarm 9p auftreten, sowie den Einfluss der zwei auf 9p gelegenen CFSs und deren assoziierte Gene (*FRA9G/CNTLN* und *FRA9C/LINGO2*) auf genomische Instabilität innerhalb dieser Region. Zu diesem Zweck wurden vier Tumormodelle mittels hochauflösender array-basierter komparativer genomischer Hybridisierung (CGH) analysiert. Ein hoher Prozentsatz der untersuchten Zelllinien zeigte Veränderungen des Chromosomenarms 9p auf. Insgesamt wurden drei Regionen zahlreicher Bruchpunkte identifiziert, einschließlich der beiden CFSs und des *CDKN2A* Locus. *FRA9G/CNTLN* and *FRA9C/LINGO2* waren oft von genomischen Anomalitäten betroffen, besonders in Gliom- bzw. Glioblastom- und Neuroblastomzellen. Darüber hinaus wurde in drei verschiedenen Tumorarten (Gliom/Glioblastom, Neuroblastom und Dickdarmkrebs) eine signifikante Anzahl von Brüchen innerhalb der von den beiden CFSs umgebenen Region beobachtet. Die durch array CGH erreichte Hochauflösung ermöglichte zudem die Identifizierung weiterer häufig geschädigter Gene, die somit als neue mögliche Tumor-Suszeptibilitätsloci in Betracht gezogen werden können.

Diese Ergebnisse weisen bei verschiedenen Tumorarten deutlich auf einen Zusammenhang hin zwischen *FRA9G/CNTLN* und *FRA9C/LINGO2* und genomischer Instabilität im Chromosomenarm 9p. Wichtig bleibt künftig die Ursachen sowie die Auswirkungen der Dysfunktion dieser neu identifizierten Gene zu erforschen.

List of abbreviations

µg	Microgram
µl	Microliter
µM	Micromolar
Alu	Alu repeats
APC	Aphidicolin
ATM	Ataxia telangiectasia-mutated, kinase
ATR	Ataxia telangiectasia Rad3-related, kinase
BAC	Bacterial artificial chromosome
BC	Brest cancer
BFB	Breakage-fusion-bridge
bp	Base pair (s)
BRCA1	"Breast Cancer 1"
BRCA2	"Breast Cancer 2"
BrdU	Bromodexoyuridine (5-bromo-deoxyuridine)
BSA	Bovin Serum Albumin
CC	Colon cancer
CDKN2A	Cyclin-dependent kinase inhibitor 2A
cDNA	Copy DNA
CFS	Common fragile site
CIN	Chromosomal intability
CISS	Chromosomal in situ suppression hybridization
CNTLN	Centlein, centrosomal protein
CNV	Copy number variation
Cy	Fluorescent carbocyanate
dNTP	Desoxynucleotides
DAPI	4,6-diamidino-2-2phenylindol
DEAC	7-diethylaminocoumarin-3-carboxylic acid
DEPC	Diethylpyrocarbonate

Ch	Chromsome
DMSO	Dimethylsulfoxid
DNA	Deoxyribonucleic acid
DNase	Deoxyrebonuclease
DSB	Double Strand Breaks (s)
DTT	1,4-dithiothreitol
EBV	Epstein-Baar virus
E.coli	Escherchia coli
EDTA	Ethylenediaminetetraacetic acid
FCS	Fetal bovin serum
FISH	Fluorescence in situ Hybridization
FITC	Fluorescein isothiocyanate
FRA	Fragile site
g	Gram
GB	Glioblastoma
h	Hour
IFN	Interferon
kb	Kilobase
kDa	Kilodalton
l	Liter
LINE	Long interspersed elements
LINGO2	Leucine rich repeat and Ig domain containing 2
LOH	Loss of heterozygosity
LRR	Leucine rich repeat
LTR	Long terminal repeats
M	Molarity
Mb	Megabase
min	Minute
MIN	Microsatellite instability
MIR	Mammalian interspersed repeats
miRNA	MicroRNA

mRNA	Messenger RNA
NB	Neuroblastoma
NCBI	National Center for Biotechnology Information
NIN	NER-related instability
PBS	Phosphate buffered saline
PCR	Polymerase chain reaction
RNA	Ribonucleic acid
RNase	Ribonuclease
rpm	Rotation per minute
RPMI 1640	Rosvell Park Memorial Institute, medium formulation 1640
RT	Room temperature
RT-PCR	Reverse transcription polymerase chain reaction
RZPD	Deutsches Ressourcenyentrum für Genomforschung
sec	Second
SD	Segmental duplication
SSC	Standard saline citrate
Taq	Thermophilus aquaticus
TBE	Tris-Borate-EDTA-buffer
TE	Tris-EDTA-buffer
U	Unit
UCSC	University of California Santa Cruz
(w/v)	Weight per volume

1. Introduction

1.1 Genomic instability in cancer

Genetic instability is defined asa set of events that are capable of rendering unscheduled aberrations within the genome. This is the distinctive feature of almost all types of human cancers. There are various forms of instabilities which are further categorized in three major groups, MIN, NIN and CIN.

Microsatellite instability (MIN, also known as MIS) is an instability of microsatellite repeat sequences which is caused by the expansion of a number of oligonucleotide repeats as a result of defects in mismatch repair pathway. There is also the NIN (NER-related instability) form of genomic instability which could be formed by increased frequencies of base-pair mutations and nuclear excision repair.

The major form of genomic instability in human cancers, however, is called chromosomal instability (CIN) which refers to an accelerated rate of structural and numerical chromosomal alterations. These alterations result in the gain or loss of whole chromosomes as well as inversions, duplications, deletions and translocations of parts of a chromosome. Aneuploidy which is an abnormal karyotype of many cancers develops as a result of chromosomal instability.

In sporadic cancers, two models are considered to explain the chromosomal instability. The first model is the mutator hypothesis in which the presence of CIN is attributed to the mutations in DNA repair genes and mitotic checkpoint genes. These genes have been linked to the repair of DNA double-strand breaks (DSBs) or DNA interstrand cross links. It has been shown that increasing spontaneous mutations in precancerous lesions drives tumor development, and that mutations occur in genes that primarily function to maintain genomic stability. The second model is the oncogene-induced DNA replication stress. According to this model, CIN in cancer results from the oncogene-induced collapse of replication forks, which leads to DNA DSBs and genomic instability. Specific genomic sites, called common fragile sites (CFSs), are sensitive to DNA damages resulting from replication stress.

1.2 Fragile sites

The first description of non-random human chromosome fragility was reported in 1965 in cells from a woman previously irradiated (Dekaban 1965). The term fragile site was first coined in 1970 to describe recurrent chromosome breaks on the long arm of chromosome 16 (Magenis *et al.* 1970). The significance of fragile site regions and their expression for the human genetics however was realized after the identification of the fragile X syndrome, which is the most common inherited form of mental retardation (Jacobs *et al.* 1980). Fragile sites are defined as heritable specific loci in mammalian chromosomes that exhibit gaps and breaks when chromosomes are exposed to specific cell culture conditions (Sutherland 1979; Sutherland *et al.* 1980; Glover *et al.* 1984; Sutherland *et al.* 1984). To date, according to NCBI Database, more than 120 different fragile sites have been identified.

Fragile sites are classified as either rare or common, according to their frequency in the population (Sutherland and Richards 1995). Rare fragile sites (RFSs) are presented in less than 5% of the population, whereas common fragile sites (CFSs) are considered to be part of normal chromosome structure and subsequently present in all individuals. They are further subdivided according their specific mode of induction *in vitro (Berger et al. 1985)*. Rare fragile sites are subdivided into folate sensitive and non-folate sensitive ones. Folate sensitive fragile sites are induced by thymidilate stress, whereas non-folate sensitive ones are obtained after exposure to distamycin A or to bromodexocyuridine (BrdU). Most of the common fragile sites are induced by aphidicolin, and the others are BrdU or 5-ayacytidine inducible. The induction of all known fragile sites requires induction during tissue culture, with the exception of a few cases of spontaneous expression in *FRA16B* and *FRA17A*.

Since both rare and common fragile sites had been demonstrated originally under artificial conditions, there was concern over their presence *in vivo*. The cloning of rare fragile site *FRA11B* (11q23.3) within the *CBL2* oncogene was the first evidence of fragile site breakage *in vivo* (Jones 1995).

1.2.1 Rare fragile sites

Rare fragile sites are segregated in Mendelian manner and have an incidence ranging from one in several thousands to one in 20 individuals (Sutherland 2003). The majority of the rare fragile sites (24/31) are folate sensitive. Since expression of these fragile sites requires lowered levels of components involved in DNA synthesis, it was considered that these sites might have special sequence composition. In fact, normal alleles at these sites were found to consist of expanded CGG microsatellite repeats (Oberle *et al.* 1991; Nancarrow *et al.* 1995; Sarafidou *et al.* 2004; Winnepenninckx *et al.* 2007). These trinucleotide repeats have two intrinsic characteristics that may affect their replication dynamic and underlie a basis for their fragility. First, these sequences are capable of adopting unusual, non-B DNA secondary structure (Pearson and Sinden 1998). Such structures can perturb DNA elongation (Usdin and Woodford 1995). The second characteristic of CGG repeats is their low efficiency of assembly into nucleosome. It means that the decondensation seen as gaps at fragile sites might reflect perturbed nucleosome assembly at these regions (Wang 1996).

Two non-folate rare fragile sites, *FRA10B* (Hewett *et al.* 1998) and *FRA16B* (Yu *et al.* 1997) have shown to comprise AT-rich minisatellite repeats and their expression is associated with expansion of one ore more of these repeats. The proposed mechanism for the expansion is a dynamic mutation process with increase of up to several kilobases of DNA. The AT-rich repeats, similar to CGG repeats, have the ability to form non-B DNA structures such as hairpins, and therefore can perturb and delay DNA replication.

The significance of rare fragile sites in human diseases is mostly related to *FRAXA* (associated with the fragile X syndrome, the most common familial severe mental retardation) and *FRAXE* (associated with X-linked non-specific mild mental retardation).

1.2.2 Common fragile sites

Common fragile sites, in contrast to rare fragile sites, are seen in all individuals and therefore are considered a component of normal chromosome structure. Common fragile sites are typically stable in culture cells grown under normal conditions. However, under conditions that

obstruct DNA synthesis, they are prone to appear as cytogenetic lesions like gaps or breaks. Such conditions comprise folate or thymidylate stress, or presence of low doses of aphidicolin (Glover *et al.* 1984; Glover and Stein 1988). Common fragile sites fall into 3 groups. The majority of the CFSs (77/89) are induced by exposure to aphidicolin (APH), an inhibitor of DNA polymerases. The other two groups can be induced by 5-azacytidine (4/79), an inhibitor of the DNA methyl-transferase, or by bromodeoxyuridin (BrdU) (7/79) (Lukusa and Fryns 2008). The exact number of common fragile sites seems to exceed the number of identified by classical cytogenetic techniques, since four new CFSs, *FRA4F* (Rozier *et al.* 2004) , *FRA7K* (Helmrich *et al.* 2007), *FRA6H* and *FRA13E* (Fechter *et al.* 2007) have been revealed applying high resolution mapping approaches.

To date, thirteen common fragile sites have been cloned and characterized at molecular levels in various ways: *FRA2G, FRA3B, FRA4F, FRA6E, FRA6F, FRA7E, FRA7G, FRA7H, FRA7I, FRA8C, FRA9E, FRA16D* and *FRAXB* (Schwartz *et al.* 2006). All are aphidicolin inducible and extend over at least 500 kb of genomic region (Paradee *et al.* 1996; Boldog *et al.* 1997).

Not all fragile sites form breaks at the same frequency and some of them are more prone to form lesions. *FRA3B* (3p14.2) is the most highly inducible common fragile site, found in treated metaphases of most humans (Smeets 1986). *FRA6E* (6q26), *FRA7H* (7q32.3), *FRA16D* (16q23) and *FRAXB* (Xp22.3) are the other highly expressed CFSs in lymphocytes (Glover *et al.* 1984). With the cloning and characterization of CFSs, it is now known that their expression could be visible over megabases of choromosomal region. Therefore, common fragile sites seem to represent regions of fragility, rather than specific loci (Handt 2000).

1.2.2.1 Genes at common fragile sites

From the thirteen CFSs which have been cloned and characterized at molecular level, most of them either lie within or span the known genes (Smith DI 2006). *FRA3B* was the first fragile site to be cloned and mapped. The identification of homozygous deletions within the *FRA3B* region in a variety of cancer types led to the identification of the fragile histidine triade gene (*FHIT*) (Druck *et al.* 1997). *FRA3B* was found to lie within the *FHIT* gene (Boldog *et al.* 1994; Wilke *et al.* 1994; Ohta *et al.* 1996). *FHIT* has a very unusual genomic structure and contains 10 small

exons which span over 1.5Mb of genomic sequence, including two large introns (Ohta *et al.* 1996). Greater that 99% of this gene is intronic sequences and only a small transcript, 1.2 kb, is encoded. There are evidences that *FHIT* acts as a tumor suppressor gene (Siprashvili *et al.* 1997; Zanesi *et al.* 2001). Fhit hydrolyzes diadenosine tetraphosphates which are produced in cells in response to stress (Kisselev L.L. 1998).

Great homology has been observed between DNA sequences surrounding the human *FHIT* and mouse *Fhit* gene, even within intronic sequences. It was also found that mouse *Fhit* lies within a CFS in the mouse (Matsuyama *et al.* 2003). These observations suggest that the very large gene and the highly unstable chromosomal region are co-conserevd, possibly due to serving some function together within the cell (Smith *et al.* 2007).

FRA16D, which together with *FRA3B* are the most active CFSs, also lies within a large gene *WWOX*. Despite its large size (1Mb), *WWOX* encodes a small 2.2-kb transcript and is believed to be a tumor suppressor gene. In response to stress, *WWOX* appears to be specifically phosphorylated and this form can bind to p53 and induce apoptosis (Chang *et al.* 2003). Thus there is potential association of *FHIT* and *WWOX* with cellular response to stress.

FRA6E is another CFS that lies within the large Parkin (*PARK2*) gene which extends over 1.3 Mb (Denison *et al.* 2003). Parkin has been shown to interact with a number of key neural proteins including synuclein (Chung *et al.* 2001) and its expression was down-regulated in 60% of primary ovarian tumors analyzed (Denison *et al.* 2003; Wang *et al.* 2004). Introduction of Parkin into the cells that did not express it, resulted in more sensitivity of those cells to apoptotic induction (Denison *et al.* 2003).

GRID2 is another extremely large gene (1.46Mb) that is localized within *FRA4F* (4q22) region (Rozier *et al.* 2004). Recurrent deletions of subregions of band 4q22 have been described in human hepatocellular carcinoma, suggesting roles for *GRID2* in hepatic carcinogenesis (Bluteau *et al.* 2002).

Many of the large CFS genes are involved in neurological development (Dussault *et al.* 1998; Doughty *et al.* 2000; Verkerk *et al.* 2003; Cam *et al.* 2004; Lorenzetti *et al.* 2004).

There is one interesting observation that so many of the large CFS genes appear to function as stress responders (Smith *et al.* 2007). One possibility underlying the mechanism for this function is that somehow the CFS regions are able to transduce cellular stresses into different

transcripts being produced from the large CFS genes. An alternative could be that the very large introns produce transcripts which somehow regulate the expression of the large CFS genes.
Re and colleagues proposed that replication stress at fragile sequences is coupled with a modified expression of the associated fragile genes (Re *et al.* 2006). They suggest that fragile sequences, sensitive to replication stress, are not located by chance within or near fragile genes, but participate together with the genes to the mechanism that regulates the cellular response to DNA damage.

1.2.2.2 Instability at common fragile sites

1.2.2.2.1 Common fragile site instability in vitro

Although CFSs are normally stable regions in cultured human cells, but under conditions that partially inhibit DNA synthesis, form gaps and breaks. In addition to displaying gaps and breaks, CFSs are hot spots for deletions and translocations (Glover and Stein 1988; Wang *et al.* 1997), increased rates of sister chromatid exchange (Glover and Stein 1987; Feichtinger and Schmid 1989; Hirsch 1991), plasmid or vector integration (Rassool *et al.* 1991; Wilke *et al.* 1996; Mishmar *et al.* 1998), interchromosomal gene amplification (Coquelle *et al.* 1997; Hellman *et al.* 2002) and regions of potential genome instability (Glover 1998). There are also reports of coincidence of viral integration sites in tumors or tumor cell lines and fragile sites (Popescu and DiPaolo 1989; De Braekeleer *et al.* 1992).

1.2.2.2.2 Common fragile site instability in cancer

All the various forms of DNA instability which have been associated with CFSs (like forming boundaries of amplified regions of genome, plasmid and viral DNA integration, sister chromatid exchange and recombination) would require DSBs as an initiating event. Therefore DSB appears to be a typical feature of common fragile sites. Aberrant repair of these fragile site-associated DSBs could eventually lead to deletions such as those that have been observed at common

fragile sites in various cancers (O'Keefe and Richards 2006). It has been suggested that fragile sites are associated with cancer development from the early stages of tumorigenesis (Gorgoulis *et al.* 2005; Halazonetis *et al.* 2008)

Studies on the most frequently expressed CFSs, *FRA16D* and *FRA3B*, have provided compelling evidence that these regions are prone to deletions and translocation in cancer cells. Identification of homozygous deletions presents a novel mechanism for gene inactivation in the absence of mutations within a coding sequence. The relative frequency of cytogenetic appearance of CFSs *in vitro* corresponds to the relative frequency of deletions observed in cancer cell lines *in vivo* (Arlt *et al.* 2002; Finnis *et al.* 2005). Deletion analysis of cell lines derived from a primary carcinoma (KM12C) and from a secondary metastasis of this same carcinoma (KM12SM) revealed precisely the same deletion endpoints in the region of *FRA16D*, despite instabilities in other regions of the genome (Finnis *et al.* 2005). Homozygous deletions of *FRA16D* have also been detected in cell lines derived from breast, lung, stomach, colon and ovary carcinomas (Bednarek *et al.* 2000; Mangelsdorf *et al.* 2000; Paige *et al.* 2000).

When looking for genes in 16q23.2, one of the frequent sites of LOH in breast cancer, Bednarek *et al.* (Bednarek *et al.* 2000) found *WWOX* gene, which lies within *FRA16D*. Several recent studies have demonstrated a tumor suppressor function for *WWOX* gene (Boldog *et al.* 1997; Bednarek *et al.* 2001; Aqeilan *et al.* 2007; Salah Z 2010). Targeted inactivation of *Wwox* led to the spontaneous occurrence of osteosarcomas in juvenile *Wwox*−/− mice and lung papillary carcinoma in adult *Wwox*+/− mice (Aqeilan *et al.* 2007). Deletions of microsatellite markers within the *FRA16D*/*WWOX* locus are prevalent in several tumor types including breast, prostate, esophageal, lung, stomach, prostate, ovary and pancreatic carcinomas (Ried *et al.* 2000; Paige *et al.* 2001; Driouch *et al.* 2002; Kuroki *et al.* 2002; Yendamuri *et al.* 2003; Kuroki *et al.* 2004; Lewandowska *et al.* 2009).

Several tumor-derived cell lines with transgenic deletion in *FRA16D*, also frequently show deletion in *FRA3B*. This could be an indicative of a common mechanism that may be causal in such deletion events (Finnis *et al.* 2005). The *FHIT* gene spans the *FRA3B* fragile site and, being a huge gene similar to *WWOX*, some homozygous deletions occur only within a large intron. Deletions mostly give rise to aberrant transcripts; however, *FRA3B*-deleted cancer cells are marked by an absence of the encoded FHIT protein, indicating that loss of function is the most likely consequence of deletion (Druck *et al.* 1997). Transgenic mice heterozygous for knockout

of the *Fhit* gene have increased susceptibility to mutagen-induced tumor formation (Fong *et al.* 2000), and since it has been found that *Fhit* gene also contains a common fragile site (Glover *et al.* 1998), probably this fragile site provides the susceptible target for the second hit in the heterozygous knockout mice. Increased sensitivity of *Fhit* heterozygous transgenic mice is supportive for the idea that individuals with higher expression of fragile sites would be more sensitive to environmental mutagenesis and thus at the greater risk of any associated type of cancer (Richards 2001). Moreover, the overexpression of *FHIT* suppresses the growth of cancer cell lines *in vitro* and *in vivo* (Siprashvili *et al.* 1997). *FHIT* is frequently involved in biallelic loss and other chromosomal abnormalities in tumors (Ohta *et al.* 1996; Kameoka *et al.* 2004; Hassan *et al.* 2010). A high frequency of homozygous and heterozygous deletions within *FRA3B* region have been detected in different cancers and cancer cell lines like esophageal adenocarcinoma (Michael *et al.* 1997), gastric cancer (Lee *et al.* 2001), head and neck squamus cell carcinoma (Virgilio *et al.* 1996), large B-cell lymphomas (Kameoka *et al.* 2004) and pancreatobiliary cancers ((Bloomston M 2009).

Other CFSs and their associated genes, including *FRA6E26, FRA9E13,* and *FRA7G (Huang et al. 1998; Bednarek et al. 2000)*, have also shown similar patterns of deletion in cancer cells. Therefore, considerable amount of studies are indicative of CFSs representing targets that are "weak links" (Huebner and Croce 2001) for genomic alterations in at least some cancer cells.

Recurrent chromosomal translocations tend to be hallmarks of particular kinds of cancer. As much as 25% of the translocation breakpoints in multiple myeloma map to *FRA16D* region (Chesi *et al.* 1998; Krummel *et al.* 2000; Mangelsdorf *et al.* 2000; Paige *et al.* 2000). These recurrent translocations result in at least one truncated allele of *WWOX* in tumor cells (Bednarek *et al.* 2000; Mangelsdorf *et al.* 2000; Ried *et al.* 2000; Krummel *et al.* 2002). The *FRA3B* fragile site, also has been reported to be the site of the chromosome 3 breakpoint in the familial clear cell renal carcinoma translocation (Ohta *et al.* 1996). Translocations in other CFSs have also been reported. *FRA6E* and *FRA6F* in acute lymphpblastic and acute myeloid leukemia (Sinclair *et al.* 2005) and *FRA2G* in members of a family with multifocal clear renal cell carcinoma have shown to have translocations. In a very recent interesting study (Gandhi *et al.* 2010) it was shown that induction of breakage at fragile sites *FRA10C* and *FRA10G* under fragile site-inducing conditions initiated and led to the generation of rearrangements in *RET/PTC1* partner genes which lie within these fragile sites. These rearrangements then contribute to papillary

thyroid carcinoma (PTC) development. This is the first direct evidence demonstrating the role of fragile sites in cancer-specific translocations.

While deletion breakpoints within CFSs in cancer cells are common, relatively fewer translocations involving CFSs have been reported. Both deletions and translocations at CFSs appear to inactivate associated genes rather than deregulate their expression.

In addition to deletion and translocation, CFSs have been associated with viral integration and gene amplification in tumor cells. Cervical carcinoma frequently exhibit human papillomavirus (HPV) integration in association wit acquiring malignant phenotype (Thorland EC 2000). This led to identify more viral integration sites at CFSs (Popescu and DiPaolo 1989; De Braekeleer *et al.* 1992; Smith *et al.* 1992; Wilke *et al.* 1996; Thorland *et al.* 2003).

Amplification and subsequent overexpression of oncogenes have been shown to be frequent in variety of neoplasias and is thought to play and important role in tumor development (Brison 1993). Human cancers are able to amplify genes extrachromosomally, in the form of "double-minutes" or "episomes", as well as intrachromosomally forming sometimes huge regions containing copies of contiguous genes. Early events of gene amplification were not available for study until model systems in cultured rodent cells were developed. Analysis of the induced amplicons in these systems revealed that the mechanism underlying the early amplification events is breakage-fusion-bridge cycles (Toledo *et al.* 1992).

According to the model introduced by McClintock (Mc Clintock 1951) an initial break (or telomere dysfunction) of a chromatid bearing the selected gene might lead to the fusion of the uncapped sister chromatids after replication. The result would be dicentric chromosome forming an anaphase bridge between the centromers, which will break while moving to opposite poles of the mitotic spindle. If this break occurs centromeric to the selected gene, a duplication of the region between the breaks is gained. Several recurrent chromosomal fusion and breakage under the appropriate selection lead to interchromosomal amplification. The amplification resulted from BFB cycle, is easily recognizable by ladder-like structure which is the consequence of the inverted position of the copies.

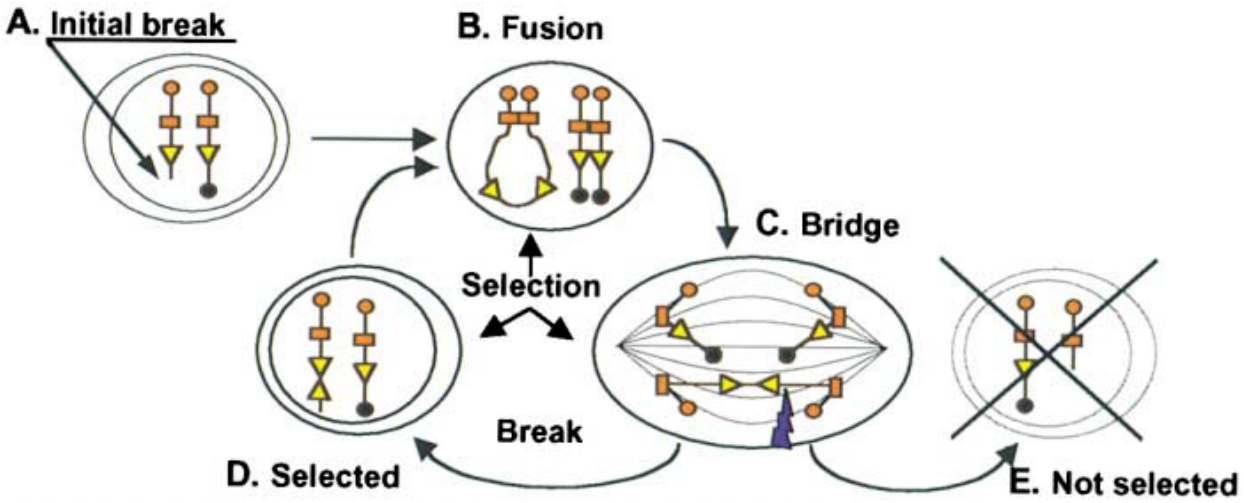

Figure 1-1. Schematic illustration of gene amplification via breakage-fusion-bridge cycles. Amplicons, yellow triangles; telomeres, orange (p-arm) or black (q-arm) circles; centromeres, orange rectangles. **(A)** Interphase; an initial break gives rise to an uncapped chromatid carrying the selected gene. (**B)** Metaphase; fusion of the 2uncapped sister chromatids results in a dicentric chromosome. (**C)** Anaphase; the dicentric chromosome forms a bridge between the opposite poles. A break of this chromosome leaves one daughter cell (**D**) with 3 copies of the selected gene, and only one copy in the other cell (**E**). Under a selection, recurrent cycles of BFB will occur, resulting in further accumulation of amplicon copies. (from Hellman *et al.* 2002)

Molecular evidence demonstrated that breakage leading to oncogene amplification preferentially occurs within CFS regions. Since human CFSs encompass large genomic regions, different breakpoints within the fragile region are expected to occur during subsequent BFB (breakage-fusion-bridge) cycles. Coquelle *et al.* (Coquelle *et al.* 1997) and Kuo *et al.* (Kuo *et al.* 1994) have provided evidence for breakage in CFSs which can drive amplification by BFB cycle in Chinese hamster ovary cell lines. It was shown that *Met* oncogene is amplified in human gastric cancer as a result of BFB cycles that initiate with *FRA7G* breakage (Hellman *et al.* 2002). A duplication of *PIP* gene in a breast carcinoma cell line has been associated to breakage in *FRA7I*. The same has been shown for other types of cancer like urothelial (Jin *et al.* 2007). In addition, an implication of *FRA5C* in amplification of *SMAD5* was shown, not only in hepatocellular cell lines, but also in primary tumors (Zimonjic *et al.* 2003). This would be an evidence for the in vivo significance of CFSs for genome instability in cancers.

It has been proposed that *ex vivo* induction of CFSs triggers and drives the amplification of drug resisted genes in rodent cells (Coquelle *et al.* 1997). Since many of the drugs used in cancer therapy are potential inducers of both fragile sites and gene amplification, they can lead to

chromosome rearrangements and further contribute to cancer development (Hellman *et al.* 2002).

1.2.2.3. Mechanism of instability at common fragile sites

1.2.2.3.1. Unstable sequences and late replication at CFSs

Sequence analysis of all cloned common fragile sites, unlike rare fragile sites, reveals no expanded di- or trinucleotide repeats or other sequences that can account for their fragility. The only feature they share with rare fragile sites is the relatively high amount of AT-rich sequence (Boldog *et al.* 1997; Mishmar *et al.* 1998; Ried *et al.* 2000; Shiraishi *et al.* 2001; Arlt *et al.* 2002). Applying Flexstab, a computer program designed to measure local variation in the twist angel between the bases within a sequence (Mishmar *et al.* 1998), revealed regions of high flexibility (termed flexibility peaks) in CFSs. This structural characteristic of DNA could be important to understand the molecular mechanism of fragility at CFSs for two reasons: First, flexible DNA at the twist angle can act as a sink for the superhelical density generated ahead of the replication fork in its progress. Accumulating superhelical density can hinder efficient topoisomerase activity and decrease the processivity of the polymerase complex (Bacolla *et al.* 1997; Gellibolian *et al.* 1997). Second, the twist angle was shown in vivo to affect the level of higher order-chromatin folding (Krajewski 1995; Krajewski and Ausio 1997). Flexibility analysis of common fragile sites *FRA2G, FRA3B, FRAXB, FRA7E, FRA7H, FRA8C,* and *FRA16D*, have shown that they contain a high number of flexibility peaks compared to non-fragile regions (Mishmar *et al.* 1998; Ried *et al.* 2000; Arlt *et al.* 2002; Limongi *et al.* 2003; Zlotorynski *et al.* 2003; Ferber *et al.* 2004). These flexible sequences are composed of interrupted runs of AT-dinucleotides and may have the potential of forming secondary structures and, hence, may affect the replication of fragile sites. The first identification of a sequence element within a CFS which increases chromosome fragility was introduced by Zhang and colleagues (Zhang 2007). They suggested that long streches of AT dinucleotides within *FRA16D* cause increased chromosome breakage by forming secondary structures that stall replication fork progress.

It has been shown that these flexible sequences have similarities to AT-rich minisatellite repeats that cause the fragility in rare fragile sites *FRA16B* and *FRA10B* (Zlotorynski *et al.* 2003). There are results from studying *FRA8C* which show a correlation between high flexibility peaks and HPV integration and translocation sites (Ferber *et al.* 2004).

If these special sequences are necessary for the fragility of CFSs, then large deletions that remove these sites should cause the loss of fragility. Arlt et al. (Arlt *et al.* 2002) found that two tumor cell lines containing a 500-kb deletion in *FRAXB* completely eliminated fragility at this site. Moreover, stable transfecting of CFS sequences at ectopic sites exhibited instability, supporting a hypothesis that sequences at CFSs are inherently unstable (Ragland *et al.* 2008).

On the other hand, an extensive study of *FRA3B* in cells with various deletions within the fragile site showed that deletion of large sequences in *FRA3B* did not affect fragility (Corbin *et al.* 2002). Moreover, the regions of frequent breakpoints in cancer cells were mapped and no correlation between landmark (flexibility peaks, deletion and translocation breakpoints) and breakpoints in *FRA3B* were found (Corbin *et al.* 2002). These results suggest that loss of large regions within CFSs reduces, but not completely demolishes the fragility.

Perhaps related to this sequence composition is the fact that common fragile sites are late replicating. It is long thought that CFSs, due to the sequences they contain, may have difficulties to replicate and that inhibition of replicative polymerases with aphidicolin further perturbs replication. It means late replication is possibly due to formation of secondary structures that inhibit replication fork progression, or other factors affecting replication dynamics at these regions. Le Beau *et al*. (Le Beau 1998) showed for the first time that sequences at *FRA3B* replicate very late and the addition of aphidicolin resulted in a further delay in replication with about 16.5% of *FRA3B* sites remaining unreplicated in G2.

Since there are other regions in the genome that replicate late, this feature alone cannot underlie the fragility at CFSs.

1.2.2.3.2 Cell cycle checkpoints and repair pathways in common fragile site instability

Little was known of cellular mechanism controlling CFS stability until recently when Casper *et al.* discovered that the Ataxia-telengiectasia and Rad3 Related (ATR) checkpoint kinase plays a major role in CFS maintenance (Casper *et al.* 2002). Cells evolve their cell cycle checkpoint to delay cell division in response to DNA damage to allow for their repair. ATR is a key player in the cellular response to stalled replication fork. It was demonstrated that in ATR-deficient cells, even without the addition of replication inhibitors, CFSs were expressed (Gorgoulis *et al.* 2005). It was also found that cells from individuals with Seckel syndrome that have hypomorphic mutation in ATR are sensitive to aphidicolin and show increased stability at common fragile sites (Casper *et al.* 2004). ATR regulatory role was the first major pathway found to be associated to CFS stability and it was very important to link the cell cycle checkpoint function to fragile site stability. subsequent investigations focused further on defining these mechanisms and a number of targets or modifiers of ATR pathway are now known to affect fragile site maintenance, including BRCA1, the Fanconi anemia (FA) pathway, SMC1 and CHK1 (Arlt *et al.* 2004; Howlett *et al.* 2005; Musio *et al.* 2005; Durkin *et al.* 2006).
Recently, it was published that in addition to ATR, ATM also plays a role in fragile site instability through a parallel pathway and the activation of ATM is independent of the activation of ATR, but they have synergic effects. Moreover, it was demonstrated that chk2 is activated by ATM in ATR deficient cells following addition of low doses of APH (Ozeri-Galai *et al.* 2008). All these data show that ATR, rather than ATM, has major (but not absolute) effect on CFS stability and the linkage with cell cycle checkpoint control.
There is little data about how lesions at fragile sites are repaired. Homologous recombination repair (HRR) plays a major role in responding to DSBs and stalled replication forks during S and G2, when the sister chromatid is present. It has been reported that on average, 70% of all gaps and breaks at *FRA3B* after aphidicolin treatment had an SCE at that site (Glover and Stein 1987). The presence of SCEs at fragile sites is an indication that some kind of repair has occurred at the site. Cells with mutation in RAD51 and other members of the HRR pathway have been reported to have reduced spontaneous and MMC-induced SCE formation, although the reduction is not severe and may even be species-specific (Fuller and Painter 1988; Tucker *et al.* 1991; Dronkert *et al.* 2000; Lambert and Lopez 2001; Takata *et al.* 2001; Stark *et al.* 2002;

Sasaki *et al.* 2004). These findings suggest that formation of DBSs at fragile sites is the result of replication perturbation and provides the first clues how lesions are repaired at CFSs.

In addition to DNA damage, recent studies have suggested that alternative chromatin structures such as changes in histone modification, loss of histone chaperones, and alterations in chromosome condensation, can trigger repair processes and cell cycle checkpoints (Koundrioukoff *et al.* 2004). These findings combined with the involvement of proteins ATR, BRCA1, SMC, and the Fanconi Anaemia pathway in fragile site expression formulate a hypothesis on the involvement of chromatin structure in fragile site expression. Chromatin structure specific to fragile sites may (1) serve as a block to slow down or stall the progress of replication forks, (2) promote formation of unusual secondary structure by fragile DNA, or (3) cause failure of chromatin condensation (Wang 2006).

Collecting data from a number of laboratories could support a working model for CFSs. It suggests that the AT-rich sequences at CFSs present difficulties during replication that are further exacerbated by APH and certain other forms of replication stress. When cells are treated with low dose APH, the polymerases slow or pause, likely leaving the helicase/topoI complex to continue unwinding DNA ahead of it, and resulting in long stretches of ssDNA that can activate the ATR-dependent DNA damage checkpoint. These ssDNA regions may form secondary structures, such as hairpins or cruciforms at the AT-repeats or AT-rich sequences associated with CFSs, which can further perturb replication as the polymerases encounter them. Although the majority of these perturbations are likely detected by the ATR-dependent DNA damage checkpoint and DNA repair machinery, some escape and present themselves as gaps and breaks on metaphase chromosomes, particularly at CFSs (Durkin and Glover 2007).

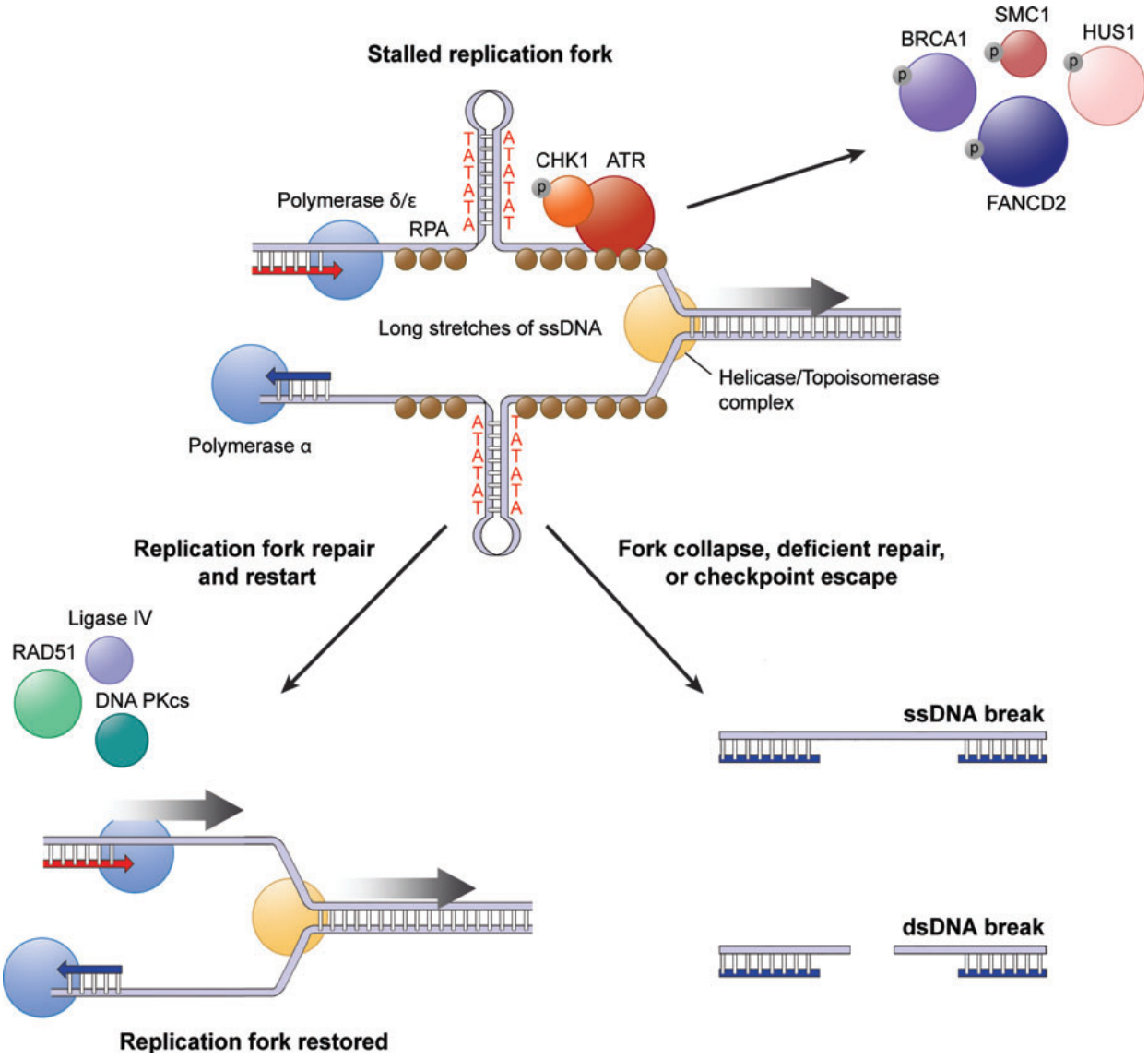

Figure 1-2. A model for common fragile site instability. This model predicts that fragile sites are derived from long stretches of unreplicated ssDNA that are exposed when a replication fork is stalled or delayed, for example by treatment with APH. The ssDNA binding protein RPA (*brown*) coats the unreplicated ssDNA and recruits the DNA damage response checkpoint proteins, including ATR (*red*), which activate S-phase or G2/M checkpoints. Repair of these regions by proteins including RAD51 and DNA-PK restores replication fork progression. However, sometimes these regions escape checkpoint activation or are left unrepaired, resulting in an unreplicated region that can appear as a fragile site on metaphase chromosomes or lead to a DSB. (according to durkin glover 2007)

1.2.2.4 Evolutionary conservation of common fragile sites

Fragile sites are quite stable in most normal somatic and germ cells. There is little evidence to link CFSs to constitutional chromosome rearrangements in humans. They also appear to be highly conserved during mammalian evolution. Orthologs of CFSs have been found in a number of other mammalian species, including other primates, cat, dog, pig, horse, cow, Indian mole rat, deer mouse and laboratory mouse (Soulie and De Grouchy 1981; Elder and Robinson 1989; Smeets and van de Klundert 1990; Stone *et al.* 1991; Stone *et al.* 1993; Yang and Long 1993; McAllister and Greenbaum 1997; Ruiz-Herrera *et al.* 2004). Of all these species, the most extensive work has been done in mouse. Three mouse fragile sites, *Fral4a2*, *Fra8el*, and *Fra6cl* have been cloned and found to be orthologs of human fragile sites *FRA3B*, *FRA16D* and *FRA4A*, respectively (Elder and Robinson 1989; Glover *et al.* 1998; Shiraishi *et al.* 2001; Krummel *et al.* 2002; Matsuyama *et al.* 2003; Rozier *et al.* 2004). The mouse fragile sites have some common features with human fragile sites, including AT-rich sequence and the presence of large genes. Furthermore, the high similarity of large intronic regions in mouse and human, suggests a functional conservation of these non-coding sequences. Such non-coding sequences may be conserved because they contain regulatory elements for associated gene function or perhaps due to the functional property of the CFS itself.

This evolutionary conservation appears to extend from mammals to lower eukaryotes like yeast. It has been demonstrated that in *Saccharomyces cerevisiae*, temperature-sensitive mutants of the *mec1* gene display double-strand breaks (DSBs) in specific genomic regions with slow-moving replication forks. *Mec1* is an ortholog of ATR which has a role in the stability of CFSs in mammalian cells.

The evolutionary conservation of CFSs is somehow puzzling. There are data demonstrating fragile sites to be significantly more frequently found at chromosomal regions that are repeatedly involved in rearrangements during evolution of the vertebrate lineage (Miro *et al.* 1987; Ruiz-Herrera *et al.* 2005; Ruiz-Herrera *et al.* 2006). These findings suggest that fragile sites are prone to *in vivo* breakage during evolution, and may fulfill an important role in genome reorganization (Debacker and Kooy 2007). On the other hand, genomic regions that are prone to instability and rearrangements would be expected to be detrimental for the organism and therefore selected against during evolution. The fact that CFSs persist in the genome from yeast

to human, suggests they have a conserved function. CFS instability may simply be a side effect of a role of these sites in high-order chromosome structure or transcriptional regulation of associated genes. Or the fragility of these sites itself serves a purpose. Since they are late replicating, they may be among the last sites to replicate and signal to the cell that the replication is complete. Cell cycle checkpoint may specifically monitor these sites, blocking into mitosis until their replication is complete (Durkin and Glover 2007).

1.3 Genome instability on the short arm of chromosome 9

Short arm of chromosome 9 is the target of some of the most often described rearrangements in cancer. LOH and chromosomal deletions on the 9p have been reported as a frequent event in several cancers including clear cell carcinoma of the ovary (Kobayashi *et al.* 2009), meningioma (Bostrom *et al.* 2001; Perry *et al.* 2002), bladder cancer (Simoneau *et al.* 1996), pancreatic cancer (Sunamura *et al.* 2002), prostate cancer (Perinchery *et al.* 1999), nasopharyngeal carcinoma (Shao *et al.* 2002), lung cancer (Neville *et al.* 1995; Mao *et al.* 1996; Sato *et al.* 2005), invasive and non-invasive pituitary adenomas (Farrell *et al.* 1997; Pack *et al.* 2005), oral cancer (Ishwad *et al.* 1996), acute lymphoblastic leukemia (Faienza *et al.* 1996), skin cancer (Carless and Griffiths 2008), thyroid cancer (Unger *et al.* 2008), osteosarcoma (Lim *et al.* 2005), breast cancer (An *et al.* 1999; Ellsworth *et al.* 2008) and neuroblastoma (Takita *et al.* 1997). As well as primary tumors, rearrangements occur also in tumor-derived cell lines. There are studies showing aberration on 9p in cervical cancer cell lines (Harris *et al.* 2003), renal cell carcinoma cell lines, glioma cell lines (Pomykala *et al.* 1994), Hodgkin lymphoma cell lines, neuroblastoma cell lines (Giordani *et al.* 2002) and breast cancer cell lines (Savelyeva *et al.* 1999). Although most of these aberrations appear to be losses than gains, there are also data showing amplification of 9p region (Savelyeva *et al.* 1999; Lim *et al.* 2005).

These findings suggest that the alteration of genetic material at 9p has an important role in the pathogenesis of different human cancers. It has been observed that LOH on 9p in neuroblastoma is more frequently detected in favorable NB stages and is statistically associated with a better clinical outcome in stage 4 patients (Mora *et al.* 2004).

The 9p21 segment including the p16/*CDKN2A*, p14/*ARF* and p15/*CDKN2B* loci has been defined as a common region for the deletions (Kamb *et al.* 1994; Nobori *et al.* 1994; Ohnishi *et al.* 1995; Tanaka *et al.* 1997; Drexler 1998; Hamada *et al.* 2000; Park *et al.* 2002). These genes are involved in the regulation of cell cycle and/or apoptosis (Sherr 2000). *CDKN2A* encodes the 16-kD p16, which is a tumor suppressor, interacts with the complex of cyclin D and the cell-cycle-dependent kinase cdk4 or cdk6, and which inhibits the phosphorylation of the retinoblastoma protein (pRB) (Serrano *et al.* 1993).

Chromosomal interstitial deletions and terminal deletions of a chromosome arm are two different critical events that may cause inactivation of tumor suppressors. Interstitial deletions are supposed to be caused by DNA double strand breaks (DSBs) and subsequent illegitimate joining of DNA ends by homologous or non-homologous end joining repair. Since there is evidence confirming that DSBs can be formed at CFSs as a result of replication perturbation, one can envisage a role for CFSs in at least a number of frequently occurring deletions in cancer cells.

To date, seven fragile sites have been recorded on chromosome 9. These include *FRA9A* to *FRA9G*. Among them, three of them are located on the short arm of chromosome 9. These are folate-sensitive *FRA9A*, and the two common fragile sites *FRA9C* and *FRA9G*.

1.3.1 *FRA9G*

Previous studies in our laboratory (Sawinska *et al.* 2007) identified *FRA9G* as a novel aphidicolin inducible common fragile site, extending over a genomic region of 302 kb at chromosome band 9p22.2.

In agreement with the known characteristics of other CFSs, *FRA9G* does not contain any expanded CGG-trinucleotide repeats or AT-rich minisatellite repeats and appears to be AT-rich (63.76%). Total amount of interspersed elements represet 58.9% of *FRA9G* sequence. This is composed mainly of LINE1 elements (35.66%), but it contains also LINE2 (3.44%), Alu (7.23%), MIR (1.2%), long terminal repeats (LTR) (8.34%) and DNA elements (3.03%). Compared to other CFSs, *FRA9G* has relatively high content of LINE1 element however it does not further help to undestand the nature of fragile site susceptibility to breakage.

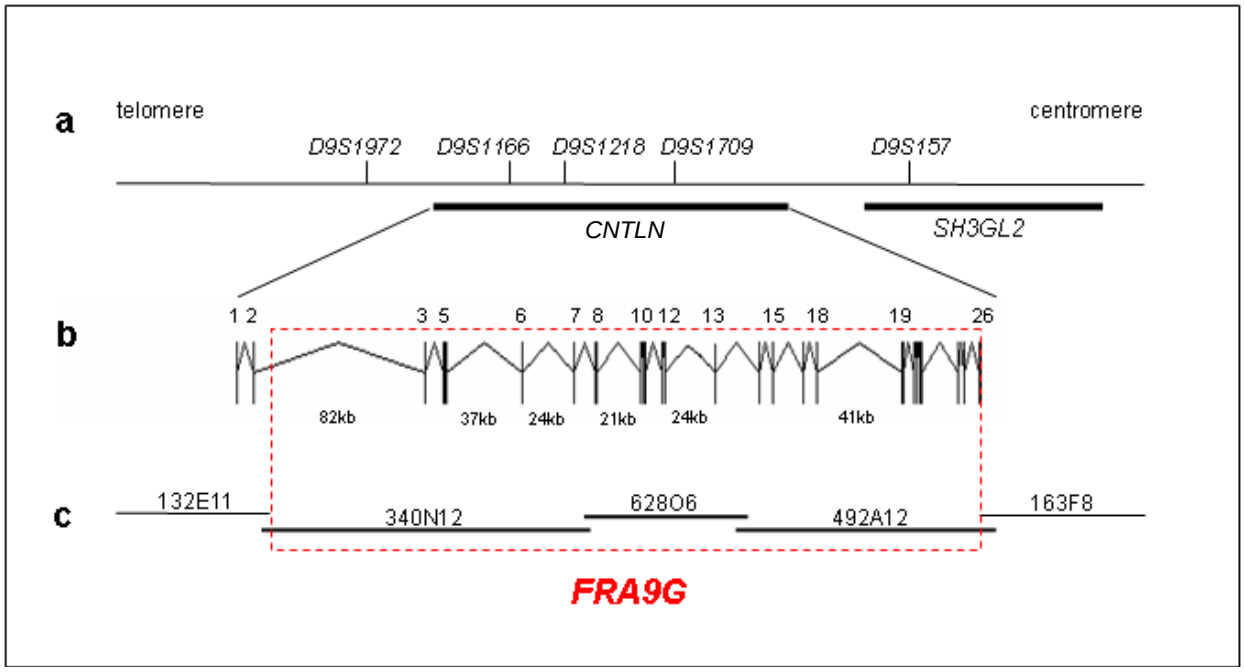

Figure 1-3. Transcriptional and physical map of the *FRA9G* region. (**a)** Location of DNA markers relative to *CNTLN* gene (*horizontal black lines*). (**b)** Genomic structure of the *CNTLN* gene. Sizes for the six largest introns are indicated. **(c)** The BAC clones that correspond to the represented region. (Fig. from Sawinska *et al*)

Similar to many other CFSs, *FRA9G* was found to be located within a single gene. According to Ensemble Database, *FRA9G* maps within *CNTLN* gene which spans 369 kb (Fig. 1-3).

1.3.2. *FRA9C*

FRA9C is a BrdU inducible common fragile site which has been long listed in the Database at short arm of chromosome 9. Recently in our laboratory and as the first BrdU inducible CFS, the chromosomal region of *FRA9C* was precisely characterized. The region that *FRA9C* spans was narrowed down to 713.5 kb between the loci identified by RP11-30O14 (centromeric signal) and RP11-438B23 (telomeric signal) (Sawinska *et al.* Unpublished data). Alignment of the sequence of *FRA9C* to Ensemble Database revealed that it spans a G/R chromosome boundary, mapping to the distal part of the 9p21.2 R band and the proximal part of the G-band 9p21.1.

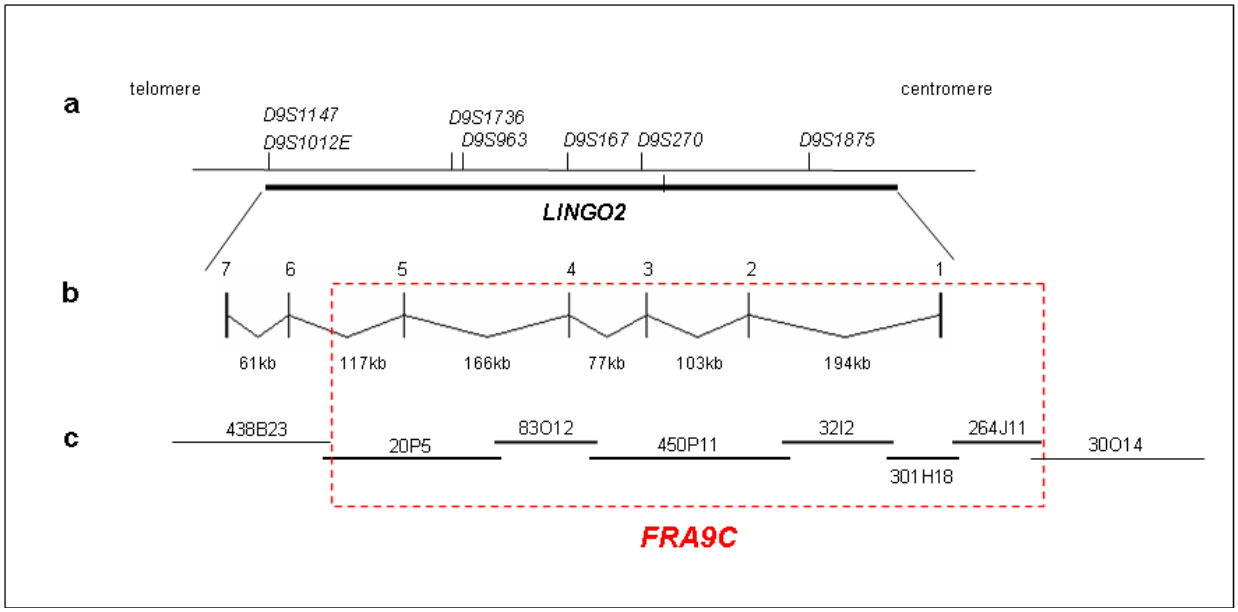

Figure 1-4. Transcriptional and physical map of the *FRA9C* region. **(a)** Location of DNA markers relative to *LINGO2* gene (*horizontal black lines*). (**b)** Genomic structure of the *LINGO2* gene. Sizes for the six largest introns are indicated. **(c)** The BAC clones that correspond to the represented region (Fig. from Sawinska *et a*l)

Little is known about the BrdU inducible common fragile sites. Most of the knowledge about CFSs have been gained from APH inducible CFSs. The sequence analysis of *FRA9C*, similar to APH inducible sites, showed AT-rich sequence (64%) and no content of expanded di- or tri-nucleotide repeats. Total interspersed elements represent 39.2% of the total sequence of *FRA9C*, consisting of Alu (3.92%), MIR (3.52%), LINE1 (17.17%), LINE2 (3.46%) long terminal repeats (LTR) (6.94%) and DNA elements (3.12%). Comparison of the *FRA9C* sequence with both telomeric and centromeric non-fragile flanking sequences shows no significant difference in quantity of particular repeat elements between these regions. To explore DNA helix flexibility in the *FRA9C* sequence, the TwistFlex program was applied and the outcome revealed 8.5 Flex Peaks per 100 kb for *FRA9C*. According to Zlotorynski *et al*, this number is 5.7 for APH inducible CFSs. Moreover, comparison of the *FRA9C* sequence with that of common fragile sites including *FRA9G*, *FRA3B*, *FRA16D*, *FRA13A* and *FRA1E*, shows a considerable variation in repeat sequences, in particular LINE1 elements (Sawinska *et al.* Unpublished data). This observation is in contrast to what has been proposed for *FRA3B*, in

which LINE1 elements are considered to have a probable major role in the DNA instability at the fragile locus (Mimori *et al.* 1999).

According to database, *FRA9C* is located within *leucine rich repeat and Ig domain containing 2 gene (LINGO2). LINGO2* is a relatively large gene of approximately 770 kb with a transcript size of 2.8 kb. It consists of seven exons ranging in size from 33 bp (exon 4) to 2.1 kb (exon 7), and big introns with the longest being 282 kb (Fig. 1-4). The genomic region of *FRA9C* extends for an approximately 620 kb of the *LINGO2* gene.

LINGO2 belongs to *LINGO/LERN* gene family, which similar to *NLRR*, *FLRT* and *LRRTM* gene families in mammals, encode for type I transmembrane proteins containing 10-12 extracellular rich leucin repeats and short intracellular tails (Carim-Todd *et al.* 2003; Lauren 2003; Haines 2005). The LERN proteins are often expressed in nervous system (Carim-Todd *et al.* 2003; Lauren 2003) and have been associated with neuronal regeneration (Ishii *et al.* 1996; Robinson 2004). It has also been suggested by some studies that these leucin rich repeat transmembrane proteins may function in the regulation of cell signaling (Fukamachi 2002; Ikeda *et al.* 2004; Haines *et al.* 2006).

1.4 Aims of this study

- To estimate the extent of genomic rearrangements affecting short arm of chromosome 9 in various tumor models. Based on a high resolution array CGH, the aim was to precisely characterize the overall genomic alterations on 9p, including deletion, amplifications and duplications and also to explore their frequency in different tumor types.

- To define the impact of the fragility at *FRA9G/CNTLN* and *FRA9C/LINGO2* on genetic alterations on 9p. As CFSs are supposed to exhibit breakages in the early stages of tumorigenesis, and also alterations in some CFS genes contribute to cancer development, one important aim of this study was to explore the frequency of *FRA9G/CNTLN* and *FRA9C/LINGO2* rearrangemnets **i**n different tumor models.

- To determine novel candidate tumor-susceptibility genes on 9p. Looking for for candidate genes associated in tumor development has been a primary task for cancer research. Herein, applying a high-resolution array would help to detect the most frequent target regions for genetic alterations on 9p, which leads to identify the most affected genes in the region.

2. Materials and Methods

2.1 Materials

2.1.1 Chemicals

5-Azacytidine	Sigma-Aldrich, Munich
β-Mercaptoethanol	Merck, Darmstadt
1,4-dithiothreitol (DTT)	Carl Roth GmbH, Karlsruhe
4,6-diamidino-2-2phenolyndole (DAPI)	Sigma-Aldrich, Munich
Acetic acid	Merck, Darmstadt
Agarose	Invitrogen, Karlsruhe
Bovin Serum Albumin (BSA)	Roche Diagnostics, Mannheim
Dextran Sulphate	Amersham Biosciences, Sweden
Diethylpyrocarbonate (DEPC)	Sigma-Aldrich, Munich
Ethanol	Sigma-Aldrich, Munich
Ethidium bromide	Sigma-Aldrich, Munich
Ethylendiaminetertaacetic acid (EDTA)	AppliChem, Darmstadt
Formamide	Merck, Darmstadt
Glycin	AppliChem GmBh, Darmstadt
Isopropanol	Merck, Darmstadt
Magnesium Chloride	Merck, Darmstadt
Methanol	Sigma-Aldrich, Munich
Phenol	Carl Roth GmbH, Karlsruhe
Phenol-Chloroform	Carl Roth GmbH, Karlsruhe
Potassium Chloride	Merck, Darmstadt
Sodium acetate	Carl Roth GmbH, Karlsruhe
Sodium chloride	J.T. Baker, Deventer, Holland
Sodium citrate	Fluka Chemie GmbH, Buchs
Sodium hydrogen carbonate	Merck, Darmstadt
Tris-(hydroxymethyl)-aminomethane-NaOH	Sigma-Aldrich, Munich
Tris-(hydroxymethyl)-aminomethane-HCl	AppliChem GmBh, Darmstadt

Tween 20	Merck-Schuchardt, Munich

2.1.2 Other Materials

Cell culture dishes	Greiner Labortechnik, Frickenhausen
Cell culture flasks	TPP, Trasadingen Schweiz
Over slips	Menzel, Braunschweig
Cryotubes	Nalgene Nunc, Wiesbaden
Microscope slides	Menzel, Braunschweig
Micro test tubes (1.5 – 2.0 ml)	Eppendorf, Hamburg
Parafilm "M"	American Natinal Can, Chicago
Pasteur pipettes	Brand, Wertheim
PCR tubes	Abgene, Surrey, UK
Pipette tips	Greiner Labortechnik, Frickenhausen
Polyethylene-tubes (15 ml, 50 ml)	Labortechnik, Frickenhausen
Optical 96-well reaction plates, MicroAmp	Applied Biosystems, Weiterstadt
Rubber cement, Figogum	Marabuwerke, Tamm
Scalpels	PFM, Köln

2.1.3 Laboratory Equipments

ABI PRISM 7000, sequence detection system	Applied Biosystem, Weiterstadt
Apparutus for gel electrophoresis	GIBCO/BRL, Eggenstein, Darmstadt
Baeuerle BS 785 Automatic Timer	St. Georgen/Schwarzwald
Biometra, TRIO thermoblock	Biometra, Göttingen
Counting cell chamber	Migge, Heildelberg
Freezer -20°C	Liebherr, Germany
Freezer -80°C	New Brunswick Scientific, USA
Heat block	Eppendorf, Hamburg
Hot cabinet, 37°C	Heraeus, Osterode
Hybridization System 4	NimbleGen Inc, USA
Incubators	W. Schreck, Hofheim

Lamin airflow cabinet Uniflow 1800	UniEquip, Martinsried
Magnetic stirrers	Heidolph-Elektro, Kehlheim
Microscope Leica DMRA 2	Leica Microsystems, Wetzler
MS 2000 Microarray Scanner	NimbleGen, USA
Nanodrop, Spectrophotometer ND-1000	Thermo Fischer Scientific, USA
Oven	Heraeus, Osterode
PCR-Thermoblock GeneAmp 9700	Applied Biosystems, Darmstadt
Photometer, Ultroscope 3000	Amersham-Pharmacia, Freiburg
Pipetboy	Integra Biosciences GmbH, Fernwald
Power supply unit Pherostab 500	BiotechFischer, Reiskirchen
Shaker IKA KS250	Janke and Kunkel, Staufen
System for gel documentation (Geldoc)	Biorad, Munich
Thermomixer compact	Eppendorf AG, Hamburg
Vaccum-Concentrator	Bachofer, Reutlingen
Vortex-Shake	Heidolph-Elektro, Kehlheim
Waterbath	Köttermann, Uetze-Hänisgen

Centrifuges

Biofuge fresco	Heraeus, Osterode
Biofuge pico	Heraeus, Osterode
Eppendorf Centrifuge 5417R	Eppendorf. Hamburg
J-6 M/E Centrifuge	Beckman Inst, Munich
J2-21 M/E Centrifuge	Beckman Inst, Munich
Avanti-J-25I	Beckman Inst, Munich

Rotors

JS 4.2	Beckman Inst, Munich
JA 10	Beckman Inst, Munich
JA 20	Beckman Inst, Munich

2.1.4 Antibiotics

Ampicilin	AppliChem, Darmstadt
Penicillin, Streptomycin	Serva, Heidelberg
Kanamycin	Serva, Heidelberg

2.1.5 Enzymes

DNA polymerase I *E.coli*	MBI-Fermentas, St.Leon-Rot
DNase I / RNase free	Roche Diagnostics, Mannheim
Klenow fragment	MBI-Fermentas, St.Leon-Rot
Pepsin	Sigma-Aldrich, Munich
Reverse transcriptase (Superscript III)	Invitrogen, Karlsruhe
RNase A	Roche Diagnostics, Mannheim
Taq DNA polymerase	Promega, Mannheim
Trypsin	

2.1.6 Fluorescent dyes

Cy3	Amersham Biosciences Europe GmbH, Germany
Cy3.5	Amersham Biosciences Europe GmbH, Germany
Cy5	Amersham Biosciences Europe GmbH, Germany
Cy5.5	Amersham Biosciences Europe GmbH, Germany
DEAC	Molecular probes Inc, Eugene, USA
FITC	Molecular probes Inc, Eugene, USA

2.1.7 Kits, Medida and solutions

First Choice Total RNA: Human Normal Tissues	Ambion, USA
Platinum SYBR Green qPCR SuperMix-UDG	Invitrogen, Karlsruhe
Qiagen Plasimd Maxi Kit	Qiagen, Hilden
QIAquick Gel Extraction Kit	Qiagen, Hilden
QIAquick PCR Purification Kit	Qiagen, Hilden
First-Strand cDNA synthesis kit for RT-PCR	Invitrogen, Karlsruhe
Fetal Bovin Serum (FBS)	Life Technologies, Munich

RPMI 1640, cell culture medium	Life Technologies, Munich
TRIZOL ™ Reagent	Invitrogen, Karlsruhe

2.1.8 Nucleic Acids

1 kb DNA-Ladder, Gene Ruler	MBI Fermentas, St.Leon-Rot
100 bp DNA-Ladder, Gene Ruler	MBI Fermentas, St.Leon-Rot
Cot-1 DNA	Life Technologies, Munich
dNTPs	Sigma-Aldrich, Munich
OLIGO(dT)23 Anchored	Sigma-Aldrich, Munich
Salmon sperm DNA	Roche-Diagnostics, Mannheim

2.1.9 Buffers and solutions

1x PBS

137 mM NaCl

2.7 mM KCl

10 mM Na_2HPO_4, pH 7.4

20x SSC

3 M NaCl

0.3 M NaCitrate, pH 7.0

TBE-buffer

50 mM Tris

50 mM boric acid

1 mM EDTA

TE

10 mM Tris.Cl 7.4 or 7.5 or 8.0

1 mM EDTA, pH 8.0

Freezing medium

20 % (v/v) DMSO

80 % (v/v) FCS

prepared freshly before use

DNA fragments separation in gel agarose

Agarose gel

1% Agarose

1x TBE-buffer

DNA-loading buffer

15% (w/v) Ficol Type 400

0.25% (w/v) Xylencyanol

0.25% (w/v) Bromophenol blue

Ethidium bromide

Stock: 10 mg/ml in H_2O

For gel: 5 ml stock/100 ml

Cell fixation and fluorescence *in situ* hybridization

Blocking solution

4x SSC

3% BSA

DAPI

Stock: 0.25 mg/ml H2O

Denaturation solution

70% deionized formamide

2x SSC

Detecrion buffer

4x SSC

1% BSA

0.1% Tween

Fixative solution

Methanol

Acetic acid

In proportion 3:1

Hybridization solution

4x SSC

20% dextran sulphate

Hypotonic solution

0.55% KCl

1% NaCitrate

In proportion

10x nick translation buffer

0.5 M Tris-HCl. pH 8.0

50 mM MgCl2

0.5 mg/ml BSA

PBS/MgCl2-solution

1x PBS

0.25 M MgCl2

PBS/MgCl2/formaldehyde-solution

1x PBS

0.25 M MgCl2

2.7% formaldehyd

Pre-treatment solution

99 ml H2O

1 ml HCl

50 µl pepsin

RNase-solution

200 µg/ml

2x SSC

2.1.10 Oligonucleotides

Below are the custom oligonucleotides were synthesized and purified by HPLC by Sigma:

CNTLN-forward primer

5' AAGGAACCACCTGTGAAACG 3'

CNTLN-reverse primer

5' GATTTCAGCCGATTTTCCAA 3'

LINGO2-forward primer

5' TGAGCTGCCTGCACTTCTAA 3'

LINGO2-reverse primer

5' TGGTGGATCCCATGAAGATT 3'

GAPDH-forward primer

5' ACCACAGTCCATGCCATCAC 3'

GAPDH-reverse primer

5' TCCACCACCCTGTTGCTGTA 3'

CNTLN (real-time)-forward primer

5' CCGATCAACGATTTCAGACA 3'

CNTLN (real-time)-reverse primer

5' GGGAATTTTCTTCTGCCAAA 3'

GAPD (real-time)-forward primer

5' TGGACCTGACCTGCCGTCTA 3'

GAPD (real-time)-reverse primer

5' CCCTGTTGCTGTAGCCAAATTC

2.1.11 Plasmids

BACs	Deutsches Ressourczentrum für Genomforschung (RZPD), Berlin

2.1.12 Software

GenePix	Agilent, USA
Leica CW4000	Leica Microsystems, San Jose, USA
NimbleScan, version 2.4.27	Roche NimbleGen, USA
SignalMap, version 1.9.0.0	Roche NimbleGen, USA
Microsoft Excel 2000	Microsoft Corp.
Microsoft Photoshop 7.0	Adobe Systems Inc.

2.1.13 Online Databases and Programs

Primer3, Web Interface Whitehead Institute for Biomedical Research	http://frodo.wi.mit.edu/primer3
National Center for Biotechnology Information (NCBI)	http://www.ncbi.nlm.nih.gov
Ensembl database	http://www.ensembl.org
UCSC Genome Browser	http://genome.ucsc.edu
Wellcome Trust Sanger institute COSMIC project	http://www.sanger.ac.uk/genetics/CGP/cosmic
RepeatMasker program	http://www.repeatmasker.org
Perfect Microsatellite Repeat Finder	http://sgdp.iop.kcl.ac.uk/nikammar/repeatfinder.html
TwistFlex program	http://margalit.huji.ac.il/TwistFlex

2.1.14 Human tumor cell lines

Cell line	Reference
LAN6	Savelyeva *et a*l, 1995
Kelly	Thiele, 1998
NGP	Brodeur *et al*, 1977
CHP-134	Schlesinger *et al*, 1976
SK-N-FI	Thiele, 1998
SK-N-BE(2)C	Thiele, 1998
HDN-33	DKFZ
Vi-856	Savelyeva *et a*l, 1995
SH-EP	Thiele, 1998
H-4	Arnstein *et al*, 1974
U-87 MG	Ponten J *et al*, 1968
U-373 MG	Ponten J *et al*, 1968
U-138MG	Ponten J *et al*, 1968
A 172	Giard DJ *et a*l, 1973
Hs-683	Owens RB *et al*, 1976
HDC-54	DKFZ, tumorgenetics department
HDC-57	DKFZ, tumorgenetics department
HDC-73	DKFZ, tumorgenetics department
HDC-75	DKFZ, tumorgenetics department
HDC-87	DKFZ, tumorgenetics department
COLO-824	Savelyeva *et al*, 1999
BT-20	Lasfargues *et al*, 1958
BT-474	Lasfargues *et al*, 1978
MX-1	Ovejera AA *et al*, 1978

T-47D	Keydar I *et al*, 1979
SK-BR-3	Fogh J *et al*, 1977
MDA-MB-436	Cailleau R *et al*, 1978
MFM-223	Hackenberg *et al*, 1991
MCF-7	Soule HD *et al*, 1973

2.1.15 Lymphoblastoid cell lines from healthy individuals

Cell line	Description
UM	Female, EBV-transformed- lymphocytes, wild type
UV	Male, EBV-transformed- lymphocytes, wild type
327M	Female, EBV-transformed- lymphocytes, wild type
327F	Male, EBV-transformed- lymphocytes, wild type
303	Male, EBV-transformed- lymphocytes, wild type
327	Female, EBV-transformed- lymphocytes, wild type

2.2 Methods

2.2.1 Array CGH

Test (human tumor cell lines) and reference (lumphoblastoid cell lines from healthy individuals) DNA Samples were applied in array-based comparative genomic hybridization experiments. Purified, unamplified, and unfragmented genomic DNA (gDNA) is required optimal sample labeling and hybridization. The whole procedure was done following manufacturer's protocol (Roche NimbleGen CGH array).

Sample preparation

Both test and reference DNA were sonicated to produce a smear of DNA from ~500 bp to ~2000 bp. On 1% agarose gel, genomic DNA should appear as a single prominent band greater than 12 kb. Degradation and/or RNA contamination appear as more than one band or as a smear, which could affect the labeling procedure. Such samples are not suitable for aCGH analysis.

Sample labeling

Cy3-Random and Cy5-Random Nanomers are diluted as below:

Random Primer Buffer	998.25 µl
β-Mercaptoethanol	1.75 µl
To the final volume of 1 ml	

Diluted primers are aliquoted and stored at -20°C.

Then 1 µg of test and reference samples were mixed with 40 µl of diluted Cy3 and Cy5, respectively. Then the samples were denaturated at 98°C for 10 min and quick chilled for 2 min. The following dNTP/Klenow Master Mix was prepared and added per sample:

10 mM dNTP Mix	10 µl
Nuclease-free water	8 µl
Klenow Fragment (3->5 exo-)	2 µl

The next step was to mix the 20 µl of dNTP/Klenow Master Mix with 80 µl of dilution of DNA samples and the Nanomers. They were then mixed well by pipetting and incubated for 2 h at 37°C.

The reaction is stopped by adding 10 µl of 0.5 M EDTA solution. After adding 11.5 µl of 5M NaCl and 110 µl of isopropanol, the samples were vortexed well and incubated for 10 min at RT. By removing the supernatant from centrifugation at 12000 x g for 10 min, pink (Cy3) and blue (Cy5) pellets were remained. The pellets were rinsed with 500 µl 80% ice-cold ethanol by 2 min centrifugation. The pellets at this stage could be stored dried at -20°C. Otherwise, the samples were diluted in 25 µl nuclease-free water, vortexed well and the concentration of each sample was caculated by Nanodrop. At this step also the pellets could be stored protected from light at -20°C.

Hybridization and washing

Using components from NimbleGen Hybridization Kit, the following hybridization solution master mix was prepared for each slide (3x720K array):

2x Hybridization Buffer	35 µl
Hybridization component A	14 µl
Alignment Oligo	3.6 µl

From the master mix, 14.4 µl was mixed with 5.6 µl of the labeled sample, incubated at 95°C for 5 min and then loaded to each slide. The mixers were loaded on the slides and sealed perfectly according to manufacturer's manual. Finally, the slides were placed in the hybridization system and incubated at 42°C for 40-72h.

All the further washing steps and scanning the slides were performed as described in NimbleGen protocol.

The results were analyzed using SignalMap and NimbleScan softwares provided by NimbleGen.

2.2.2 Cytogenetic techniques

Preparation of metaphases

In order to excite cells division and also to increase the amount of the cells in metaphase, fresh medium was added to cells one day prior to metaphases preparation. For harvesting, cells were centrifuged at 800 rpm for 6 min at room temperature, following the cells pellet was resuspended in 10-12 ml (depending on the pellet size) of fresh hypotonic solution and incubated for 15-25 min at RT. Longer hypotonic incubation (45-60 minutes) or the use of more hypotonic buffer resulted in longer, thicker, stickier chromosomes, very difficult to spread, yielding poor banding but still good FISH signals. Too short hypotonic treatment leaves cell membranes and cell/nuclear debris around the chromosomes, which do not spread properly and have poor banding and hybridization quality.

After hypotonic treatment and before centrifugation (800 rpm, 5 min, room temperature), 1ml of fixative solution (3:1 parts absolute methanol/glacial acetic acid) was added. For fixation, the cell pellet was resuspended in 5 ml of fixative solution and incubated for 15 min at RT. The fixative solution preserves the cells in their "swollen" state after hypotonic treatment, removes lipids and dentures proteins thus making the cell membrane very fragile, which helps chromosome spreading. After incubation, the cell suspension was again centrifuged at 800 rpm for 5 min, the supernatant removed and pellet cells were washed in fixative solution. This procedure was repeated three times. After the last centrifugation step, cells pellet was supernatant in fresh fixative and stored for years at -20°C. Prior to slide preparation, the supernatant was removed and replenished with fresh fixative when stored longer than 5-6 days in refrigerator or more than two weeks in a freezer.

Hypotonic solution	absolute methanol, glacial acetic acid, in proportion 3:1
Fixative solution	0.55 % KCL 1 % NaCitrate, in proportion 1:1

Slides preparation

Glass slides were washed and rinsed in double distilled water. With an automatic pipette, 20-30 µl of cell suspension was evenly distributed on several locations on the slide and spread the liquid by gently moving the pipette tip parallel to the surface. As the fixative gradually

evaporated, the surface of the slide became "grainy" (cells visible). Afterwards, the slide was faced down into the steam of the hot water bath (~60°C) for 2-4 seconds and then air-dried.
An alternative method consisted in dropping 2-3 drops of cells suspension using Pasteur pipette on the preheated for several seconds (water bath, ~60°C) slide from 10-15 cm distance. Cells were evenly distributed on the surface. Excess liquid was drained on a paper towel and the slide was air-dried. The degree of spreading was adjusted using the different temperature of water bath, with higher temperatures increasing chromosomes spreading.
The quality of the slides was verified with the help of light-optical microscope.

Aging of slides-dry heat

Prior to fluorescence *in situ* hybridization, slides were aged either by incubating 2-3 days at RT, or at 37°C for 2 days, or overnight at 65°C. However, aging has to be gentle enough to allow optimal access of the labeled DNA probe to the target chromosomal DNA. Very fresh slides, if not aged, might either lose most of the nuclei/chromosomes during denaturing or the shape of the chromosomes will become much distorted ("puffy" chromosomes). Too long aging can sharply decrease the efficiency of hybridization.

Fluorescence *in situ* hybridization

In fluorescence *in situ* hybridization (FISH), a DNA probe is labeled with a fluorescent dye or a hapten (usually in the form of fluor-dUTP or hapten-dUTP, which is incorporated into the DNA using enzymatic reactions, such as *nick translation* or *PCR*). The labeled DNA is purified, concentrated, resuspended in hybridization buffer (containing formamide) and is hybridized onto chromosomes and nuclei on slides (cytogenetic preparations). After overnight hybridization, the slides are rinsed in washing solutions and, if needed, one or several layers of fluorescent-labeled antibodies are added to detect hapten-labeled DNA. The slides are mounted with antifade solution and are visualized at the fluorescent microscope, using appropriate filters.

Chemical coupling – synthesis of labeled nucleotides

As previously described (Henegariu *et al.* 2000), labeled nucleotides were synthesized by chemically coupling allylamine-dUTP to succinimidyl-ester derivatives of fluorescent dyes: DEAC (diethyl aminomethyl coumarin), FITC (fluorescein isothiocyanate), Cy3, Cy3.5, Cy5,

Cy5.5. The latter require fluorescently-labeled antibodies or specific proteins for visualization/detection. The reactive nucleotide (allylamine-dUTP), are all available commercially as dry powders, in 5-10-25 mg aliquots. Most of the days can be dissolved in DMSO, but some, for instance CB and 488 (the acetylazide derivative of Alexa 488, respectively) are soluble in water. Chemical coupling reactions were carried out at 2:1 molar concentration (dye: dUTP) in 80-100 mM bicarbonate buffer, adding the allylamine-dUTP (20 mM stock solution, in 0.2 M bicarbonate buffer) first, and the reactive dye last.

Aminoallyl-dUTP	1 mg AA-dUTP/100 µl 0.2 M bicarbonate buffer
Bicarbonate buffer	0.2 M NaHCO3 (pH 8.3)
Glycine	2 M glycine, pH 8
Tris-HCl	1 M Tris-HCl, pH 7.75

After 3-4 hours of incubation at RT, glycine was added to every reaction in order to stop reaction, then Tris-HCl to stabilize the nucleotides and H2O. Nucleotides could be used immediately or stored at -20°C.

***Nick translation* – enzymatic DNA labeling**

The labeling of FISH probes was carried out by *nick translation* with fluorescence dyes-dUTP such as Cy3-dUTP, Cy3.5-dUTP, FITC-dUTP, DEAC-dUTP, Cy5-dUTP and Cy5.5-dUTP.
A standard *nick translation* reaction included:

2-3 µg	DNA
10 µl	0.1 M β-Mercaptoethanol
10 µl	1× *nick translation* buffer
10 µl	10× dNTP-mix
3 µl	DNase I (0.03 U/µl)
2µl	E.coli DNA-polymerase I (10 U/µL)
H2Odd	to 100 µl final volume

The reaction was mixed on ice and subsequently incubated at 15°C for 45-55 min. During incubation **DNase I** in the presence of Mg++ becomes a single stranded endonuclease and creates random nicks in the two strands of any DNA molecule. ***E.coli* polymerase** I which

through its 5'-3' exonuclease activity removes nucleotides "in front" of itself, while the 5'-3' polymerase activity adds nucleotides to all the available 3' ends created by the DNase. This exonuclease/polymerase activity, moves (or "translates") any single stranded nick in the 5'-3' direction. When nicks on opposite strands meet, the DNA molecule breaks.

The enzymatic activity was stopped by incubation of vials on ice. The size of labeled DNA fragments used for hybridization was verified by electrophoresis and 8 µl of every sample was run on 1 % agarose gel. Their size needs to be between 200-500 bp long, otherwise, a relatively high backgrounds starts to become visible on the slides and the hybridization signals become more punctuate.

10 × nick translation buffer	0.5 M Tris-HCl (pH 8.0), 50 mM $MgCl_2$, 0.5 mg/ml BSA
10 × dNTP-mix	50 µl 1 mM dNTP (dATP, dCTP, dGTP), 15 µl 1 mM dTTP, 35µl 1 mM labeled dUTP

Preparation of DNA probes for *in situ* hybridization

After *nick translation*, the labeled DNA needs to be processed and purified before it is used as a probe in FISH.

Chromosomal *in situ* suppression (CISS) hybridization

Since the interspersed elements are present in a probe, application of the standard procedure results in hybridization signals distributed over the whole chromosome complement due to the ubiquitous presence of repetitive sequences throughout the genome. These elements can be suppressed in a given probe, while a highly specific signal is produced by the target site specific sequences. The method has been called chromosomal *in situ* suppression (CISS) hybridization. The labeled probe fragments are denaturated together with an excess of unlabeled competitor DNA (Cot-1 DNA). Thereafter, pre-annealing is allowed for a given period of time. During this time, repetitive elements of the probe will hybridize rapidly with abundant chromosome specific sequences remain single-stranded. Accordingly, the resulting double-stranded repetitive elements in the pre-annealed probe can no longer hybridized to their chromosomal DNA targets. Remaining single-stranded repetitive sequences will hybridized to chromosomal repetitive targets during the subsequent *in situ* hybridization.

For each *nick translation*, DNA probe was mixed Cot-1 fraction of human genomic DNA (10 µg Cot-1 DNA pro 100 µl of *nick translation* volume) and 4 µl of salmon sperm (20 µg per 100 µl of *nick translation*). The mix was precipitated with 2.5 volume of absolute ethanol, incubated for 30 min at -80°C, and afterwards centrifuged at 13000 rpm for 30 min, at 4°C. The dried pellet was dissolved at 65°C in 15 µl per slide of deionized formamide and after addition of 15 µl of hybridization buffer, well mixed and denaturated for 10 min at 90°C. Pre-annealing was performed for 30-60 min at 37 °C. After incubation, the probe was completely prepared for hybridization with the pre-treated metaphase chromosomes.

Deionized formamide	deionized with 100 g *Mixed Bed Resin*/1 l formamide
Hybridization buffer	4× SSC, 20 % dextran sulphate

Pretreatment and *in situ* hybridization of metaphase chromosomes

Before hybridization of DNA probe to the metaphase preparation, the slides were treated with RNase and pepsin. For RNase treatment, which serves to remove endogenous RNA and may improve the signal to noise ration in hybridization to DNA targets, 300 µl of RNase-solution was put onto microscope slides, covered with cover slips and incubated for 1 h at 37°C. Afterwards, the slides were rinsed three times with 2× SSC for 5 min each, at 42°C. After this incubation, the digestion of proteins that surround the target nucleic acid was performed with 50 µg/ml pepsin in 0.01 M HCl-solution at 42°C for 10 min to increase accessibility. Following, the slides were washed twice for 5min each, at 42°C, at first in 1 × PBS and then in PBS/$MgCl_2$-solution. The next fixation was performed in 1%iger formaldehyde-solution (in PBS/$MgCl_2$-solution) for 10 min at room temperature and after this the slides were washed in 1×PBS for 5 min at 42°C. Finally the slides were dehydrated in ethanol series (70 %, 90 %, 100 %), each for 3 min at RT and air-dried. Immediately before hybridization with DNA probes, chromosomes were denaturated in 70 % formamide (FA)/2 × SSC in Coplin jar) at 70-74 °C, followed by rising, 3 min each in 70 %, 90 % and 100 % ice-cold ethanol at room temperature. After air-drying, previously prepared probe mixture was spotted onto thee cell sample and glass cover slips were carefully applied. Drying up of probe was prevented through sealing the edges of slides with *rubber cement* (Fixogum) during overnight hybridization at 37 °C in a humidified chamber.

2.2.3 Nucleic acid manipulations

2.2.3.1 Total RNA extraction

Total cellular RNA from cell lines was isolated using TRIZOL. This reagent is a monophasic solution of phenol and guanidine isothiocyanate, which is able to effectively dissolve cellular components ensuring the integrity of the RNA molecules through the isolation procedure. After addition of chloroform, the TRIZOL containing solution separates onto an aqueous RNA containing phase and an organic phase. RNA can be easily recovered from aqueous phase by precipitation with isopropanol.

Cell culture medium was discarded from the culture dishes and then TRIZOL was added directly to cells. Lyzed cells were transferred into the RNase-free polypropylene tubes and incubated for 5 min at RT. To separate the aqueous phase, 0.2 ml of chloroform per 1 ml TRIZOL was added to each tube. Samples were mixed by vortexing for 1 min and then centrifuged at 10,000x g for 10 min at 4°C. After centrifugation, the upper colorless aqueous phase was collected and RNA was precipitated with equal volume of isopropanol alcohol. The RNA pellet, obtained after centrifugation for 15 min at 12,000x g, was then washed once with 75% ethanol and air0dried for 5 min. RNA was dissolved in RNase-free water and the amount of RNA in each sample was estimated on a spectrophotometer, reading the absorbance at 260 nm.

2.2.3.2 Reverse transcription of total RNA and RT-PCR

To generate the first strand cDNA, total RNA was reversely transcribed using the SuperScript™ III Reverse Transcriptase from Invitrogen according to the manufacturer's instructions. The First- Strand cDNA synthesis reaction was conducted as below:

RNA and oligo(dT)$_{12-18}$ primers were denaturated at 65°C for 5 min and placed on ice and mixed with dNTPs:

1µl Oligo(dT) primer (50µM)
1 µg RNA
10 mM dNTPs (10mM)
H2O up to final volume of 13 µl

To the chilled RNA/oligo mixture, the following master reaction mix was added:

4 µl 5x First Strand Buffer
1 µl 0.1 M DTT
1 µl SuperScript RT (200 units/µl)

The reaction mixture was mixed well and incubated for 60 min at 50°C. Then the reaction was terminated at 85°C for 5 min. The final samples could be diluted and stores at -80°C.

To amplify *CNTLN* and *LINGO2* cDNA, the first strand cDNA was used for PCR amplification with the specific primers described before. The primers were designed with the Primer3 software and were ordered from Sigma.

PCR reactions were set up as below:

2 µl RT reaction
5 µl 10x PCR Buffer
0.5 µl dNTPs
1 µl primer forward
1 µl primer reverse
0.5 µl *Taq* DNA polymerase (5 U/µl)
H2O to the final volume of 50 µl

And cycling conditions were:

	94°C	2 min
35 cycles	94°C	30 sec
	55°C	45 sec
	72°C	60 sec
	72°C	7 min

The fragment of cDNA of the housekeeping gene *GAPDH*, amplified with the primers described in 2.1.10, was used for normalization of the results.

2.2.3.3 Quantitative RT-PCR

For quantifying the expression of *CNTLN* in normal tissues, the total RNA of normal human tissues (Ambion) were subjected to reverse transcription and then the obtained cDNA was

analyzed by real-time RT-PCR. The analysis was performed using SYBR green assay (Invitrogen) according to manufacturer's protocol. The primers were designed with the Primer3 software in a way that they cross exon-intron boundaries. They were the ordered from Sigma. The PCR reaction for the First-Strand cDNA was as below:

13 µl	Platinum SYBR Greenq PCR SuperMix UDG (2x)
1.25 µl	forward primer (6pmol/µl)
1.25 µl	reverse primer (6pmol/µl)
2.5 µl	template cDNA
7 µl	H2O

The reaction was carried out in ABI PRISM 7900 detection system (Applied Biosystems) using the following conditions:

40 cycles	95°C	15 min
	94°C	15 sec
	55°C	30 sec

The results obtained from *CNTLN* qPCR were normalized by *GAPD* housekeeping gene qPCR results.

2.2.3.4 Genomic DNA extraction

To isolate the genomic DNA, cells from 150 mm plates were trypsinized and collected in 15 ml falcon tubes. They were then washed using 10 ml PBS and centifugating at 800 rpm for 5 min. The pellet was then resuspended in 2 ml of lysis buffer and incubated for 1h at 56°C.

Lysis Buffer	8.3 g	NH4Cl
	1 g	KH2CO3
	0.37	EDTA
	H2O up to 1 L	

Five ml of phenol/chloroform was added to the lyzed solution, vortexed and centrifuged at 3000 rpm for 5 min. The aquouse layer was then collected and transferred to a new 15 ml falcon tube and again 5 ml phenol/chloroform was added, followed by centrifugation. Afterwards, the

aqueous phase was transferred to a 50 ml falcon tube containing 30 ml of Ethanol 100% and 3ml NH4AC (3 M). It was mixed gently until DNA was precipitated.
Genomic DNA was then spooled onto a glass rod and washed by dipping the rod into 1 ml of 70% ethanol. In the end the DNA was detached from the rod and dissolved completely in water.

2.2.4 Culture of cells

All cells were grown at 37°C in a cell incubator in a 5% carbon dioxide/100% humidity atmosphere. All cell culture media were supplemented with 100 U/ml penicillin, 100 µg/ml streptomycin and 10% fetal bovine serum. Most adherent cells were detached from the surface of the cell culture flasks with the help of a trypsin / EDTA solution. Before the detachment the growth medium was removed and the cells were washed by the careful addition and subsequent removal of 10–20 ml PBS. Then 40 µl trypsin/EDTA solution per square centimeter surface was added and the cells were kept for 5–10 minutes at 37°C in a cell incubator. When the cells were detached they were washed in 10–20 ml growth medium to inactivate the trypsin/EDTA and used for further experiments.

2.2.5 Freezing and thawing of cells

In order to freeze mammalian cells, $1*10^6$ to $1*10^7$ cells were suspended in 500 µl of the respective growth medium. To the cell suspension 500 µl freezing medium was added and the samples were transferred immediately to -80°C. After one week at -80°C the cells were transferred to liquid nitrogen containers and stored at -196°C. In order to thaw cells, 37°C warm growth medium was added to the frozen cells with a Pasteur pipette. One washing step was performed in 10 ml growth medium to remove the DMSO. After that the cells were seeded in fresh medium in a cell culture flask.

2.2.6 5-Azacytidine treatment

The cell lines were maintained in RPMI 1640 supplemented with 10% fetal bovine serum. Ninety six hours after treatment with 20mM of 5-aza-2'-deoxycytidine, cells were harvested and subjected to subsequent experiments.

3. Results

3.1 Chromosomal rearrangements on 9p in different tumor types

To investigate and characterize the precise genomic rearrangements throughout 9p, fine tiling custom array CGH (comparative genomic hybridization) technology was applied on four different tumor types including glioblastoma/glioma, neuroblastoma (NB), colon cancer (CC) and breast cancer (BC). Sixty-bp probes where applied for the entire 9p arrays and custom design arrays containing *FRA9G*, *CDKN2A* and *FRA9C*, with intervals of 40 and 80 bp, respectively. Due to the high resolution of the probes, we were able to define the precise location of the breaks and genomic alterations on the target sequence. The number of probes was enough to cover the whole length of 9p sequence. In addition to array-based experiments, fluorescence *in situ* hybridization (FISH) was performed to validate the results obtained from the aCGH experiments.

3.1.1 Copy number changing profiles

Copy number changes are the most frequently known type of human structural genomic variations. They comprise gains and losses of DNA fragments that are generally 500 bp, or longer, in length (Gokcumen and Lee 2009).

The aCGH output files of all the cell lines from four different tumor types were loaded to UCSC Genome Browser to analyze their copy number changes on entire 9p. Figure 1-1 overviews the copy number changes of 9p region in GB/glioma (A172, H4, Hs-683, U138-MG, U-373 MG and U-87 MG), NB (SK-N-BE2C, CHP-134, Kelly, LAN-6, NGP and Vi-856,), CC (HDC-54, HDC-57, HDC-73 and HDC-87) and BC (BT-20, COLO-824, MCF-7, MDA-MB-436, MX-1 and SKBR3). The copy number changes of each cell line are shown as losses (red) and gains (green) on individual tracks. The top position along the chromosome 9 is indicated in Mb scale.

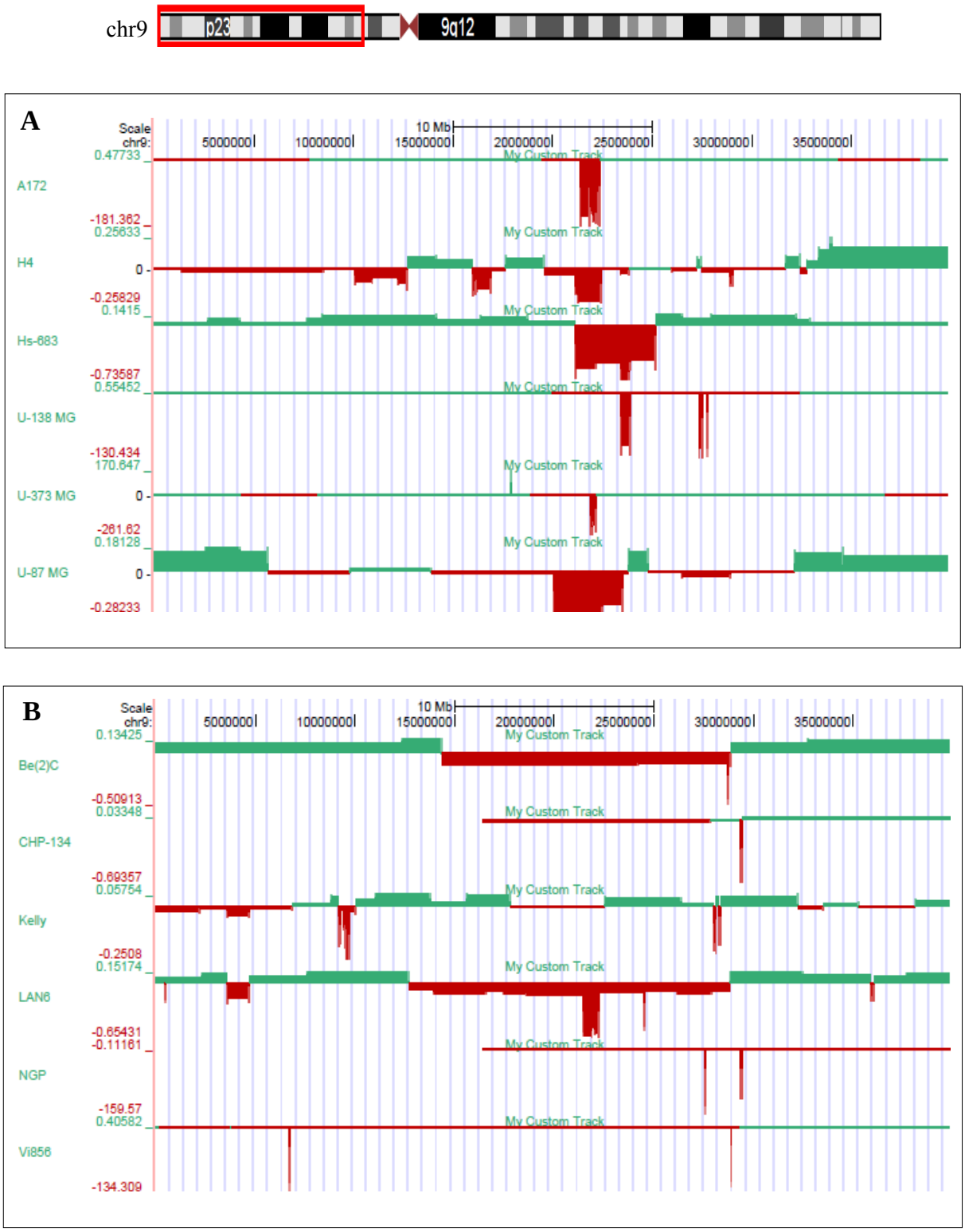
chr9
p23
9q12
A
Scale
chr9:
10 Mb
5000000
10000000
15000000
20000000
25000000
30000000
35000000
0.47733
A172
-181.362
0.25633
H4
0
-0.25829
0.1415
Hs-683
-0.73587
0.55452
U-138 MG
-130.434
170.647
U-373 MG
0
-261.62
0.18128
U-87 MG
0
-0.28233
My Custom Track
B
0.13425
Be(2)C
-0.50913
0.03348
CHP-134
-0.69357
0.05754
Kelly
-0.2508
0.15174
LAN6
-0.65431
-0.11161
NGP
-159.57
0.40582
Vi856
-134.309

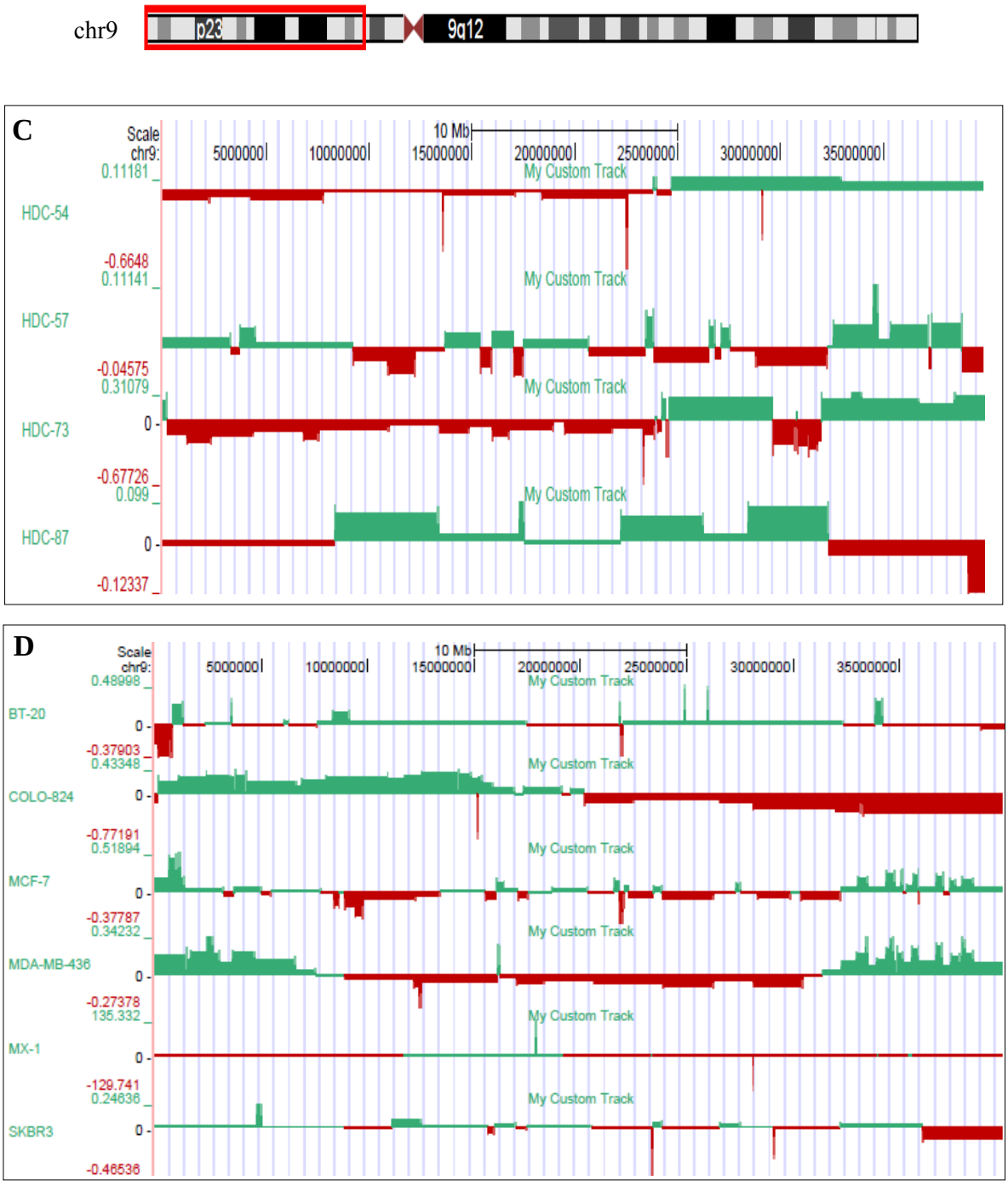

Figure 3-1. Copy number changes along the short arm of chromosome 9 in different cancer cell lines. On the very top is an ideogram of chromosome 9. The output data files from array CGH experiments of 9p arm are loaded in the database and copy number changes of individual cell line are displayed on each track. The x axis above the graphs represents position along the length of the chromosome in Mb scale. Chromosomal aberrations are shown as gain (green) and loss (red). Custom tracks for (A) glioma/GB, (B) NB, (C) CC, and (D) BC cell lines are displayed.

Figure 3-1.A displays the copy numbers along 9p in GB/glioma cells. All six cell lines show copy number changes on their 9p, including clusters of loss in a region located in between 20 to 25 Mb from telomere. In H4 cells, other regions of copy number loss were observed at 29, 16-17 and 10-12 Mbs. U138-MG cells also contained a region of loss at 28 Mb.

In NB cells (Fig. 3-1.B) different regions of losses were observed as well. All six NB cells shared a copy number loss in the sequence from 28 to 30 Mb. In Kelly, LAN-6 and Vi-856 there were also losses on distal 9p, at 10, 4 and 7 Mb, respectively.

Colon cell lines, HDC-54 and HDC-73, showed a large fragment of loss which started from approximately 24 Mb from telomere and extended to the distal end of 9p (Fig. 3-1.C). There were also homozygous copy losses within this large region of loss in these two cell lines. HDC-73 cells also showed a region of copy number loss spanning region of 29 to 31 Mb from telomere.

All six BC cells showed copy number changes, including losses and gains, on their 9p arm (Fig. 3-1.D). BT-20 cells had copy gains on very distal (locations 2 and 8 Mb) and proximal (point 34 Mb) 9p. COLO-824 cells had a large fragment of copy gain starting approximately 16 Mb from telomere extending all along 9p to the distal end. MX-1 cells had a gain region spanning from position 12 to 20 Mb from telomere.

Overall, the copy number profiles along 9p show an individual pattern of alterations in different tumor types. Furthermore, most of the copy numbers were losses rather than gains.

3.1.2 *FRA9G, CDKN2A* and *FRA9C* are breakpoint-clustering loci on 9p

High-resolution aCGH, allowed us to precisely define the location of overall breakpoints occurring along short arm of chromosome 9 and therefore to estimate the impact of a particular CFSs on genomic alterations along 9p. To achieve this, 29 cell lines from different types were applied, including 6 glioma/GB cell lines (A172, H4, Hs-683, U138-MH, U-373 MG and U-87 MG), 9 NB cell lines (SK-N-BE2C, SK-N-FI, SH-EP, HD-N-33, CHP-134, Kelly, LAN-6, NGP, Vi-856,), 5 CC (HDC-54, HDC-57, HDC-73, HDC-75, HDC-87) and 9 BC (BT-20, COLO-824, MCF-7, MDA-MB-436, MX-1, T47D, MX-1, MFM-223, SKBR3).

In glioma/GB cells (Fig. 3-2), the percentage of the breakpoints within *FRA9G* and *FRA9C* were 12% and 2.5%, respectively. Forty five percent of the total breakpoints were located in the region in between the two CFSs, and clustered within the *CDKN2A* locus.

In NB cells (Fig. 3-2), *FRA9C* contained a large cluster of the breakpoints within its sequence (38% of total breaks). *FRA9G* in NB cells comprised a tital of 10% of all breakpoints. The region in between the two CFSs in NB cells contained 27% of the breakpoint, from which almost all of them clustered in *CDKN2A* locus.

In CC, no breakpoints were detected within either *FRA9G* or *FRA9C*, and 37% of the breakages occurred in the region flanked by the two CFSs, forming a cluster on distal side of *CDKN2A* locus. Colon cancer presented less number of breakpoints along 9p, compared to the other three groups.

In BC, the percentage of the breaks within *FRA9G* and *FAR9C* were 5% and 4%, respectively. Only 16% of total breaks occurred in the region between the CFSs. Instead, three clusters of breakpoints were observed in these cells, one on proximal 9p (p13.3), one on central 9p (p22.3) and the other one on distal 9p (p24.4)

These results propose various non-random clusters of breakpoints along 9p of different tumor cell types. In glioma/GB cells, *FRA9G* and *CDKN2A* locus comprise majority of the breaks. In NB, regions spanning *CDKN2A* and *FRA9C* contain the clusters of breakpoints. In CC more than one third of the breaks occur between the two CFSs, nearby *CDKN2A* region. Breast cell lines show a more evenly distributed pattern of breakpoints, containing more than half of their breaks (56%) on distal part of 9p, whereas in glioma/GB, NB and CC, proximal 9p is the main target for breakages on 9p.

Altogether, these data demonstrate non-random involvement of *FRA9G*, and *FRA9C* in instability events on 9p of different tumor cells. While *FRA9G* is predominantly involved in glioma/GB rearrangements, *FRA9C* is the main target of genomic alterations in NB cells.

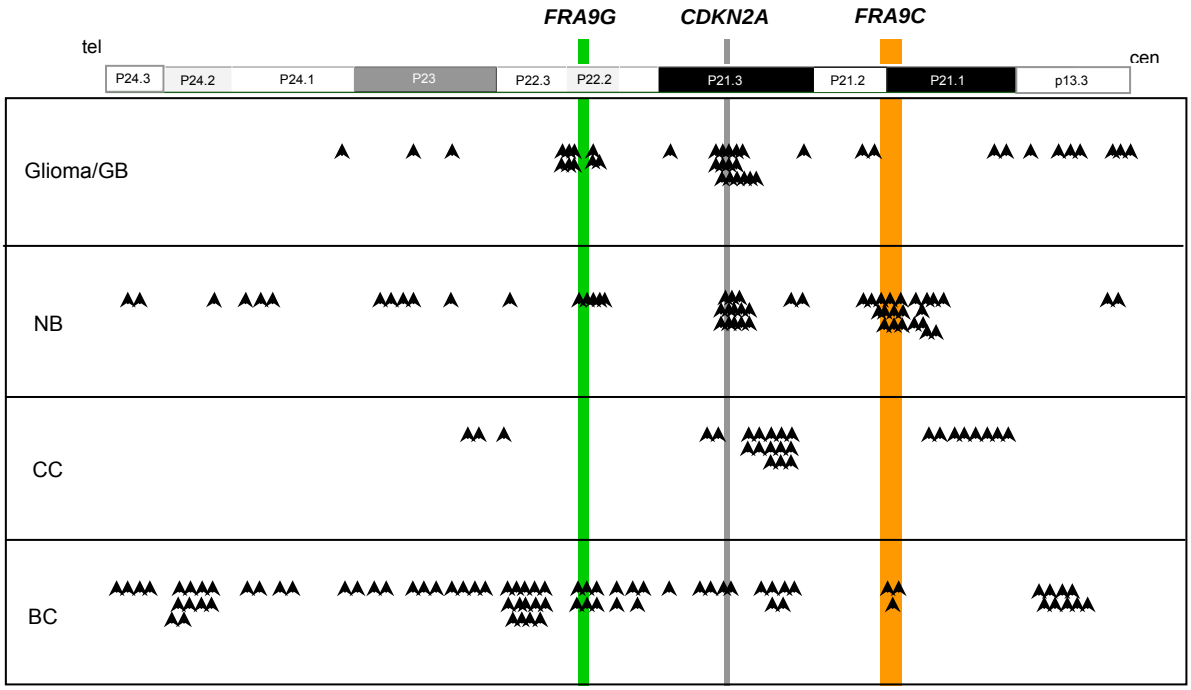

Figure 3-2. Schematic diagram for distribution of the breakpoints along 9p arm in four different tumor cell types. On top is the ideogram of the 9p arm. Location of *FRA9C*, *CDKN2A* and *FRA9C* loci are indicated by color bars. The arrows represent the precise location of each breakpoint observed in aCGH results. The percentages of the breakpoints on 9p within *FRA9G* and *FRA9C* are written next to their location. The percentage written in between *FRA9G* and *FRA9C* represents the breakpoints occurring in the region flanked by the two CFSs. In three tumor cell types, including glioma/glioblastoma, neuroblastoma and colon, the majority of the breakpoint occurs within *FRA9C*, *FRA9G* and the region in between the two CFSs. Only in breast cancer cells, more than half of the breakpoints present to be on distal 9p.

3.1.3 *FRA9G, CDKN2A* and *FRA9C* demonstrate multiple rearrangements within their sequence in tumor cells

To explore precisely the nature of genomic alterations occurring within the sequence of *FRA9G*, *CDKN2A* and *FRA9C*, aCGH data from the region spanning the three loci sequences and the 1 Mb regions flanking them were taken for analysis. High-resolution custom array allowed detecting copy number changes encompassing large genomic fragments, as well as micro-deletions and micro-duplications.

In addition, FISH validation was performed for some cases to confirm the rearrangements observed in array results.

3.1.3.1 *FRA9G*

Seven out of 29 cell lines presented rearrangements within their *FRA9G* sequence. These cells included one glioblastoma (U-373 MG), one glioma (H4), three NB (SK-N-BE(2)C), SK-N-FI, Vi-856), and two BC (MX-1, COLO-824). As examples, aCGH plots of four cell lines representing the genomic alteration in this region are shown in Figure 3-3.

H4 cells showed two breakpoints distal to *FRA9G*. This resulted to a deleted region of approximately 1 Mb (Fig. 3-3.A). In U-373 MG cells, two breakages distal to *FRA9G* were detedted, leading to the duplication of an approximately 500 kb fragment (Fig. 3-3.B). In SK-N-FI cells, four breakpoints were found within and flanking *FRA9G*, resulting to heterozygous deletion of two fragments of less than 1 Mb in size (Fig. 3-3.C). COLO-824 cells showed four breakpoints within *FRA9G* which led to two micro interstitial deletions within the CFS sequence (Fig. 3-3.D). Altogether, a combination of various rearrangements, including deletion and duplication of small or large fragments of chromosome, either within or in the vicinity of *FRA9G,* were observed in different tumors.

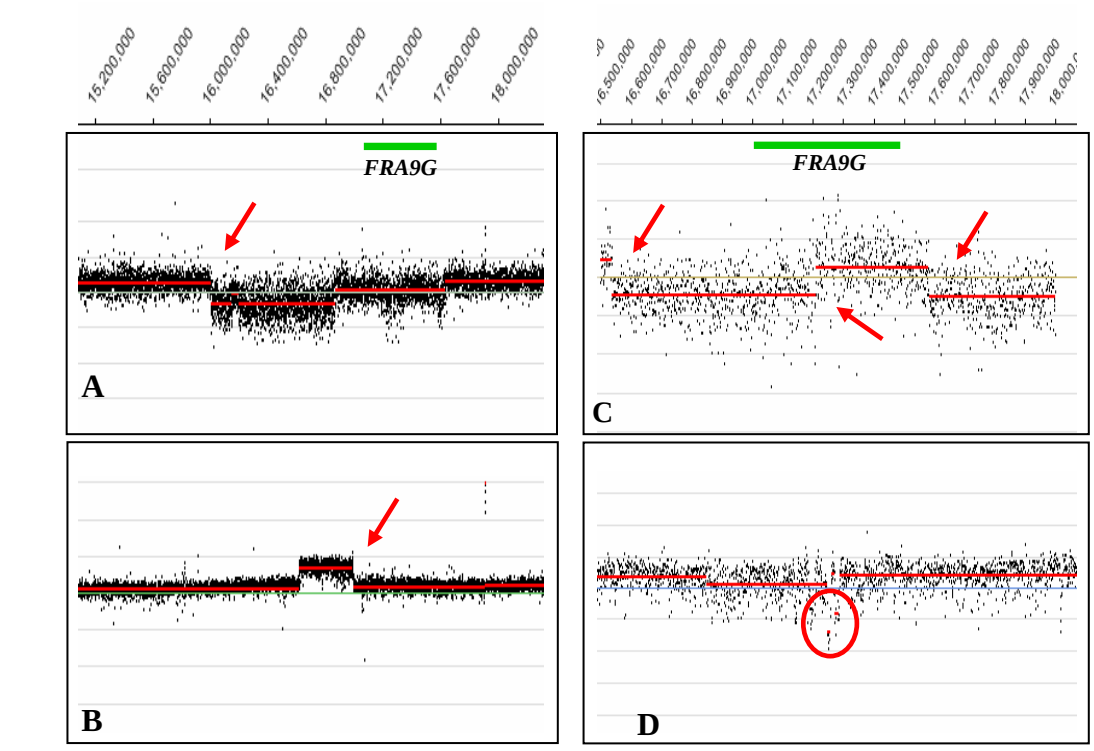

Figure 3-3 Array CGH plots representing rearrangements in *FRA9G* sequence in (A) H4, (B) U-373 MG, (C) SK-N-FI and (D) COLO-824. On top is the position along the length of chromosome 9. The green bar corresponds to the location of *FRA9C*. The red circle and arrows indicate the location of the deletion, duplication and breakage sites occurring within or in the vicinity of *FRA9G*.

3.1.3.2 *CDKN2A*

Fourteen out of 29 cell lines presented genomic alterations either within or in the vicinity of their *CDKN2A* locus. These cells include all the glioma/GB cells (A-172, U-87 MG, U-373 MG, U-138 MG, Hs-683, H4), five NB (LAN-6, SK-N-FI, SK-N-BE(2)C, SH-EP, Vi-856), one CC (HDC-54) and two BC (MCF-7, COLO-824). The aCGH plots of four cell lines in Figure 3-4 represent the arrangements observed within *CDKN2A* in the cells.

U-373 MG cells showed a micro-deletion in the *CDKN2A* gene (surrounded in red circle in Fig. 3-4 A), which occurred, in addition, within a larger deleted fragment in this region. In SH-EP cells, a similar pattern of a homozygous micro-deletion within a previously heterozygous deleted region was observed in a fragment that spanned over the *CDKN2A* locus, but the micro-deletion occurred not within, but distal to *CDKN2A* (Fig. 3-4 B). Moreover, there was a micro-deletion 444 kb proximal to *CDKN2A*. In MCF-7 cells, the occurrence of three breaks led to the deletion of a region that spanned over *CDKN2A* sequence (Fig. 3-4 C). In BT-20 cells, a 65-kb deletion spanned over the *CDKN2A* sequence (Fig. 3-4 D). A micro-duplication was also observed in these cells distal to *CDKN2A*.

Overall, more than half of all cell lines shows alterations in the region where *CDKN2A* is located. All the rearrangements in *CDKN2A* sequence were deletions.

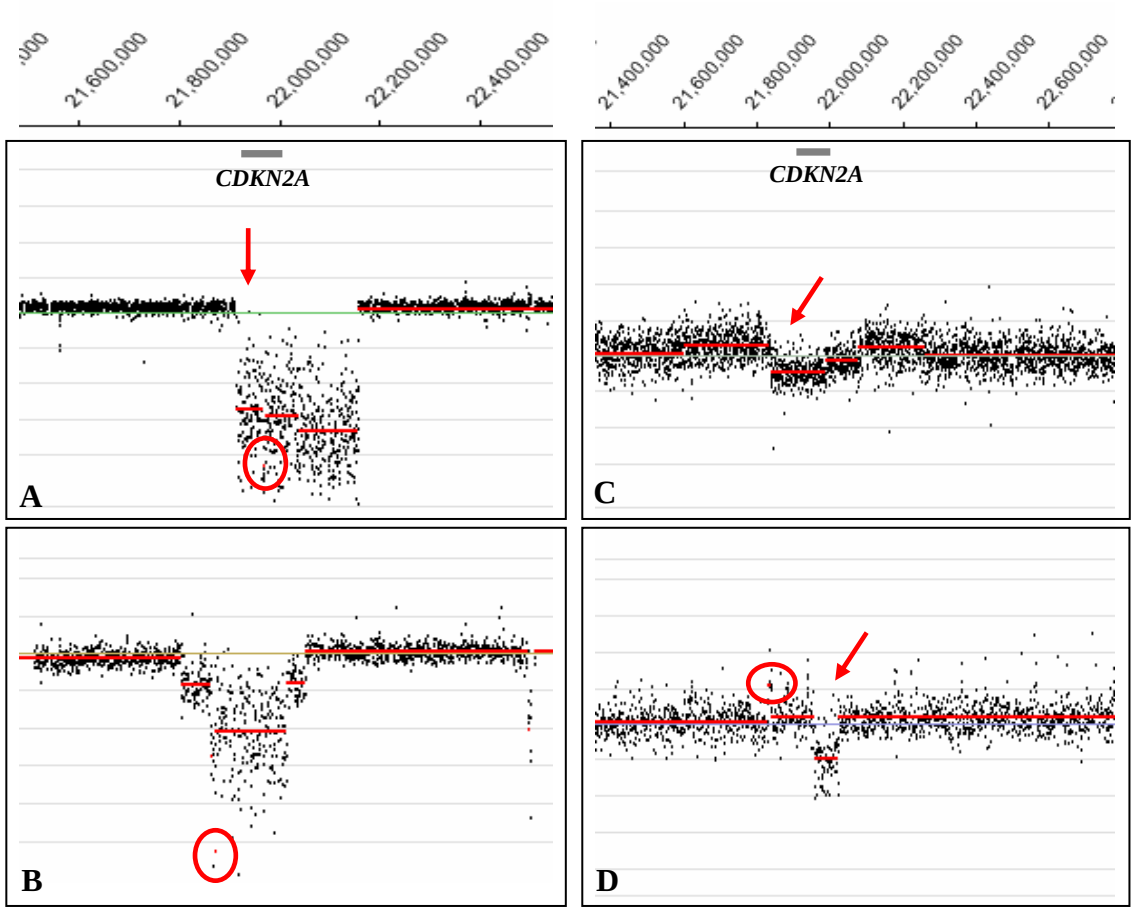

Figure 3-4 Array CGH plots representing rearrangements in *CDKN2A* sequence of (A) U-373 MG, (B) SH-EP, (C) MCF-7, (D) BT-20. On top is the position along the length of the chromosome 9. The gray bar corresponds to the location of *CDKN2A*. The red circle and arrows indicate the location of the deletion, duplication and breakage sites occurring within or in the vicinity of *CDKN2A*.

3.1.3.3 *FRA9C*

Out of 29 examined cell lines, 11 demonstrated genomic alterations within or in the vicinity of their *FRA9C* sequence. These cells included one glioblastoma (U-138 MG), six NB (LAN-6, Kelly, SK-N-FI, SK-N-BE(2)C, SH-EP, Vi-856), two CC (HDC-54, HDC-73) and two BC (MX-1 and COLO-824). Array plots for LAN-6, SH-EP, COLO-824 and Kelly are presented in Figure 3-5.

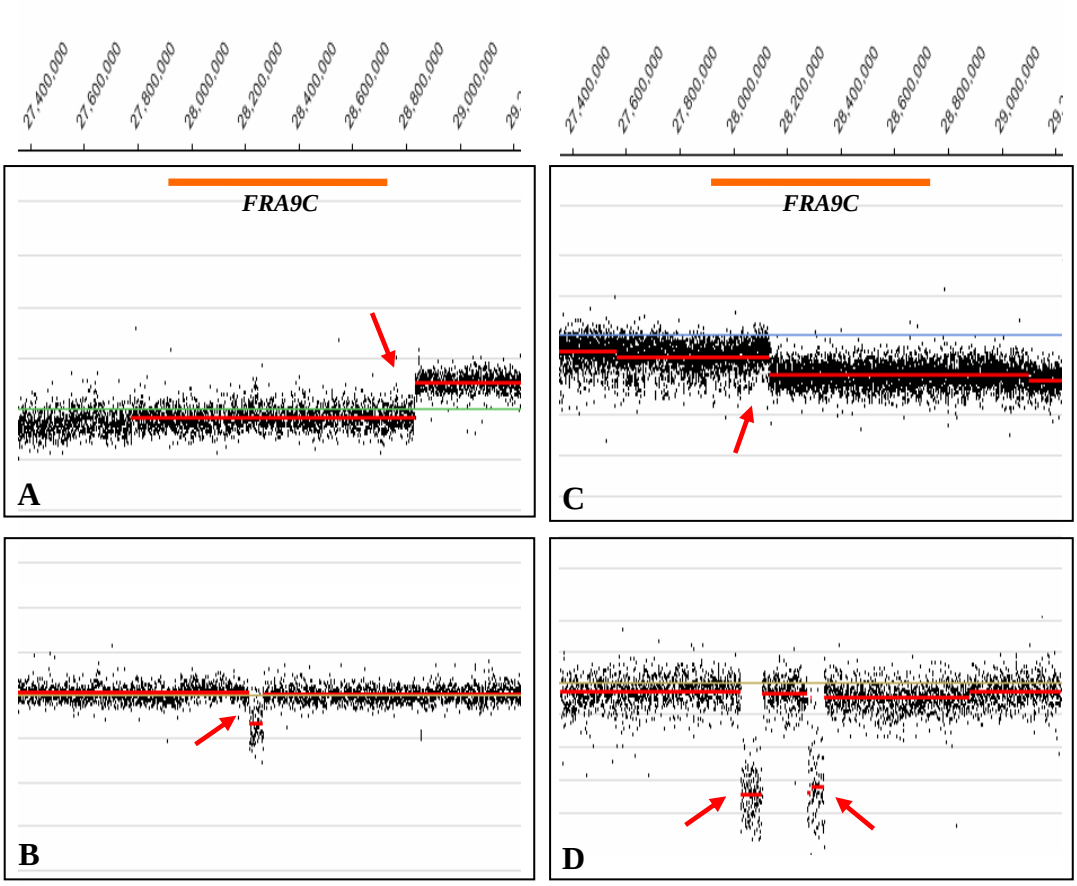

Figure 3-5 Array CGH plots representing rearrangements in *FRA9C* sequence of (A) LAN-6, (B) SH-EP, (C) COLO-824, (D) Kelly. On top is the position along the length of the chromosome 9. The orange bar corresponds to the location of *FRA9C*. The red arrows indicate the location of the deletion and break points occurring within or in the vicinity of *FRA9C*.

In LAN-6 (Fig. 3-5.A), a break occurred approximately 120 kb proximal to *FRA9C* and resulted into a heterozygous deletion which extended for almost 16 Mb to the distal end of 9p. SH-EP cells showed a 51 kb deletion within their *FRA9C* (Fig. 3-5.B). The deleted fragment seemed to be a heterozygous loss. In COLO-824 cells, a break occurred within *FRA9C*, which subsequently led to a duplicated fragment that extended over the distal side of the breakage and spanned the whole *FAR9G* sequence, as well (Fig. 3-5.C). In total, COLO-824 presented multiple and very complex rearrangements on the short arm of chromosome 9. Kelly cells showed rearrangements within *FRA9C* (Fig. 3-5.D). Two regions of loss were detected in this cell line, each to be 93 kb and 77 kb in size.

Together, analysis of *FRA9C* sequence revealed frequent occurrence of rearrangements within or in the vicinity of this region in different tumor cells.

3.1.3.3.1 Fluorescence *In situ* hybridization (FISH) confirms aCGH data

To validate aCGH findings, FISH analysis using BAC clones spanning the *FRA9C* region were performed on a number of cell lines that were earlier subjected to aCGH. BAC clones from RP11- library that was used for our *in situ* experiments are listed in the Table 3-1.

Table 3-1. List of the BAC clones with their chromosomal band location and corresponding locus

BAC clone	chromosomal location	Corresponding locus
RP11-29P12	9p21.1	*FRA9C*
RP11-30O14	9p21.1	*FRA9C*
RP11-29M23	9p21.1	*FRA9C*
RP11-159L16	9p21.1	*FRA9C*
RP11-450P11	9p21.1/21.2	*FRA9C/LINGO2*
RP11-83O12	9p21.2	*FRA9C/LINGO2*
RP11-438B23	9p21.2	*FRA9C/LINGO2*
RP11-421H8	9p13.3	-

LAN-6

Array data showed a breakage in the close proximal side of *FRA9C* which lresulted in the heterozygous deletion of the whole CFS sequence. To validate this observation, we applied BAC clones RP11-450P11 (Cy5-labeled) and RP11-159L16 (FITC-labeled) which corresponded to *FRA9C/LINGO2* and the centromeric adjacent region of the breakpoint, respectively. Heterozygous loss of green signal (FITC), shown in Figure 3-6, confirmed the deletion of *FRA9C* sequence.

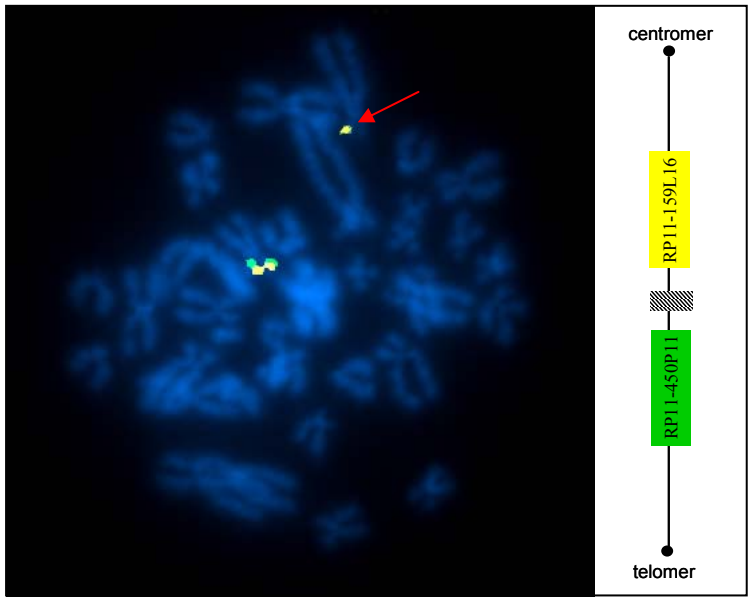

Figure 3-6. Fluorescence *In situ* confirmation of rearrangements in LAN-6 cells. The chromosomes were counterstained with DAPI. Two-color FISH for LAN-6 cells using BACs RP11-159L16 (yellow) and RP11-450P11 (green). Heterozygous deletion of the green signal (indicated by red arrow) corresponds to *FRA9/LINGO2* region.

COLO-824

Three BAC clones were applied for *in situ* hybridization in COLO-824 cell line. BACs RP11-438B23 and RP11-83O12 spanned within the *FRA9C*/*LINGO2* region and were labeled with Cy3 (red) and FITC (green), respectively. BAC clone RP11-30O14, which was the most centromeric to the other two, corresponded to a proximal adjacent sequence to *FRA9C* and was labeled with DEAC (purple). Figure 3-7 shows a duplicated signal for all the three BACs. This is in accordance to the previous M-FISH karyotyping data in our lab which showed that complex genomic rearrangements affect 9p and that there are four derivative chromosomes, with material of 9p in all analyzed metaphases of COLO-824 cells. In addition, one extra signal from BAC RP11-438B23 (red) was observed. These FISH results confirm the amplification events which were earlier detected in aCGH results.

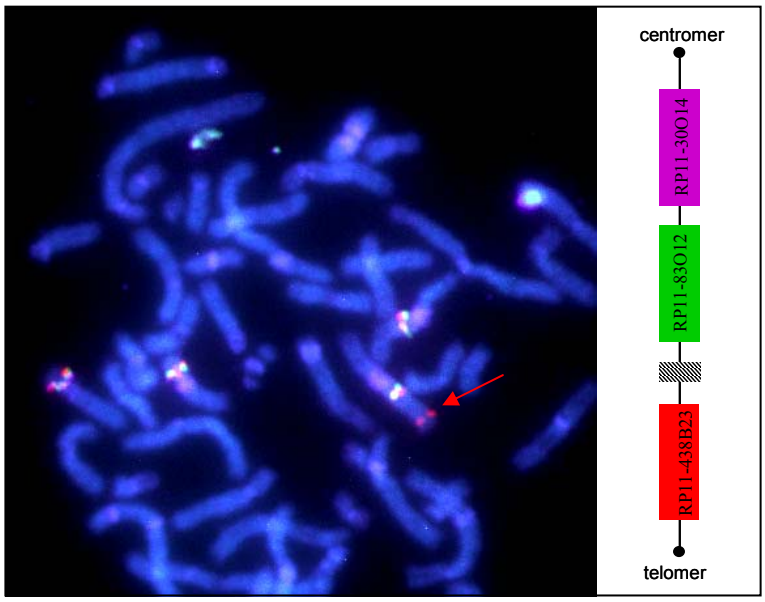

Figure 3-7. Fluorescence *In situ* confirmation of rearrangements in COLO-824 cells. The chromosomes were counterstained with DAPI. Three-color *in situ* hybridization performed using BACs spanning *FRA9C*/LINGO2 region revealed amplification of the signals from all the three BAC clones. BACs RP11-83O12 (green) and RP11-30O14 (purple) showed a duplication represented by four signals corresponding to a aneuploidy karyotype of this cells. There is one extra signal for BAC RP11-438B23 (red) which is indicated by red arrow.

HDC-73

In the aCGH analysis, a region of deletion proximal to *FRA9C* was detected in HDC-73 cells. To confirm this, three-color *in situ* hybridization was performed using BAC clones spanning from the distal to the proximal region of the deletion. BAC clones RP11-29P12 corresponding to the normal region distal to the deletion, and RP11-421H8 spanning a region proximal to the deletion were labeled with Cy3.5 (pink) and Cy5.5 (light blue) respectively. RP11-29M23, which was labeled with Cy5 (yellow), was used to represent the region of deletion. The FISH-mapping studies in our lab had already revealed a triploid karyotype for HDC-73 cells, and as is shown in Fig. 3-11.A, this phenomenon was observed for BACs RP11-421H8 and RP11-29P12. In two out of three spots, which are indicated by red arrows in Figure 3-8, the yellow signal from RP11-29M23 is missing. This confirms the loss of deleted region previously observed in the array data.

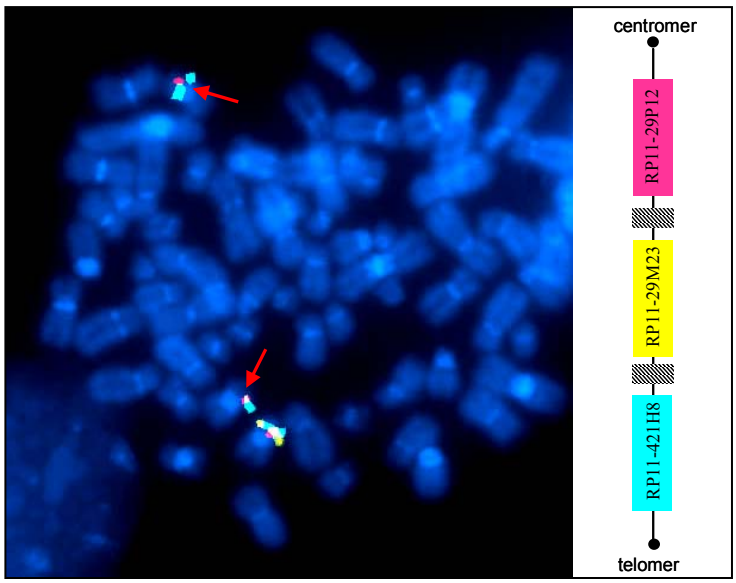

Figure 3-8 Fluorescence *In situ* confirmation of rearrangements in HDC-73 cells. The chromosomes were counterstained with DAPI. Three BACs including RP11-29P12 (pink), RP11-421H8 (light blue) and RP11-29M23 (yellow) were used on metaphases of HDC-73 cells. According to the triploid karyotype of HDC-73 cells, our analysis showed three spots containing pink and light blue colors representing RP11-29P12 and RP11-421H8, respectively. However, in two of three spots, the yellow signal of RP11-29M23 was missing. This is exactly corresponding to the region of deletion previously detected in array experiments.

3.1.4 Differentiated pattern of 9p rearrangements in four tumor types

3.1.4.1 Frequencies of involvement of target regions of 9p in chromosome alterations

Array CGH data for the group of 29 cell lines (6 glioma/GB, 9 NB, 9 BC and 5 CC) were quantified for rearrangements on their short arm of chromosome 9. Out of 29 cell lines, 22 (73%) demonstrated rearrangements on 9p. Glioma/GB cell lines showed the highest rate of aberrations on 9p, 100% (Fig. 3-9). The other three groups, including NB, CC and BC cells, each presented 9p aberrations with rates of 66%, 40%, and 66%, respectively.

FRA9G rearrangements were observed in all four types of cells which comprised of 26% of all the examined cells. *FRA9G* aberration rates in glioma/GB, NB, CC and BC cells was 33%, 33%, 0% and 22%, respectively. In 70% of the cells, the aberrations occurred within *FRA9G*.

CDKN2A showed to be a main target of rearrangements in all four types of cell lines. Among the 29 cells analyzed in aCGH experiments, 48% (14 out of 29) showed damage in p16. The

highest percentage was presented by glioma/GB cells, which was 100% (Fig. 3-9). NB cells also had a high damage in p16 gene (55%). Colon cell lines and BC displayed 20% and 11%, respectively.

FRA9C was rearranged in 40% of all the four types of cells examined. The total number of rearrangements in *FRA9C* in different groups was 16% (GB/G), 66% (NB), 40% (CC) and 22% (BC) (Fig. 3-9). From all the cells presenting rearrangements in the *FRA9C* region, two thirds (65%) of the damage occurred within the CFS. The rest showed aberrations in the vicinity of *FRA9C*.

Altogether, aCGH and FISH results indicate a frequent occurrence of rearrangements either within or in the vicinity of *CDKN2A* and the two CFSs (*FRA9G* and *FRA9C*), in various tumor types. In particular, *FRA9G* and *CDKN2A* in both glioma/GB and NB cells, and *FRA9C* in NB present a predominant involvement in genomic rearrangement. These rearrangements include both losses and gains, which vary in size from very small regions from a few kliobases to large fragments of several Mb from the chromosome.

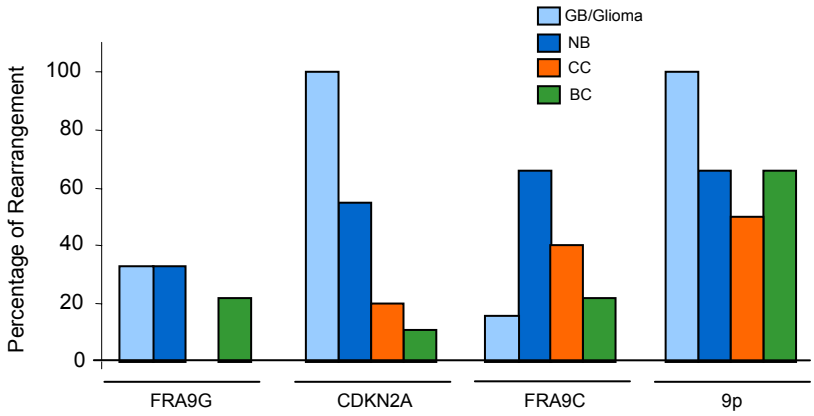

Figure 3-9. Percentage of overall rearrangements along entire 9p and also within or in the vicinity of *FRA9G*, *CDKN2A* and *FRA9C* in glioma/GB, NB, CC and BC cells. Y axis represents the percentage of rearrangements. The graph presents the data revealed by the custom aCGHs (with the resolution of 40 and 80 bp).

3.1.4.2 Large scale analysis of target regions of 9p

In order to have more accurate validation of the results obtained from the aCGH experiments, the same quantification analysis was further applied to a larger number of cell lines. Array CGH data, (with the resolution of 1 Mb) were retrieved from database (COSMIC project) and investigated for the overall rearrangements on total 9p, and *FRA9G, CDKN2A* and *FRA9C* in particular.

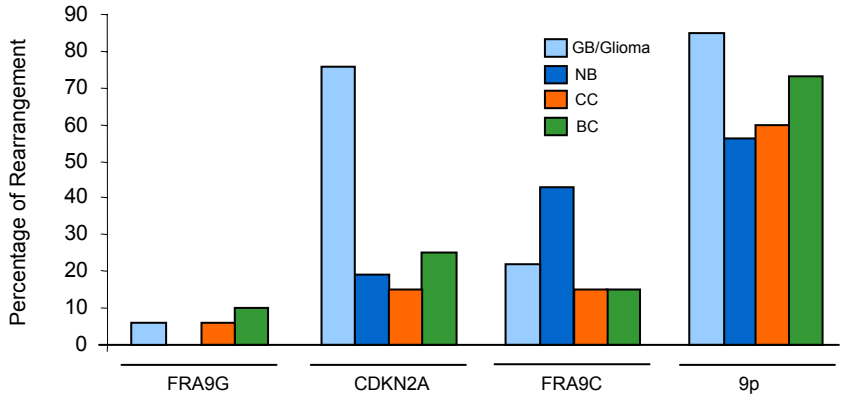

Figure 3-10. Percentage of overall rearrangements along entire 9p and also within or in the vicinity of the three cluster forming loci, *FRA9G, CDKN2A* and *FRA9C* in database aCGH experiments. Y axis represents the percentage of rearrangements. The graph displays percentage of rearrangements based on analysis of the aCGH results obtained from the database (group of 173 cell lines, with the resolution of 1 Mb).

A group of 173 cell lines, including 59 (glioma/GB), 37 (NB), 32 (CC) and 45 (BC) were obtained from the database and analyzed (Fig. 3-10). In 68% of all cell lines, rearrangements on 9p arm was observed. Almost 90% of the glioma/GB cells showed rearrangements on 9p. NB, CC and BC cells exhibited 9p rearrangement rates of 55%, 60% and 75%, respectively.

No rearrangements in *FRA9G* was observed in NB cells while glioma/GB, CC and BC cells presented 5%, 5% and 10% rearrangements, respectively.

As for *CDKN2A*, nearly 80% of glioma/GB cells showed deletion in *CDKN2A* locus. This number was 20% for NB, 15% for CC and 28% for BC cells.

FRA9C was rearranged in more than 40% of the NB cells, whereas this value was 25%, 15% and 15% for glioma/GB, BC and CC, respectively.

To sum up, applyin the analysis to the aCGH data of a larger number of cell lines (173) obtained from the database, presented a similar pattern for alteration in *FRA9G*, *CDKN2A* and *FRA9C*.

The differences seen in a few cases could be due to the lower resolution of the arrays used in producing the results of database, and therefore probably micro-deletion and duplications were not detected in those experiments.

3.1.4.1 Breakage at *FRA9C* coincides with deletion at *CDKN2A* locus

While analyzing rearrangements occurring in 9p, cell lines bearing rearrangements in both *FRA9C* and *CDKN2A* were observed. Upon close look on the mode of deletion in these two regions in a same cell line, we encountered samples in which a heterozygous deletion in *FRA9C* was extended to a homozygous deletion of *CDKN2A* gene (Fig. 3-11.A). In fact, it seems that this occurs in two steps in the region. In one step, a breakage ocurrs in the fragile site which makes a heterozygous deletion, and in the other step, occurrence of a breakage leads to the complete deletion of the gene locus on the chromosome.

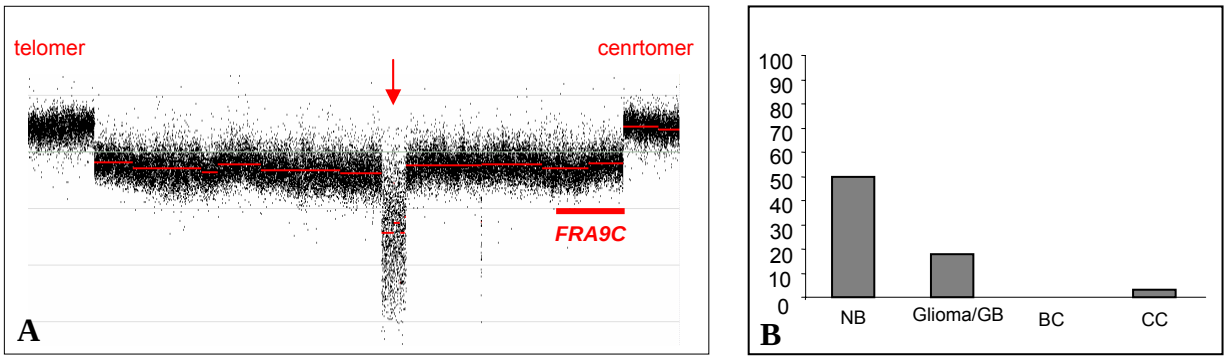

Fig 3-11. *FRA9C* involvement in *CDKN2A* deletion. (A) Shows the array CGH plot for LAN-6 cells. The heterozygous deletion of *FRA9C* which occurs due to a break within the fragile locus, led to a distal heterozygously deleted region on the distal side, in which a second hit of breakage events could lead to homozygous deletion of *CDKN2A* locus. (B) The graph presents the percentage of the different cancer cells (data obtained from the database) that demonstrated such a model for their *CDKN2A* deletions.

A larger number (173 cell lines) of array data from the database were explored in order to know if the examples observed in aCGH results were more than just a coincidence, and if so, how often they ocurr in cancer cells. The results are presented in Figure 3-11.B. In NB cells, half of the *CDKN2A* homozygous deletion cases were similar to the pattern observed earlier. In nearly 20% of the glioma/GB cells, deletion of *CDKN2A* was derived directly from breakage in

FRA9C, too. In CC and BC, there was either very little (3%) or no occurrence of this phenomenon, respectively.
Collectively, our observations indicate an active role of *FRA9C* in homozygous deletion of *CDKN2A* locus in NB cells.

3.2 Identification of cancer susceptibility candidate genes on 9p; CFS genes as novel candidates

To explore tumor-associated susceptible loci along 9p, a total of thirty cell lines (grouped in four types, including NB, glioma/GB, CC and BC) were inspected for the chromosomal aberrations within the genes located on 9p.
To achieve this aim, genes that (according to their aCGH results) showed breakpoints or regions of losses/gains either within or in the vicinity of their sequence were considered to be affected. Then, genes presenting genomic alteration in more than one cell line were taken into consideration. Genes that are only altered in one cell line were excluded. The results of the evaluation are summarized in a schematic diagram in Figure 3-12.
From total gene alterations considered for all the cell lines, 70% of them occurred in the region between *FRA9C* and *FRA9G*. This rate was 75% and 87% for neuroblastoma and glioma/GB cell lines. There were few numbers of alterations on 9p of colon cell lines, from which almost all of them occurred between the two fragile sites. Breast cell lines showed the most scattered pattern of alteration points, presenting less than half of them in between *FRA9G* and *FRA9C*. Genes residing in this region which showed highest occurrence of aberrations included, *MTAP/CDKN2A, LINGO2, BNC2, IFN* gene cluster, *CNTLN* and *ELAVL2*, respectively.
Furthermore, each group of cell lines was separately investigated for the specific genes as the target for aberrations. *LINGO2* showed to be altered in almost 66% of all the NB cell lines. This score comprised 45% 33% and 33% of NB cells for *MTAP/CDKN2A*, *CNTLN* and *BNC2*, respectively. In GB/Glioma cell lines, *MTAP/CDKN2A* and *IFN* gene cluster presented highest range of alteration, 100% and 85%, respectively. In addition, alterations in *ELAVL2* gene was observed in half of the glioma/GB cell lines.

Collectively, our analyses propose that the proximal part of 9p, specifically the region lying in between the two fragile sites, is a hotspot for gene alterations in cancer cells. Genes located in this region, including, *ELAVL2*, *CDKN2A*, *MTAP*, *INF* gene cluster and *BNC2*, which are known to have critical functions in different biological processes, presented high levels of damage in various tumor cells. This suggests that these genes may be candidates for tumor-susceptibility loci on 9p. However, not all of these genes are contributing the same level of rearrangements in different cell types. *CDKN2A*, *MTAP* and *INF* gene cluster appear to be mostly deleted in NB and glioma/GB cells, whereas *ELAVL2* shows to be more involved in glioma/GB cells. And *BNC2* gene damage is more highlighted in NB cells.

Furthermore, based on the results in this study, it is suggested that CFS genes of this region, including *CNTLN* and *LINGO2*, as new candidate tumor-susceptibility genes on 9p in NB and GB/Glioma. The significance of *FRA9G/CNTLN* and *FRA9C/LINGO2* loci in 9p rearrangement events attracts more consideration when their damage frequency is compared to that of *CDKN2A/p16* locus, which has been long been reported in literature as a main target of rearrangement events in various tumors. As is presented in Table 3-2, *FRA9G* and *FRA9C* show 15% damage when calculated in all cell lines together, and considering the length of the two CFSs which comprise less than 3% of whole 9p, we propose that *FRA9G/CNTLN* and *FRA9C/LINGO2* not only play an important role in rendering instability on 9p, but are also frequent targets of such instabilities in the region.

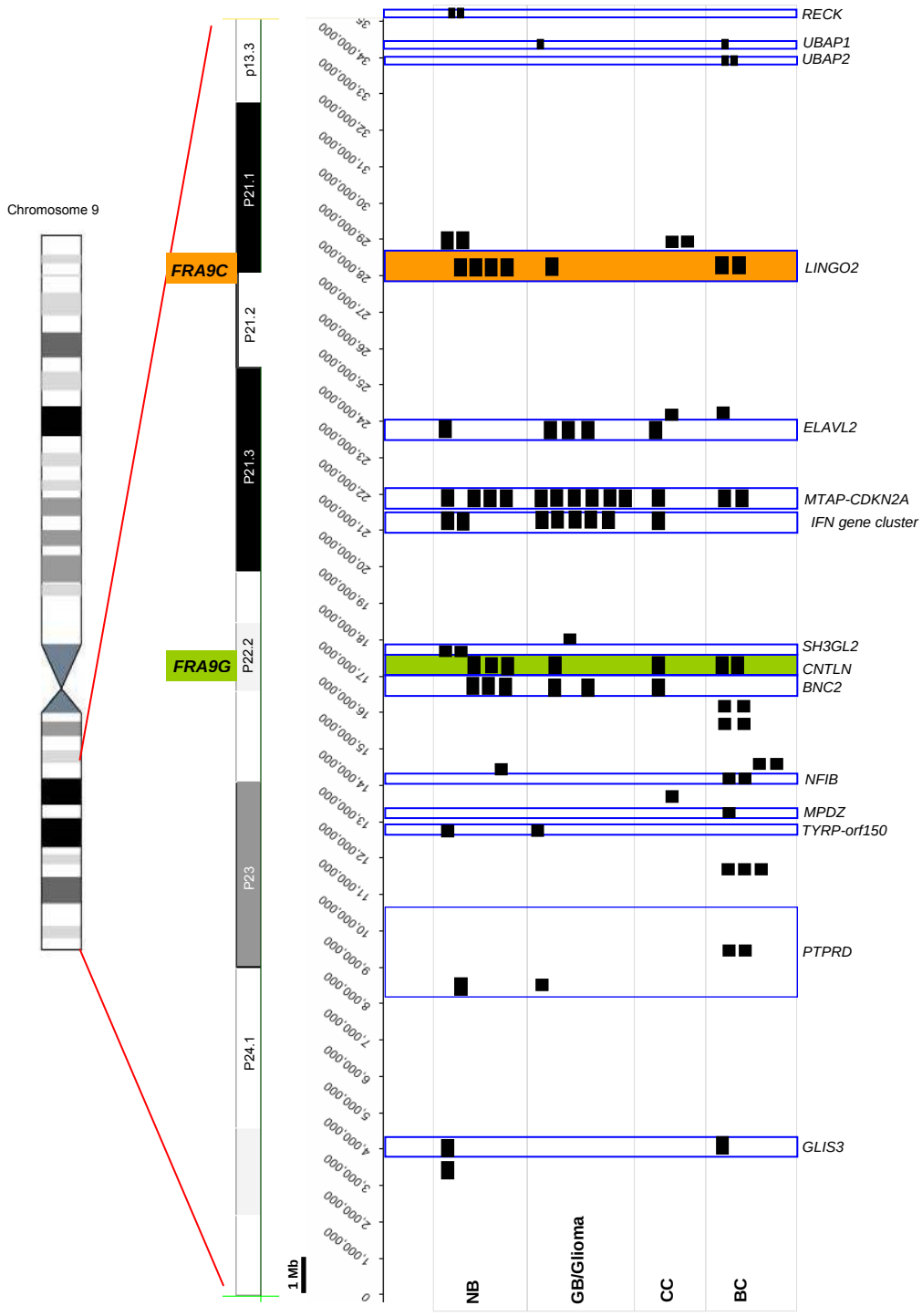

Figure 3-12. Schematic map for distribution of damaged genes along 9p in 29 cell lines of four tumor types. On the left is the ideogram of chromosome 9, ideogram of 9p arm and positions along the length of 9p are presented, respectively. Only genes that showed to be damaged in more than one cell line were taken into this map. Each cube represents the damage of the related gene in an individual cell line. The region flanked by *FRA9G* and *FRA9C* shows to have the most affected genes within it. *FRA9G* and *FRA9C* related genes, as well, are highly damaged in NB and glioma/GB cells.

	FRA9G	*FRA9C*	*CDKN2A*
Glioma/GB			
H4			
U-87 MG			
Hs-683			
U-373 MG			
A-172			
U-138 MG			
Neuroblastoma			
LAN-6			
Kelly			
NGP			
CHP-134			
SK-N-BE(2)C			
SK-NF-I			
HD-N-33			
SHEP			
Vi-856			
Colon Cancer			
HDC-54			
HDC-73			
HDC-87			
HDC-75			
HDC-57			
Breast Cancer			
COLO-824			
BT-20			
BT-474			
MX-1			
T47D			
SKBR3			
MDA-MB-436			
MFM-223			
MCF-7			

Table 3-2. Twenty nine cell lines tested for 9p rearrangements using aCGH-based analysis, presented by the frequency of rearrangements in three loci, including *FRA9G*, *FRA9C* and *CDKN2A*. Red boxes indicate the damaged sequence of each locus in individual cell lines. Comparison of the number of damage in *CDKN2A* locus, as a well-known frequent target for genetic alteration, to that of *FRA9G* and *FRA9C* suggests these two CFSs as novel candidate tumor-susceptibility loci in different tumor cells.

3.2 Sequence analysis of unstable regions of 9p

Since it has been proposed that DNA sequences within CFSs could count for the reason of fragility observed in their region, we analyzed the DNA sequence of the three breakpoint-clustering regions which were already identified in our aCGH results.

3.3.1. DNA repeat composition and flexibility

Earlier, three regions of breakpoint clusters, including *FRA9G*, *CDKN2A* locus and *FRA9C* were shown to contain the majority of breakpoints within or nearby their sequence. To analyze the DNA sequence of those regions for their DNA repeat composition and flexibility, the 1 Mb cores of the clusters, as well as their centromeric and telomeric flanking regions of the same size, were taken and subjected to RepeatMasker and TwistFlex programs.

The total DNA repeats that were analyzed for the three clusters of breakpoints were composed of MIR (1.9%, 3.5%, 3.6%), ALU (5.2%, 4,6%, 3,6), LINE1 (17.1%, 25.3%, 17.3%), LINE2 (2.7%, 3.8%, 3.7%), LTR (6%, 10.1%, 6.4%) and DNA elements (3.6%, 2.7%, 3%) for *FRA9G*, *CDKN2A* and *FRA9C* regions, respectively (Fig. 3-13.A). The CG content of the unstable regions showed similar ranges to the non-fragile genome. For *FRA9G*, *CDKN2A*, *FRA9C* and non-fragile regions, 38.3%, 38.1%, 36% and 38% CG content was obtained, respectively.

The comparison of DNA repeat elements in the three clusters of breakpoints did not show a significant difference between the core regions and their flanking sequences and also the non-fragile genome.

Then, DNA helix flexibility in breakpoint-clustering regions was calculated. The outcome revealed an average of 3, 6.5 and 7.5 flexibility peaks per 100 kb for *FRA9G*, *CDKN2A* and *FRA9C*-containing clusters, respectively. Non-fragile genome showed approximately 4 Flex peaks per 100 kb (Fig. 3-13.B).

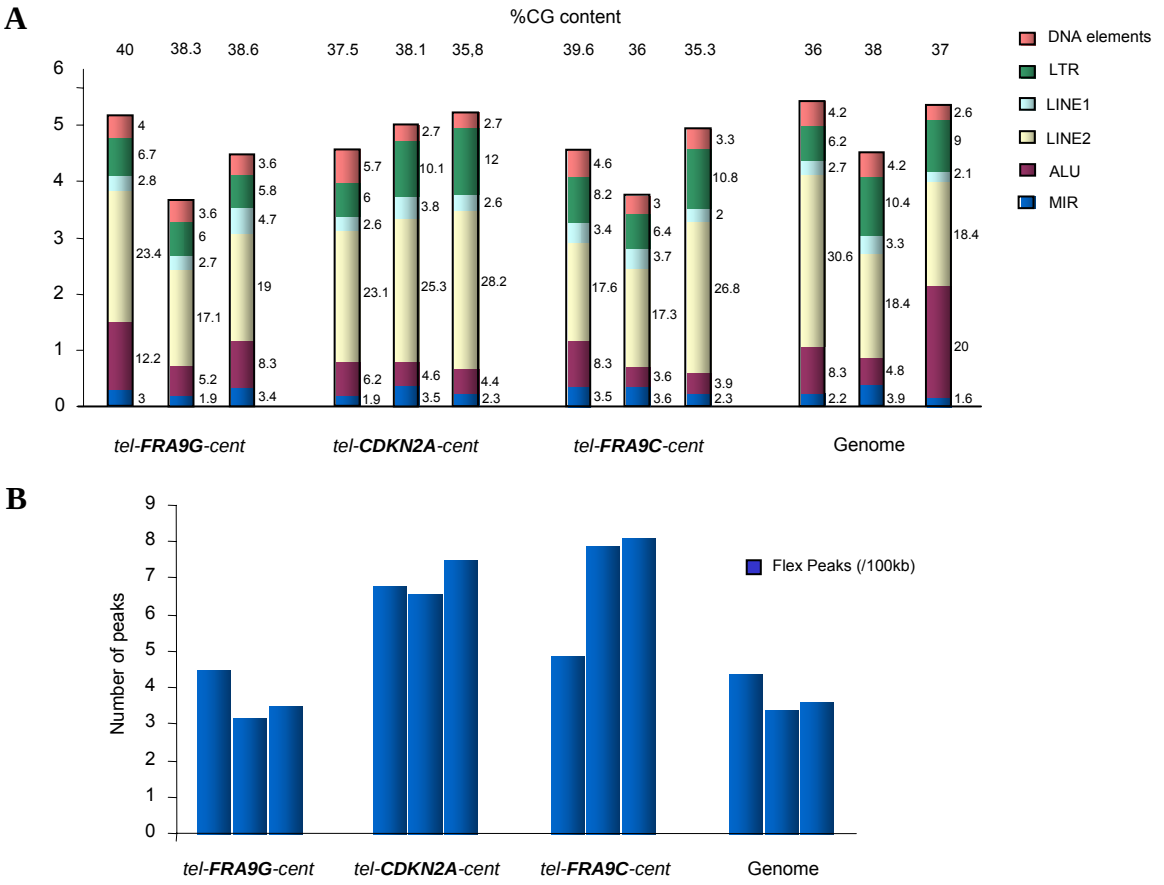

Figure 3-13. DNA sequence analysis of three breakpoint-clustering regions on 9p. Each cluster was divided into three regions of 1 Mb in size and named after the core region of instability within them, including *FRA9G*, *CDKN2A* and *FRA9C*. The analysis was done separately for the 1 Mb core sequence and its 1 Mb flanking sequences. (A) Shows the repeat composition of the 1 Mb-sequence in the core of each cluster, as well as 1 Mb flanking sequences of each cluster ("tel" for telomeric side and "cent" for centromeric side), compared to that of non-fragile regions of the human genome. X axis represents the percentage of each element. On the top, the percentage of CG content for each group is indicated. No significant differences were observed between and within the four groups of sequences. (B) The number of flexibility peaks within the three breakpoint-clustering regions and human genome. *FRA9C* and *CDKN2A*-containing regions presented higher number of peaks compared to *FRA9G* and human genome**.**

The 1Mb-sequence of each breakpoint clustering region was studied more closely as windows of 100 kb in size. In all the three clustering regions, there was one single 100 kb window that contained the majority of the breakpoints in that region. In addition, a window of region-of-no-flexibility peaks was identified that had no breaks within its sequence. All the four 100 kb sequences (three from breakpoint clusters and one from the window of no breaks) were picked up and subjected to repeat elements analysis.

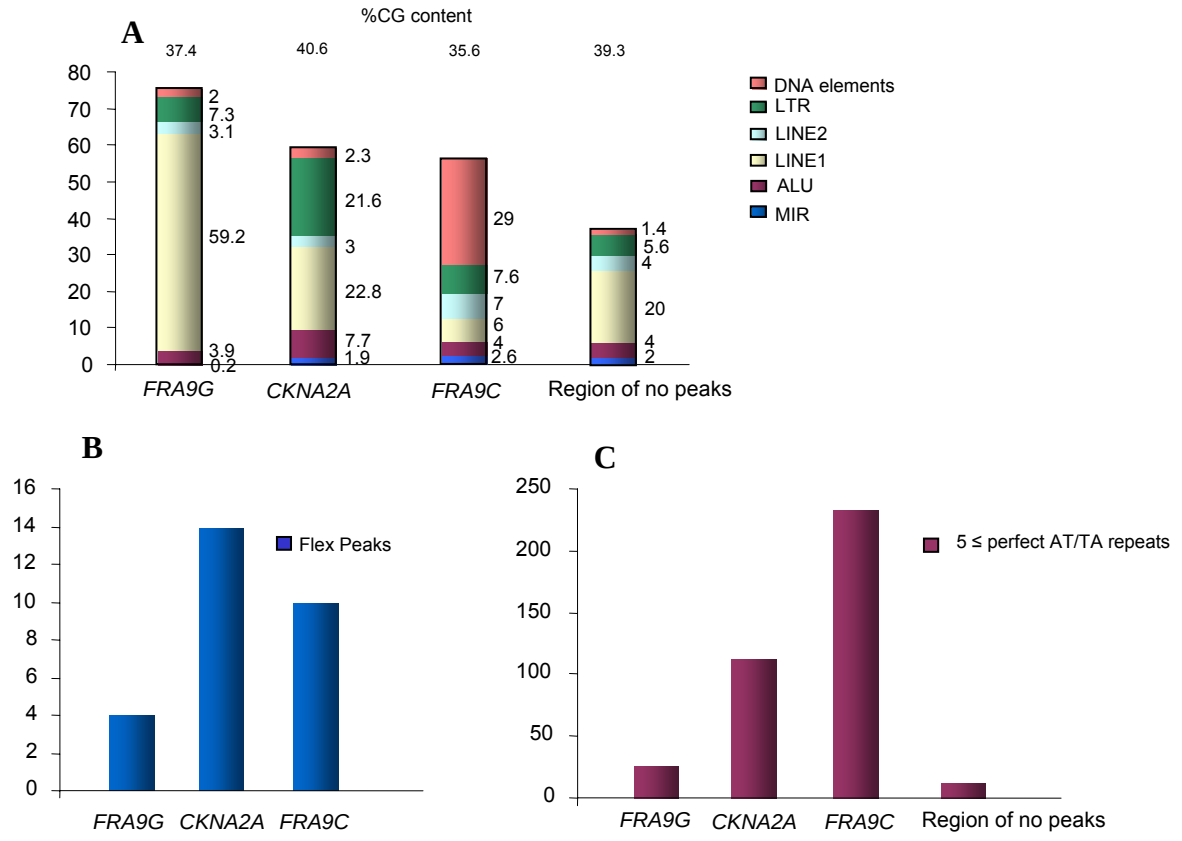

Figure 3-14. DNA sequence analysis of the 100 kb windows within the breakpoint clusters. These 100 kb windows of *FRA9G*, *CDKN2A* and *FRA9C* showed to have the majority of the breakpoints within the clusters. The region of no peaks was a 100 kb window within which no breakpoints or flexibility peaks were observed. Comparison of (A) DNA repeats composition, (B) number of flexibility peaks and (C) number of equal or more than 5 perfect AT/TA repeats of the described windows are displayed. (A) Except from LINE1 elements in *FRA9G* window, and DNA elements in *FRA9C* window, no other distinct features were observed in different regions. (B) Number of flexibility peaks in *CDKN2A* and *FRA9C* showed higher rates than proposed for CFSs average, which is said to be 5. (C) Number of equal or more than 5 perfect AT/TA repeats was also much higher in *CDKN2A* and *FRA9C* window, compared to that of *FRA9G* and region of no peaks.

The results for *FRA9G*, *CDKN2A*, *FRA9C* windows and the window of no FlexPeaks were MIR (0.2%, 1.9%, 2.6%, 2%), ALU (3.9%, 7.7%, 4%, 4%), LIINE1 (59.2%, 22.8%, 6%, 20%), LINE2 (3.1%, 3%, 7%, 4%), LTR (7.3%, 21.6%, 7.6%, 5.6%) and DNA elements (2%, 2.3%, 29%, 1.4%), respectively (Fig. 3-14.A). The 100 kb-window within *FRA9G* revealed almost threefold LINE1 elements content compared to the other three windows. DNA elements content in *FRA9C* window was relatively higher compared to the *FRA9G* and *CDKN2A* windows and also the single non-fragile genome sequences. Other repeat elements showed varied rates in

different sequences and no significant differences among them were observed. In addition, The CG content of the four windows did not present to be a significant feature (Fig. 3-14.A).
The helix flexibility content of the 100 kb windows of *FRA9G*, *CDKN2A* and *FRA9C* was explored and the results showed 4, 14 and 10 flexibility peaks for each of them, respectively (Fig. 3-14.B). The number of peaks in *CDKN2A* and *FRA9C* windows was even much higher than the average that has been proposed for aphidicolin-induced common fragile sites (5 peaks per 100kb). This indicates that helix flexibility is an important element in the fragility of the *CDKN2A* and *FRA9C* regions.
High number of flexibility peaks influences chromatin condensation process and increases the susceptibility to fragility. Moreover, it has been suggested that AT/TA perfect repeats within a fragile site can efficiently stall the replication fork and consequently result in instability. Comparison the frequency of equal or more than 5 perfect AT/TA repeats in the three regions of breakpoint cluster and the single region of no breaks and FlexPeaks, revealed recurrent repeats within *CDKN2A* and *FRA9C* –located region (Fig. 3-17.C). The high number of flexibility peaks and AT/TA perfect repeats in these two regions may be of critical importance in the instability observed within them. Whereas, both FlexPeaks and AT/TA perfect repeats within *FRA9G*-located region present much less degrees than that of other two fragile regions, they are relatively similar to what is observed in the non-fragile sequence.

In conclusion, DNA sequence analysis revealed a variation in DNA repeat composition of less stable regions, among the unstable regions of 9p and also between them and their flanking sequence. This did not give any clue to the nature of their susceptibility to breakages. Only regarding flexibility peaks, clusters in the region spanning *FRA9C* and *CDKN2A* presented a higher number of peaks in comparison to *FRA9G* and human genome.

3.3.2 Segmental duplication (SD) and copy number variation (CNV)

The segmental duplications, which might range from only a few to hundreds of kilobases, share a high degree of sequence identity and have been associated to chromosomal rearrangements in recent primate evolution and instability in human carcinoma cells. In order to estimate the SD content of the region of high instability on 9p and to estimate SDs involvement in rearrangements on 9p, distribution of segmental duplications (SDs) along the proximal 9p

region which spanned over the three breakpoint clusters was analyzed based on UCSC genome database (Fig. 3-15). A high content of SDs within *FRA9C/LINGO2* locus, as well as in a telomeric vicinity of *CKNA2A*, where *IFN* gene cluster resides was observed.
A cluster of copy number variation was also observed within *FRA9C* sequence.

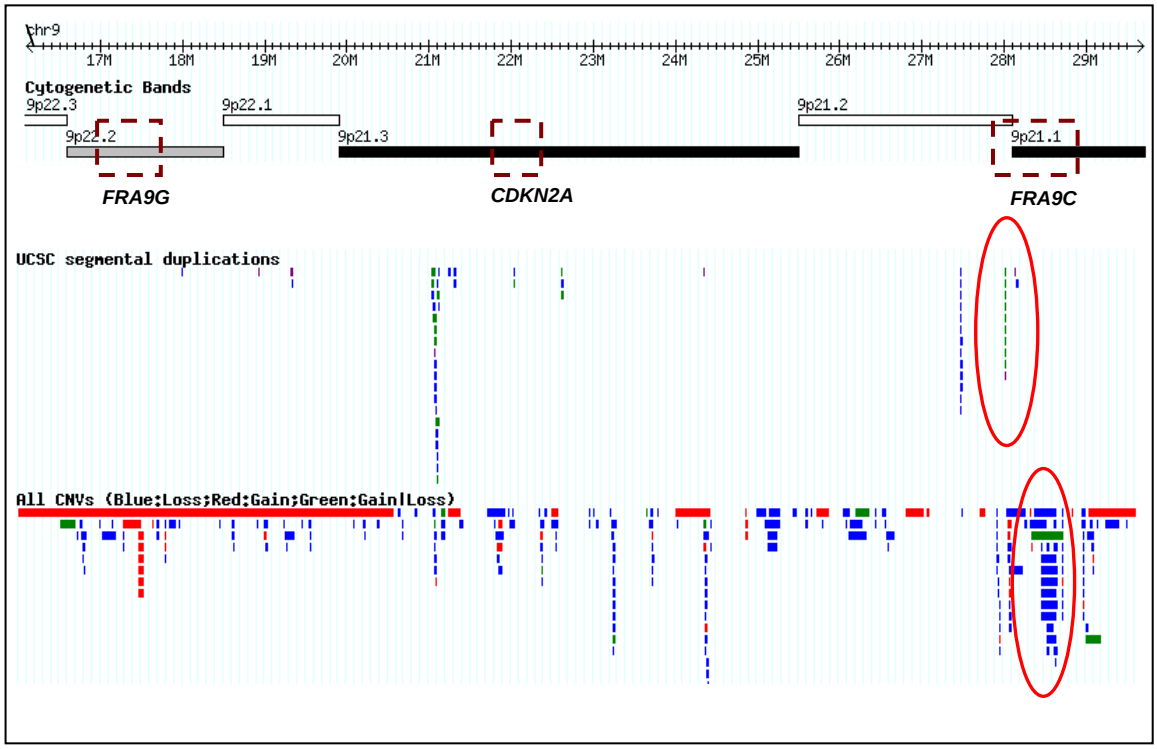

Figure 3-15. Distribution of segmental duplications (SDs) along the region of 9p of which clusters of breakpoints locate. A high content of SDs is observed within and in the vicinity of *FRA9C* and *CDKN2A* loci. In the lower track, where CNVs along the region are displayed, there is also a population of CNVs for *FRA9C* locus.

SDs analysis suggests that a high number of SDs within or in the vicinity of *FRA9C* and *IFN* gene cluster might be associated to the high frequency of instability observed in this region of various tumor cells.

3.4 Fragile site genes expression analysis

Since *FRA9G/CNTLN* and *FRA9C/LINGO2* loci demonstrate to be hot spots for genomic rearrangement events, one could envisage an important functional role for the genes located in these loci in normal and malignant cell procedures. Therefore, as the first step in characterizing their function, we explored expression of CFS genes, *CNTLN* and *LINGO2* in normal and tumor cells.

3.4.1 *FRA9G/CNTLN* expression; ubiquitous in normal cells, differentiated in tumor cells

The expression of *CNTLN* was examined in various human tissues and cell lines. Reverse transcriptase-PCR analysis in twenty one tissues demonstrated that *CNTLN* was expressed in all human tissues including adipose, trachea, bladder, brain, cervix, colon, esophagus, heart, kidney, liver, lung, ovary, placenta, skeletal muscle, small intestine, spleen, testes, thymus, thyroid and breast (Fig. 3-16.A).

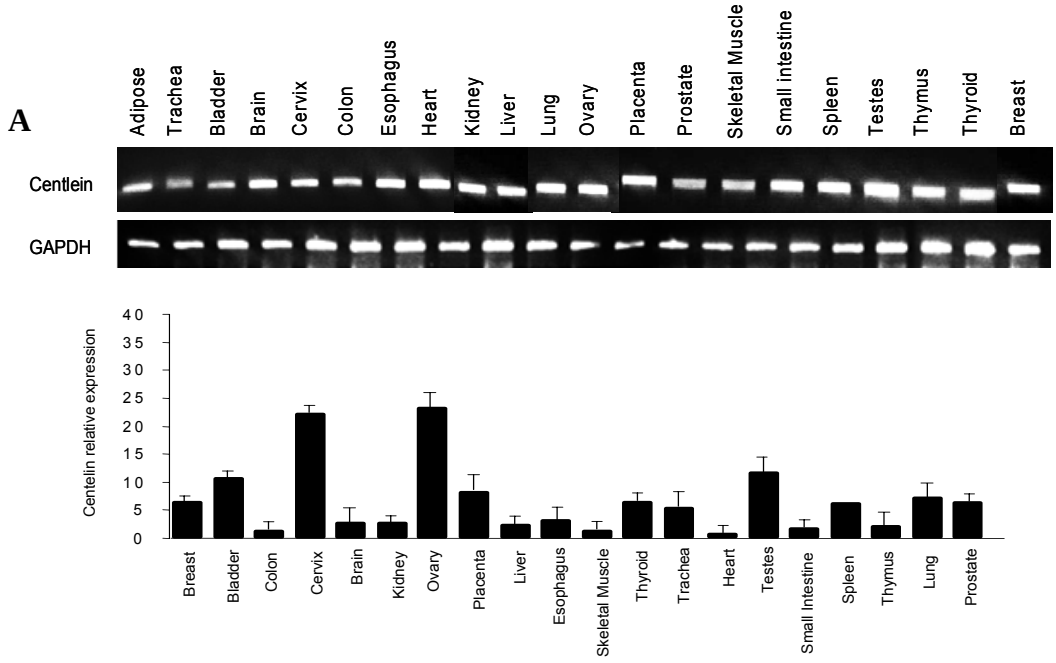

Figure 3-16. mRNA expression analysis for CFS gene *CNTLN*. (A) Shows the ubiquitous expression of *CNTLN* mRNA in human normal tissues. (B) Presents the quantification of *CNTLN* expression, in which normal ovary and cervix cells showed highest level of mRNA expression in normal human tissues.

In addition, real-time quantitative PCR experiments showed ovary and cervix to have the highest mRNA expression of *CNTLN* among normal human tissues (Fig.3-19.B).

Expression of *CNTLN* was further investigated in human cancer cell lines. *CNTLN* expression was detected in seven out of the nine BC cell lines, including MX-1, T47D, BT-20, MDA-MB-436, BT-474, SKBR3, and MCF-7 (Fig. 3-17.A). No *CNTLN* expression was observed in COLO-824 and MFM-223. Moreover, *CNTLN* was expressed in most of the glioma/GB cell lines examined in this study, including H4, Hs-683, A-172, U-138, and U-87 (Fig.3-17.B). *CNTLN* expression was not detected in U-373.

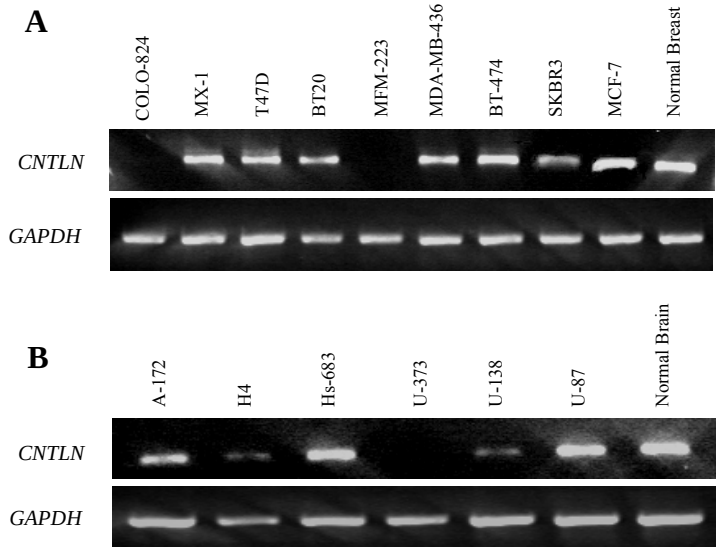

Figure 3-17. *CNTLN* expression analysis in tumor cells, (A) breast cell lines and (B) Glioma/glioblastoma cell lines. RT-PCR results showed differential expression of *CNTLN* in these cells.

These results indicate that *CNTLN* is ubiquitously expressed in human normal tissues. Moreover, differential expression of *CNTLN* in the cell lines implies aberration of this gene in some cancer cells. Such aberrations could be due to structural changes which were also earlier detected in the aCGH results.

3.4.2 *FRA9C/LINGO2* expression; differential in normal and tumor cells

LINGO2 expression in a range of normal human tissues was investigated. Expression of *LINGO2* was observed in a few tissues, including brain, kidney ovary, placenta, prostate and testes (Fig. 3-18).

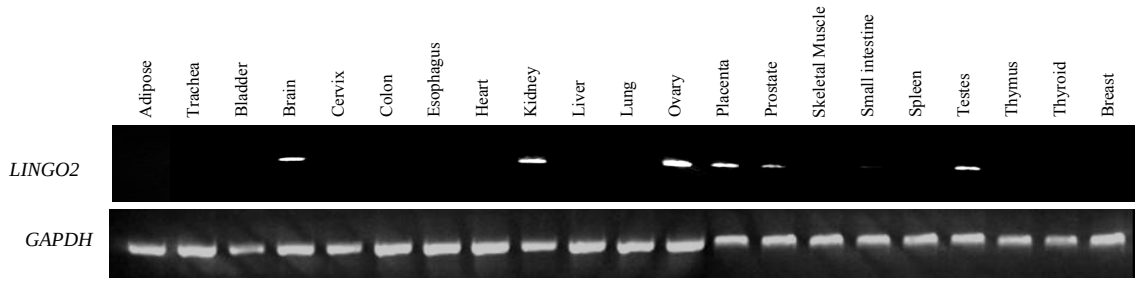

Figure 3-18. *LINGO2* expression in normal human tissues. RT-PCR results showed a differential expression of *LINGO2* in a few number of normal tissues.

As brain tissue was among the few tissues showing *LINGO2* expression, the probable disturbance of the gene expression in brain associated cell lines (glioma/glioblastoma) was investigated. One glioma (Hs683) and one glioblastoma cell line (U-138) did not reveal *LINGO2* expression (Fig. 3-19 A). To explore whether epigenetic silencing via methylation is the cause of expression inhibition in these two cell lines, *LINGO2* expression was examined before and after cell treatment with 5-azacytidin. *LINGO2* expression was reversed in Hs-683 cells after methylation inhibition, whereas U-138 still showed no expression (Fig. 3-19 A). This observation is in accordance with the data achieved for U-138 in aCGH experiments earlier. In addition, *In situ* hybridization was performed to confirm the integrity of *LINGO2* gene locus in Hs-683, and to prove the genomic aberration in U-138. BAC clones RP11-264J11 and RP11-123J20 covering *LINGO2* and *CNTLN* regions respectively, were applied and the expected duplicate signal of both BAC clones were observed in Hs-683 cells , whereas the signal from BAC RP11-264J11, which locates within the rearranged sequence in U-138 cells was missing (Fig. 3-19 B). The lack of purple signals form BAC RP11-264J11 in U-138 cells is an indication of rearrangements in *LINGO2* sequence and could explain the lack of *LINGO2* expression observed in these cells.

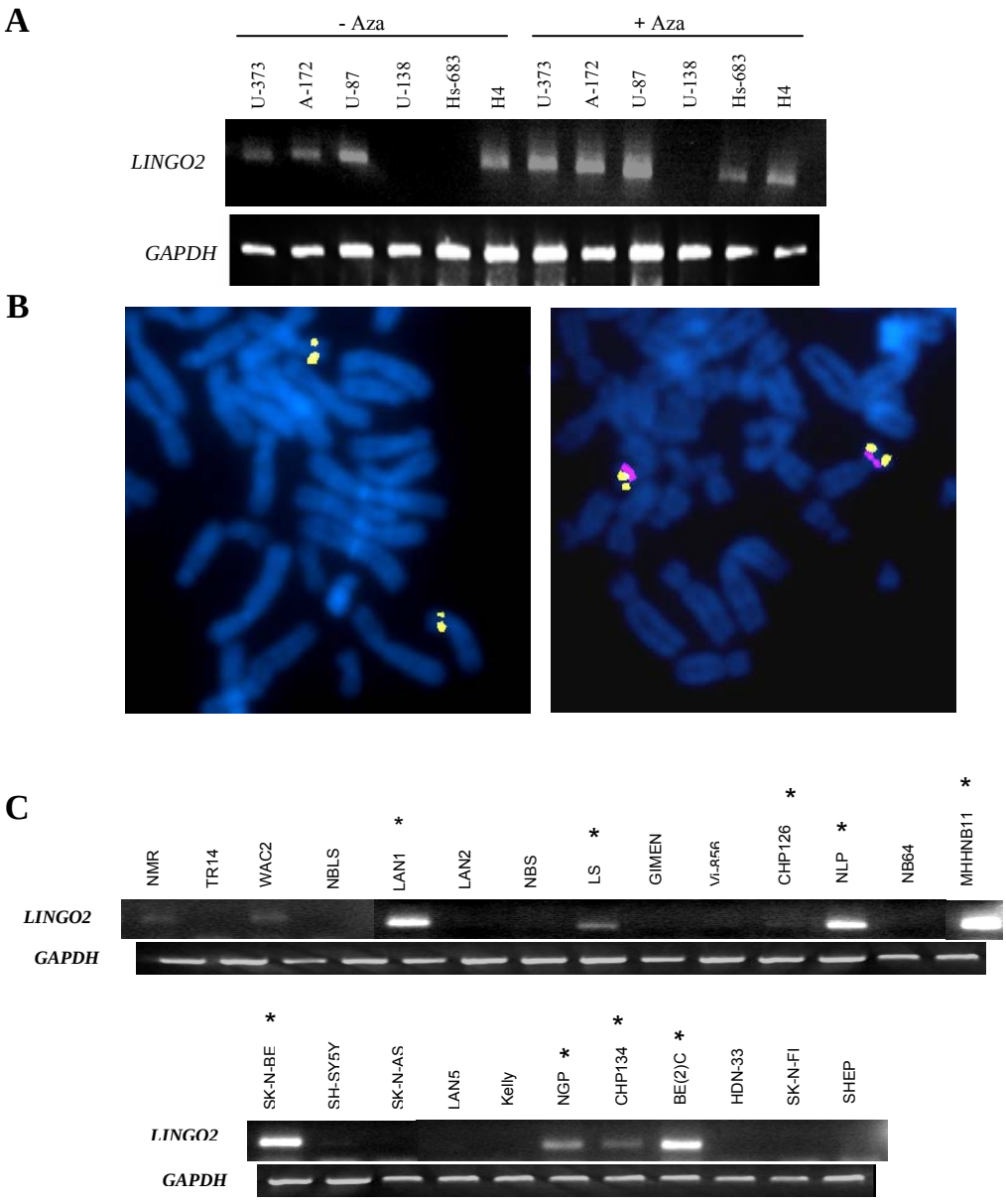

Figure 3-19. *LINGO2* Expression in glioma/GB and NB cells. (A) RT-PCR for *LINGO2* expression in glioma/glioblastomacells, before and after treatment with azacitydine. Hs-683 and U-138 showed no *LINGO2* expression before azacitydine treatment. After methylation inhibition by azacitydine treatment, the expresseion was reversed only in Hs-683 and not U-138. (B) Fluorescence hybridization of *LINGO2* sequence in Hs-683 and U-138 cells showed the signal of BAC RP11-264J11 (purple) in Hs-683 (on right-hand side), and not U-138 cells (on left-hand side). This is an indication of genomic rearrangements in this region of U-138 cells which could justify the lack of *LINGO2* expression in these cells. (C) RT-PCR for *LINGO2* expression in neuroblastoma cell lines. A differential pattern of expression was detected with expression mostly observed in *MYCN*-amplified cells (indicated by asterix on top).

LINGO2 expression was also investigated in NB cells. Twenty five NB cells were examined for *LINGO2* mRNA, including NMR, TR14, WAC2, NBLS, LAN1, LAN2, NBS, LS, GIMEN, Vi856, CHP126, NLP, NB64, MHH-NB-11, SK-N-BE, SH-SY5Y, LAN5, Kelly, NGP, CHP134, N-BE(2)C, HDN33, SK-N-FI and SH-EP (Fig. 3-19 C). A differential expression of *LINGO2* in NB cells was observed, with a tendency of expression mostly in *MYCN* positive cells (indicated in the figure by an asterix on top).

In conclusion, *LINGO2* shows a differential pattern of expression in normal tissues, as well as in the tumor cell lines. Also, there is an indication that epigenetic mechanism of hypermethylation could be involved in control of *LINGO2* gene expression.

4. Discussion

One of the primary missions of cancer research is to discover candidate genes involved in tumor development. Chromosomal fragile sites (CFSs) are particularly sensitive to DNA breaks and are frequent sites of rearrangement or loss in many human cancers. Studies on the most expressed CFSs, *FRA3B* and *FRA16D*, have revealed that CFSs are the sites for deletion and loss of heterozygosity (LOH) in many cancers (Huebner and Croce 2001; Yang *et al.* 2002; Finnis *et al.* 2005; O'Keefe and Richards 2006). Common fragile sites are supposed to be the genomic regions which exhibit breakage at the very early stages of tumorigenesis (Bartkova *et al.* 2005; Gorgoulis *et al.* 2005; Halazonetis *et al.* 2008). Identification of CFS genes and their involvement in chromosomal rearrangements in different cancer types may lead to discovery of new cancer-susceptibility genes.

The short arm of chromosome 9 is involved in genomic rearrangements in several types of cancer. Inversions, translocations, deletions and LOH on 9p have been reported in various cancers. Different regions on 9p have been reported to be targeted by these genetic aberrations. Several studies demonstrate the incidence of LOH, mainly on 9p21 region, in a variety of malignancies like neuroblastoma (Mora *et al.* 2004), lung cancers (Sawada *et al.* 2003; Shibukawa *et al.* 2009) and renal carcinoma (Grady *et al.* 2001; Sanz-Casla *et al.* 2003). Also deletions in regions 9p22-p24 have been repeatedly observed in wide range of tumors like breast cancer (An *et al.* 1999) and neuroblastoma (Giordani *et al.* 2002). In fact, these findings imply the involvement of even more than one region of LOH on 9p in many cancers.

Two CFSs are located on 9p region. A study by Savelyeva and colleagues (Savelyeva *et al.* 2001) demonstrated that heterozygous *BRCA2* mutation carriers exhibit high levels of genomic instability on 9p23-24, including inversions, duplications and amplifications. This led to a proposition that there is a particular tendency of distal 9p to spontaneous instability, which could be possibly due to the presence of a fragile site in the vicinity of the aberration region. Finally, FISH mapping studies revealed *FRA9G* as a new CFS at 9p22.2 (Sawinska *et al.* 2007). There is also *FRA9C* which is listed in the databases as a CFS mapped on proximal 9p, and its precise location was not characterized until recently in a work done by Sawinska *et al*, (2008, unpublished). *FRA9C* lies on a region spanning distal 9p21.1 and 9p21.2 boundary.

In this study, the probable involvement of these two CFSs and their encompassing genes, *FRA9G/CNTLN* and *FRA9C/LINGO2*, in chromosomal rearrangement events on 9p is explored.

4.1 *FRA9C* and *FRA9G* are frequently involved in 9p instability

By applying aCGH technique, it is feasible to define the possible impact of *FRA9G* and *FRA9C* on the chromosomal aberrations on 9p. While overall 9p region rearrangements in all four cell types were approximately 73%, the damage rate presented in *FRA9G* and *FRA9C* (26% and 40%, respectively) showed to comprise a significant part of this whole damage on 9p. In total, *FRA9C* showed higher degrees of aberrations compared to *FRA9G*.

FRA9C was predominantly damaged in NB cells. In glioma/GB cells, although 100% of the cells had rearrangements on 9p, only less than 20% of them exhibited *FRA9C* alterations, whereas the rate of 9p and *FRA9C* alterations in NB were both almost similar and as high as 70%. This observation implies the particularly important role of *FRA9C* in NB genetic aberrations on 9p. Analysis of a larger number of cell lines from the database, showed a similar pattern for *FRA9C* in NB cell lines. However, in general, rates retrieved from the database results were lower than what was observed in the custom aCGH data. This could be explained by the higher resolution of the custom array used in this study (40 bp), as compared to the probes used in producing the results in the database (1Mb).

The total breaks occurring on the entire 9p in each tumor cell type were counted, and BC cell lines showed the highest number of breaks. However, it should be noted that due to very complex rearrangements observed in two BC cell lines, MX-1 and COLO-824, a considerable part of the breaks counted for breast tumors were actually coming only from these two cell lines, whereas there were cell lines showing no breaks on 9p, including MFM-223 and BT-474. So the assumption of BC having more breaks on 9p should be considered cautiously.

Type and number of cells	total breaks	*FRA9G*	*FRA9G-FRA9C*	*FRA9C*
Glioma/Glioblastoma (6)	40	12%	45%	2.5%
Neuroblastoma (9)	49	10%	27%	30%
Colon Cancer (5)	26	0	37%	0
Breast Cancer (9)	76	5%	16%	4%

Table 5-1. The percentage of overall breaks occurring within and in between the *FRA9G* and *FRA9C*.

In NB, almost 30% of the breakpoints were within or in the vicinity of *FRA9C* (Table 5-1). In glioma/GB, regions flanking the vicinity of *FRA9G* contained 12% of the total breakpoint occurring in this type of cancer. The sequence of *FRA9G* and *FRA9C* which are 400 kb and 800 kb constitutes only 2.5% of the whole 9p length. This suggests that there is a significant involvement of these two fragile sites towards genomic aberrations of this region. In addition, the majority of the breakpoints on 9p showed to occur in the 13 Mb region spanning over *FRA9G* and *FRA9C* sequence and the sequence flanked by these two CFSs. This region contained more than half of the breaks in NB, glioma/GB and CC (Table 5-1). This observation could be a supporting evidence for the important role of the two fragile sites in 9p instability.

Apart from *FRA9G* and *FRA9C* sequence in NB and glioma/GB cells, a third cluster of breakpoints which were observed in these two types of cells located at *CDKN2A* and the region around it. Cyclin-dependent kinase inhibitor 2A (*CDKN2A*) is a tumor suppressor gene (TSG) which encodes for $p16^{INK4A}$ and $p14^{ARF}$. The alterations of the *CDKN2A*/p16 have been reported in many cancers and its deletion is known to impair both the Rb and p53 pathways (Mora *et al.* 2004). The observation which showed *FRA9G* and *FRA9C* as being largely active in rearrangement events on 9p, and the fact that the highly damaged locus of *CDKN2A* lies in between the two CFSs, further highlights the possible role of the two CFSs in the instability of this TSG. In fact, we observed the damage of *CDKN2A* locus in the cell lines that either one or both of the fragile sites were active in them.

Based on the concordance of the location of fragile sites with chromosomal breakpoints, it has been hypothesized that common fragile sites may play a mechanistic role in the occurrence of chromosomal rearrangements observed in tumor cells (Yunis and Soreng 1984; Corbin *et al.* 2002). In the results of this study, the breakage at *FRA9C* in three NB cell lines, including LAN-6, SK-N-BE(2)C and Vi-865, led to the heterozygous deletion of a distal fragment which

spanned over the *CDKN2A* locus. And in one of these cell lines, LAN-6, there was another interstitial deletion occurring with the deleted part, that led to the homozygous deletion of *CDKN2A*. Further investigations from the database reveal that a similar phenomenon also occurrs in the 50% of NB cells and 20% of glioma/GB cells. The observation that breakage at *FRA9C* coincides with deletion of *CDKN2A*, suggests the existence of an association between the two events, in terms of a possible mechanistic role for the CFS in alterations occurring in the TGS.

In addition to the findings that suggest a contributory role of fragile sites in tumorigenesis, and given that CFSs are normal components of human chromosomes, one can assume that they also play a protective role against cancer. This function could be related to CFS genes. Common fragile site genes generally extend over long genomic regions and most of them contain several genes. Only six common fragile sites are restricted by single genes *FRA1E*/*DPYD* (Hormozian *et al.* 2007), *FRA3B*/*FHIT (Ohta et al. 1996)*, *FRA16D*/*WWOX* (Ried *et al.* 2000; Bednarek *et al.* 2001), *FRA13A/NBEA* (Savelyeva *et al.* 2006), *FRA9G/CNTLN* (Sawinska *et al.* 2007) and *FRA9C/LINGO2* (Sawinska *et al*, 2008, unpiblished data*)*. Genes located at CFSs are highly susceptible to genomic instability especially in cancer cells. The studies on these genes in the context of their role in cancer development have revealed an important role for most of the large CFS genes as tumor suppressor (O'Keefe and Richards 2006; Smith DI 2006; Lukusa and Fryns 2008). Several studies on the two most expressed fragile sites (*FRA3B* and *FRA16D*), implies a tumor suppressor function for the genes within the fragile sites and genetic alteration of *FHIT* and *WWOX* (*FRA3B* and *FRA16D* associated genes) has been frequently reported. (Giarnieri *et al.*; Lewandowska *et al.* 2009; Ludes-Meyers *et al.* 2009; Hassan *et al.* 2010). These findings indicate that at preliminary stages of tumor development, the altered expression of genes located at fragile sites maay elicit a cellular response against hazards. In addition, observation that CFSs and the large genes are evolutionary co-conserved further suggests that these genes and the unstable regions share some function within normal cells (Krummel *et al.* 2002).

Herein, CFS genes *CLNTLN* and *LINGO2*, associated to *FRA9G* and *FRA9C*, respectively, were investigated in the context of genomic alterations on 9p in different tumors.

4.2 Fragile site genes; tumor-associated function

4.2.1 *FRA9G/CNTLN*

CNTLN gene which encodes for a centrosomal protein is located at *FRA9G*. Similar to many fragile site genes, it is a gene with very large introns. Centrosome abnormalities, which are also associated with high degree of aneuploidy, are prevalent in almost all types of solid tumors and certain cases of hematological cancers (D'Assoro *et al.* 2002; Fukasawa 2005).

Recently, the rat protein of this gene has been isolated and shown to possess coiled-coil domains, but lack known functional domain (Makino *et al.* 2008). Their results indicated that centlein is a centrosomal protein in interphase and mitosis. They showed the expression of Centlein in various rat normal tissues and cell lines. *CNTLN* expression was also detected in HeLa cells.

The aCGH results in this study showed *FRA9G/CNTLN* to be disturbed by rearrangements in seven cell lines (out of 29). Three of these cell lines were NB, including SK-N-BE(2)C, SK-N-FI and Vi-856. The whole region of the gene was heterozygously deleted in SK-N-FI and SK-N-BE(2)C. In Vi-856, the gene sequence was damaged by two breakpoints. In BC cells COLO-824 and MX-1, in spite of the amplification of the large parts of the 9p which spanned over the *CNTLN/FRA9G* region, breakages were observed exactly within the *CNTLN* locus which led to interstitial deletion of parts of the gene. These observations imply that deletions in *CNTLN* gene may be an advantage for tumor progression. Still, when the expression of *CNTLN* at RNA level was analyzed in COLO-824 and MX-1, one could detect *CNTLN* expression only in MX-1 cells. This suggests that alterations were probably heterozygous in MX-1 cell line. Moreover, in MFM-223 cells which did not present genetic alterations at *FRA9G/CNTLN*, no gene expression was detected. One could envisage an epigenetic inhabitation of expression via hypermethylation of *CNTLN* in MFM-223 cell line.

One important observation regarding the deletions in *CNTLN* gene was that all the interstitial deletion occurred within the large introns. One hypothesis regarding the presence of large introns in CFS genes has suggested a regulatory role in gene expression and response to stress. A study looking for prostate cancer susceptibility alleles, localized on such allele within one of the large introns of *FHIT* gene. This atudy suggests that DNA changes within the sequence of such introns could dramatically impact the gene function. There are also studies indicating that

there are many more RNA species encoded within the genome than was predicted previously. Taken together, these studies further support the hypothesis that large introns within the CFS genes may be producing RNA species which function regulates gene expression. The results revealed in this study, show that introns of *CNTLN* gene are frequent targets for genomic deletions and therefore are also in favor of this hypothesis.

A ubiquitous expression of *CNTLN* gene in all the 21 human normal tissues tested here was detected. This observation, given the differentiated expression of the gene observed in tumor cells, indicate an important function of the gene product in the biology of the cell and cancer development, which as far needs defined to be defined.

4.2.2 *FRA9C /LINGO2*

LINGO2 (leucin-rich repeat and Ig domain containing 2), located at *FRA9C* region, belongs to the *LINGO/LERN* gene family which is often expressed in the nervous system (Carim-Todd *et al.* 2003). Every member of this family has shown distinct patterns of expression in mouse embryos, as *Lingo2/LERN3* expression has been seen in a population of cells lying adjacent to the epithelial lining of the alofactory pit (Haines and Rigby 2008). Unlike the expression of most of the *LINGO/LERN* genes that increases as the embryo develops and is low in the adult, *LINGO2* has been detected in mouse adult brain (Haines and Rigby 2008) and appeared to be restricted to neural tissues. *LINGO2* encodes a leucin-rich repeat (LRR) transmembrane protein, the function of which is unknown. Many examples of LRR proteins are found to be expressed in the nervous system. Duplications of *LRRN6A*, which maps to the centromeric end of a region of genomic instability at 15q24, have been defined as a susceptibility factor for panic and anxiety disorders (Gratacos *et al.* 2001). LERN1 (leucin-rich repeat neural protein 1) has similarity to the proteins involved in axional guidance and migration, nervous system development and regeneration. *LINGO1* has recently been associated with an increased risk of essential tremor (ET) and Parkinson disease (PD) (Clark *et al.*; Haubenberger *et al.* 2009). *LINGO2* is a less well characterized paralog of *LINGO1* which is biologically a plausible candidate gene for neurodegenerative disease. Given the high degree of homology between *LINGO1* and *LINGO2* protein (61%), *LINGO2* has been suggested to be a reasonable candidate gene for ET and PD (Vilarino-Guell *et al.*).

Many of the large CFS genes are involved in neurological development. The first CFS gene identified in this regard was Parkin, which has shown to be mutated in some patients with autosomal recessive juvenile Parkinsonism. The *PARK2* gene is among several other genes located at *FRA6E* (Denison *et al.* 2003). Spontaneous deletion of Parkin in mice results in the Quaker (viable) phenotype. Another CFS gene is GRID2 (delta2 glutamate receptor gene) that is located within *FRA4F* (Chauvet *et al.* 2004; Rozier *et al.* 2004). Deletion of GRID2 in mice results in phenotype Lurcher, which is associated with ataxia. *RORA*, another large CFS gene, encodes an orphan retinoic receptor and is mapped to *FRA15A*. The gene product binds to the hypoxia inducible factor and therefore may be involved in cellular responses to stresses (Chauvet *et al.* 2004). A number of other large fragile site genes that appear to be significantly involved in neurological development are *CNTNAP2/FRA7I* (Verkerk *et al.* 2003), *LRP1B/FRA2F* (Cam *et al.* 2004) and *IL1RAPL1/FRAXC* (Zhang *et al.* 2004).

In this study, a very limited expression of *LINGO2* in human normal tissues, including brain, kidney, ovary, testes, prostate and placenta was detected. *LINGO2* expression was observed, in accordance to few other reports, not only in a part of nervous system (brain), but also, in contrast to what was speculated in those studies, in a few number of other tissues.

The aCGH data presented here show that that 6 out of 9 NB cell lines are damaged within or very close to their *LINGO2/FRA9G* locus. Moreover, in two BC cell lines, MX-1 and COLO-824, interstitial deletions within the fragile site gene were detected. In total, one third of all the cell lines showed rearrangements in their *LINGO2* locus. Four of the NB cells, including SH-EP, Vi-856, SK-N-FI and Kelly, plus the two BC cell lines bore the deletions in their largest intron, 4-5. In LAN-6, the deletion was in the proximal vicinity of the gene and only 30 kb and 50 kb downstream to mir-876 and mir-873, respectively. In SK-N-BE(2)C, in addition to an interstitial deletion particularly affecting the regulatory 5' upstream region of the gene, the whole *LINGO2* sequence was heterozygously deleted. The brain cell line, U-138, showed a breakpoint within intron 3-4 of *LINGO2*. These findings indicate that *LINGO2* locus is frequently affected by rearrangements in cancer cells, especially in NB. The observation that the majority of the genetic alterations in *LINGO2* gene happen within the large introns, is a strong support for the regulatory role of the large introns in CFS genes that has been also proposed by some other studies. It is also suggested that the instability-induced alterations in some CFS genes contribute to cancer development, in a two step process. First the initial alterations occur

primarily within intronic regions (as these genes are greater than 99% intronic). Then these alterations, which are not benign, alter the repertoire of transcripts produced from these genes (Smith DI 2006).

Here, the expression analysis of *LINGO2* gene at RNA level in NB and glioma/GB cell lines presented a differential expression pattern. Twenty five NB cells show a very differential pattern of expression for *LINGO2*. In more than half of the cell lines *LINGO2* was not detected at RNA level. From 10 cell lines showing *LINGO2* expression, 8 were *MYCN* amplified. The *MYCN* gene is a proto-oncogene and belongs to the MYC family of transcription factors. Among the prognostic indicators of NB, *MYCN* amplification has been associated to poor prognosis. However, the significance of *MYCN* expression in the clinical and biological behavior of neuroblastoma is still not clear. Whether the co-existence of *MYCN* amplification and *LINGO2* expression in NB is a cause and effect or just two parallel pathways during the pathogenesis of neuroblastoma, needs to be further investigated. This would allow us to have a better understanding of the biological function of the *LINGO2* gene.

In two brain cell lines, U-138 and Hs-683, lack of *LINGO2* expression showed to be the result of two different mechanisms, chromosomal deletion and hypermethylation inhibition.

Hemi- and Homozygous deletions of fragile site gene *FHIT* have been frequently reported in various cancers (Fong *et al.* 1997; Sozzi *et al.* 1997; Wistuba *et al.* 1997). Also, several studies demonstrating the absence of point mutations in two common fragile site genes, *WWOX* and *FHIT*, have suggested that other mechanisms, in addition to deletions, regulate their expression. A recent study showed promoter hypermethylation as a critical regulator of FHIT expression in lung cell lines (Verri *et al.* 2009). A similar result has been shown to exist for *WWOX* gene expression in pancreatic cancer cell lines (Kuroki *et al.* 2004). Due to high frequency of methylation events in *FHIT* and *WWOX* in association with loss of expression, it is suggested that CFS genes could enrich a hypermethylation panel for various types of cancer. Recent data concerning lung carcinogenesis indicates that extensive DNA damage through double strand breaks could in part be responsible for the acquisition of aberrant promoter hypermethylation. It has been suggested for *FHIT* gene that both deletions and methylation events are two independent factors that contribute to functional loss of expression (Verri *et al.* 2009).

Further studies on expressional pattern of *LINGO2* in cancer and modes of expression inhibition of this CFS gene could further shed light on its possible role in carcinogenesis.

4.3 Non-fragile site genes located at unstable regions of 9p

In addition to common fragile site genes, *CNTLN* and *LINGO2*, there are several other genes located on the three localized clusters of breakpoints which are revealed from the results of this study.

According to literature, *CDKN2A*/p16 is considered to be the main target for 9p rearrangements in tumors. LOH, as well as point mutations and hypermethylation have been described as inactivation mechanisms for *CDKN2A*. Mcdermott and colleagues (McDermott *et al.* 2006) showed that lack of p16 protein specifically leads to disturbance of centrosome function. In fact, there are several oncogenic and tumor-suppressor proteins which have been found to be involved in the regulation of centrosome function and duplication. When those proteins are damaged, it results in mitotic defects that are associated with numeral and functional abnormalities of centrosomes. The most frequently damaged region revealed by our array experiments was 9p21.3. In addition to *CDKN2A*, there were few other genes that present relatively high degree of genomic alterations, including *MTAP*, *ELAVL2* and *IFN* gene clusters.

MTAP gene (methylthioadenosin phosphorylase) resides approximately 100 kb from *CDKN2A* and is reported to be frequently co-deleted with it. It encodes a ubiquitous enzyme which is essential in methionine and purine metabolism and is frequently deficient in cancer cell lines and some malignancies (Kamatani *et al.* 1981; Schmid *et al.* 1998; Garcia-Castellano *et al.* 2002).

ELAVL2 (embryonic lethal, abnormal vision, Drosophila-like 2) resides approximately 2 Mb proximal to *CDKN2A* and encodes for a neural-specific RNA-binding protein. It is a regulator of MYCN expression in neuroblastoma and is involved in neural differentiation (Chagnovich and Cohn 1996; Chagnovich *et al.* 1996; Ball and King 1997). Co-deletion of *ELAVL2* with *MTAP* and *CDKN2A* genes has also been observed (Kamath *et al.* 2008).

The *IFN* gene cluster resides 500-1000 kb, telomeric to *CDKN2A*. This cluster contains *IFN*-β and almost 25 genes and pseudogenes for *IFN*-α and *IFN*-γ. Frequent homozygotic deletions of *IFN*-α and *IFN*-β have been observed and their loss sensitisez cells to the growth inhibitory actions of exogenous IFNs (Haus 2000). Deletions of the *IFN* gene cluster have been reported in glioma cell lines (James *et al.* 1993), lung cancer (Olopade *et al.* 1993), head and neck cancer (Lydiatt *et al.* 1998), and leukemias (Usvasalo *et al.*). *IFN* gene cluster also have been

demonstrated to be deleted in whole or in part in more than half of the *CDKN2A*-deficient cell lines (Zhang *et al.* 1996).

In the more telomeric cluster, where *FRA9G/CNTLN* is located, there are two neighboring genes to *CNTLN*, including *BNC2* and *SH3GL2*. *BNC2* encodes for basonuclin2 which is a recently discovered zinc-finger protein which is highly expressed in normal keratinocytes, ovary, testes, kidney and lung, however it is present in virtually every cell type. It is mostly localized in the nucleus and is likely related to mRNA splicing processes and in general is suggested to function as a transcriptional regulator (Romano *et al.* 2004; Vanhoutteghem and Djian 2006). One interesting observation about this gene is that it has the potential to generate 90,000 mRNA isoforms encoding more than 2000 different proteins. In fact, there are few genes known to generate such extraordinary number of splicing isoforms. There are two recent studies implying *BNC2* as a tumor-associated gene. First, which reported the homozygous deletion spanning 9p22.3-p22.2 (region where harbors *BNC2* gene) and the decreased expression of *BNC2* mRNA in Barett's esophagus (BE) carcinoma (Akagi *et al.* 2009). Second, the study by Song et al, which reported that SNP microarray analysis in ovarian cancer revealed a cluster of frequent SNPs on 9p22.2, nearby *BNC2* gene (Song *et al.* 2009).

SH3GL2 (SH3-domain GRB2-like 2), the other neighboring gene to *CNTLN*, encodes for an evolutionary conserved amino acid domain protein involved in signal transduction, mobility, enzymatic activation and transcriptional regulation. This gene is predominantly expressed in the brain (Giachino *et al.* 1997) and is suggested to be a candidate tumor suppressor gene. Frequent deletion and abnormalities of *SH3GL2* have been associated to development of breast carcinoma (Sinha *et al.* 2008), dysplastic lesions of head and neck carcinoma (Ghosh *et al.* 2009), laryngeal carcinoma (Shang *et al.* 2007) and gastric cancer (Sun *et al.* 2006).

The aCGH results also revealed a cluster of breakpoints localized at 9p22.2, a region that spans over *BNC2*, *CNTLN* and *SH3GL2* genes. Three NB, two brain and one CC cell lines showed deletion within *BNC2* gene. *SH3GL2* gene presented breakages within two NB cell lines. The 9p22.2 region has been frequently demonstrated to be the target for chromosomal deletions in various cancers. The observation in this study, which is in line with the results of other studies, suggests an important function of the genes located in this region in tumor biogenesis.

Since almost all of these genes in the instability area are related to normal and malignant function of different cell types, one can assume that they are actively transcribed. This predicts

an open chromatin structure for these regions in order to be accessible to transcription factors and gene expression control. The open configuration of chromatin structure have been proposed to be predisposed to double strand breaks, which have been reported to be the main reason for DNA instabilities.

Several studies have shown that miRNAs play an important role in certain human cancers, including B cell chronic lymphocytic leukemias (Calin *et al.* 2002), and Burkitts lymphoma, colon cancer, lung cancer, and breast cancer (Esquela-Kerscher and Slack 2006; Sevignani *et al.* 2006). Furthermore, miRNAs can downregulate a large number of target mRNAs and since many of these targets are either tumor oncogenes or tumor suppressors, it is suggested that miRNAs can influence susceptibility and predispose individuals to different cancers. It has been reported that more than 50% of miRNA genes are located in cancer-associated genomic regions and fragile sites, as well as in minimal regions of LOH and minimal regions of amplification (minimal amplicons) (Calin *et al.* 2004).
Five miRNA genes are located on the short arm of chromosome 9. Two of them, mir-873 and mir-876 are located on very close centromeric side of *FRA9C/LINGO2* locus. The other two, including mir-31 and mir-491 are located on the vicinity of distal *CDKN2A*. The fifth one which is mir-101-2 is located on distal end of 9p arm. Therefore, four out of five miRNA genes on 9p are located close to the two clusters of breakpoints earlier identified by aCGH results.

4.3 Sequence analysis of the breakpoint-clustering regions on 9p

Unlike rare fragile sites which CGG tinucleotide repeats expansion and AT-rich minisatellite repeats are described as molecular basis for their instability, there is not a consensus agreement on a common molecular feature shared by common fragile sites that could lead to their fragility. Common fragile sites are relatively AT-rich sequences and do not contain any expanded repeats or specific sequences. Moreover, comparison of different common fragile sites, including *FRA9C*, *FRA9G*, *FRA3B*, *FRA16D*, *FRA13A* and *FRA1E*, show a considerable variation in DNA repeat sequences, in particular LINE1 elements (Sawinska *et al.* 2007). This observation is in contrast to what has been proposed for *FRA3B*, in which LINE1 elements are considered to have a probable major role in the DNA instability at the fragile locus. Only *FRA9G* seems to

have a slightly higher degree of LINE1 elements. The same results were obtained when the three regions of breakpoint-clustering on 9p were analyzed for their DNA repeat elements. No significant differences were observed between the DNA sequence of the three regions of clusters and that of non-fragile genome. Only in the core region of *FRA9G* breakpoint clusters, within a part that the majority of the breakpoint occurred in, a relatively high number of LINE1 elements were presented. This might suggest an involvement of LINE1 elements in *FRA9G* region instability. One could not imply this for the other two unstable clusters.

El Achkar and colleagues showed that the majority of common fragile sites are located at the interface of G/R boundaries of chromosome (El Achkar *et al.* 2005). G-bands are AT-rich and gene-poor and undergo DNA replication late in the S phase of the cell cycle. R-bands are CG-rich and gene-rich and undergo replication early in the S phase. R- and G-bands are different in their structure and function. The DNA replication kinetic at the R-band/G- band transition is still unknown but it is likely that these regions are difficult to duplicate and particularly sensitive to treatments that disturb the replication, leading to fragility.

A study by Mishmar *et al*, identified enrichment of clusters of DNA sequences with high flexibility, termed "flexibility peaks", in the *FRA7H* sequence (Mishmar *et al.* 1998). These are short regions of a few hundred nucleotides that show high local variation in twist angle, which may affect chromatin condensation and fragility. Since then, some other studies have shown high frequency of these regions in common fragile sites. As it has been shown by Zlotorynski *et al,* aphidicolin-induced fragile sites mapped to G band, perform an average of 5.7 flexibility islands per 100 kb (Zlotorynski *et al.* 2003). Very recently, in a model proposing mechanisms underlying instability at two common fragile sites, it was speculated that the breakpoint-clustering regions at common fragile sites is flanked by the high-flexibility peaks and the R/G band boundaries.

In the present study, analyzing *FRA9C* and *CDKN2A* regions of instability revealed an average of 8 flexibility peaks per 100 kb. This is slightly higher than what is proposed for aphidicolin-induced fragile sites. *FRA9G* region, as an aphidicolin-induced FS, showed even lower number of peaks than the average 3.5 peaks/100 kb.

The sequences enriched with AT-dinucleotide-rich stretches are potentially capable of forming secondary structure and therefore causing replication fork collapse and double strand breaks (Le Beau *et al.* 1998; Hellman *et al.* 2000; Palakodeti *et al.* 2004; El Achkar *et al.* 2005). In a study

by Zhang and colleagues, it was demonstrated that sequences enriched in perfect polymorphic AT repeats within *FRA16D*, can efficiently cause stalling of replication fork, and this is directly dependent on the length of an AT repeat (Zhang 2007). However, it still remains to be elucidated whether these motifs have crucial role in CFS stability and if this could be the case for the other CFSs. It has been proposed that expanded perfect AT-rich repeats, which are prone to form hairpin or cruciform structures (non-B DNA forms), can stall a replication fork (Mangelsdorf M. 1997; Hewett *et al.* 1998). In addition, the binding of ligands for AT-rich DNA minor groove, or interrupting replication compelled by incorporation of BrdU, which replaces thymidine in such highly AT-rich sequences, may lead to hindering of chromosome condensation. Failure of chromosome condensation might generate unstable chromatin in this region and be expressed as gaps or breaks in metaphase chromosomes.

Altogether, based on the results in this study, DNA sequence analysis in terms of DNA repeats elements did not reveal any specific feature element as an important factor undertaking the fragility in any of the three breakpoint-clustering regions on 9p. However, regarding flexibility peaks, clusters in the region spanning *FRA9C* and *CDKN2A* presented a higher number of peaks in comparison to *FRA9G* and human genome. This suggests firstly that the twist angle of DNA in *FRA9C* and *CDKN2A* loci could partly be of some importance for breakages occurring within them, and secondly that probably no common DNA feature is shared by CFSs and regions of high instability in the genome as a cause for their fragility.

4.5 Conclusions and Perspective

Here, 9p instability in four tumor models was investigated by using high-resolution array CGH. Then the results obtained from aCGH were then confirmed using FISH experiments.

The results clearly showed frequent 9p rearrangements in more than 70% of the cell lines. The size, localization and number of breakpoint throughout the entire 9p were precisely determined and the results presented various pattern of 9p instability in different tumor types. Overall, three clusters of localized breakpoints were identified on 9p, including *FRA9G/CNTLN*, *CDKN2A* and *FRA9C/LINGO2*. The percentage of rearrangements observed in these three clusters in all the examined cell lines was 26% *(FRA9G/CNTLN*), 50% (*CDKN2A)* and 40% (*FRA9C/LINGO)*. *CDKN2A* is a commonly known tumor suppressor gene which has been frequently reported to

be deleted in cancer. Based on the results of this study, the two common fragile sites and their associated genes, *FRA9G/CNTLN* and *FRA9C/LINGO*, are proposed to be new candidates of tumor-susceptibility loci. In addition, high-resolution aCGH allowed detecting recurrent damages in several genes in different tumor models. These genes included *BNC2* and *SH3GL2* (in NB), *ELAVL2* (in glioma/GB) and *MTAP* and *IFN* gene cluster (in glioma/GB, NB and CC). This finding is in agreement with previous studies which have proposed these genes to be associated with different cancer types.

There were miRNA clusters close to *FRA9C* (mir-873 and mir-876) and *CDKN2A* region (mir-31 and mir-491), which is in accordance to the finding that miRNA clusters mostly reside at tumor-susceptibility chromosome areas.

Moreover, *LINGO2* expression analysis in this study indicated hypermethylation as an inhibitory mechanism for expression of the gene in certain cells. It has been suggested that hypermethylation can trigger chromosomal instability.

In the quest to identify novel candidates for genomic instabilities in cancer, one important task would be to investigate the dysfunctions in these novel tumor-associated genes genes and also to explore the causes and impacts of such abnormal functions in the process of tumor development.

Akagi, T., T. Ito, M. Kato, Z. Jin, Y. Cheng, T. Kan, G. Yamamoto, A. Olaru, N. Kawamata, J. Boult, H. J. Soukiasian, C. W. Miller, S. Ogawa, S. J. Meltzer and H. P. Koeffler (2009). "Chromosomal Abnormalities and Novel Disease-Related Regions in Progression from Barrett's Esophagus to Esophageal Adenocarcinoma." Int J Cancer **125**(10): 2349-59.

An, H. X., A. Claas, L. Savelyeva, S. Seitz, P. Schlag, S. Scherneck and M. Schwab (1999). "Two Regions of Deletion in 9p23-24 in Sporadic Breast Cancer." Cancer Res **59**(16): 3941-3.

Aqeilan, R. I., F. Trapasso, S. Hussain, S. Costinean, D. Marshall, Y. Pekarsky, J. P. Hagan, N. Zanesi, M. Kaou, G. S. Stein, J. B. Lian and C. M. Croce (2007). "Targeted Deletion of Wwox Reveals a Tumor Suppressor Function." Proc Natl Acad Sci U S A **104**(10): 3949-54.

Arlt, M. F., D. E. Miller, D. G. Beer and T. W. Glover (2002). "Molecular Characterization of Fraxb and Comparative Common Fragile Site Instability in Cancer Cells." Genes Chromosomes Cancer **33**(1): 82-92.

Arlt, M. F., B. Xu, S. G. Durkin, A. M. Casper, M. B. Kastan and T. W. Glover (2004). "Brca1 Is Required for Common-Fragile-Site Stability Via Its G2/M Checkpoint Function." Mol Cell Biol **24**(15): 6701-9.

Bacolla, A., R. Gellibolian, M. Shimizu, S. Amirhaeri, S. Kang, K. Ohshima, J. E. Larson, S. C. Harvey, B. D. Stollar and R. D. Wells (1997). "Flexible DNA: Genetically Unstable Ctg.Cag and Cgg.Ccg from Human Hereditary Neuromuscular Disease Genes." J Biol Chem **272**(27): 16783-92.

Ball, N. S. and P. H. King (1997). "Neuron-Specific Hel-N1 and Hud as Novel Molecular Markers of Neuroblastoma: A Correlation of Hud Messenger Rna Levels with Favorable Prognostic Features." Clin Cancer Res **3**(10): 1859-65.

Bartkova, J., Z. Horejsi, K. Koed, A. Kramer, F. Tort, K. Zieger, P. Guldberg, M. Sehested, J. M. Nesland, C. Lukas, T. Orntoft, J. Lukas and J. Bartek (2005). "DNA Damage Response as a Candidate Anti-Cancer Barrier in Early Human Tumorigenesis." Nature **434**(7035): 864-70.

Bednarek, A. K., C. L. Keck-Waggoner, R. L. Daniel, K. J. Laflin, P. L. Bergsagel, K. Kiguchi, A. J. Brenner and C. M. Aldaz (2001). "Wwox, the Fra16d Gene, Behaves as a Suppressor of Tumor Growth." Cancer Res **61**(22): 8068-73.

Bednarek, A. K., K. J. Laflin, R. L. Daniel, Q. Liao, K. A. Hawkins and C. M. Aldaz (2000). "Wwox, a Novel Ww Domain-Containing Protein Mapping to Human Chromosome 16q23.3-24.1, a Region Frequently Affected in Breast Cancer." Cancer Res **60**(8): 2140-5.

Berger, R., C. D. Bloomfield and G. R. Sutherland (1985). "Report of the Committee on Chromosome Rearrangements in Neoplasia and on Fragile Sites." Cytogenet Cell Genet **40**(1-4): 490-535.

Bloomston M, K. J., Butterfield M, Dillhoff M, Muscarella P, Ellison EC, Melvin WS, Croce CM, Pichiorri F, Huebner K, Frankel WL (2009). "Coordinate Loss of Fragile Gene Expression in Pancreatobiliary Cancers: Correlations among Markers and Clinical Features." Ann Surg Oncol **16**(8): 2331-8.

Bluteau, O., J. C. Beaudoin, P. Pasturaud, J. Belghiti, D. Franco, P. Bioulac-Sage, P. Laurent-Puig and J. Zucman-Rossi (2002). "Specific Association between Alcohol Intake, High Grade of Differentiation and 4q34-Q35 Deletions in Hepatocellular Carcinomas Identified by High Resolution Allelotyping." Oncogene **21**(8): 1225-32.

Boldog, F., R. M. Gemmill, J. West, M. Robinson, L. Robinson, E. Li, J. Roche, S. Todd, B. Waggoner, R. Lundstrom, J. Jacobson, M. R. Mullokandov, H. Klinger and H. A. Drabkin (1997). "Chromosome 3p14 Homozygous Deletions and Sequence Analysis of Fra3b." Hum Mol Genet **6**(2): 193-203.

Boldog, F. L., B. Waggoner, T. W. Glover, I. Chumakov, D. Le Paslier, D. Cohen, R. M. Gemmill and H. A. Drabkin (1994). "Integrated Yac Contig Containing the 3p14.2 Hereditary Renal Carcinoma 3;8 Translocation Breakpoint and the Fragile Site Fra3b." Genes Chromosomes Cancer **11**(4): 216-21.

Bostrom, J., B. Meyer-Puttlitz, M. Wolter, B. Blaschke, R. G. Weber, P. Lichter, K. Ichimura, V. P. Collins and G. Reifenberger (2001). "Alterations of the Tumor Suppressor Genes Cdkn2a (P16(Ink4a)), P14(Arf), Cdkn2b (P15(Ink4b)), and Cdkn2c (P18(Ink4c)) in Atypical and Anaplastic Meningiomas." Am J Pathol **159**(2): 661-9.

Brison, O. (1993). "Gene Amplification and Tumor Progression." Biochim Biophys Acta **1155**(1): 25-41.

Calin, G. A., C. D. Dumitru, M. Shimizu, R. Bichi, S. Zupo, E. Noch, H. Aldler, S. Rattan, M. Keating, K. Rai, L. Rassenti, T. Kipps, M. Negrini, F. Bullrich and C. M. Croce (2002). "Frequent Deletions and Down-Regulation of Micro- Rna Genes Mir15 and Mir16 at 13q14 in Chronic Lymphocytic Leukemia." Proc Natl Acad Sci U S A **99**(24): 15524-9.

Calin, G. A., C. Sevignani, C. D. Dumitru, T. Hyslop, E. Noch, S. Yendamuri, M. Shimizu, S. Rattan, F. Bullrich, M. Negrini and C. M. Croce (2004). "Human Microrna Genes Are Frequently Located at Fragile Sites and Genomic Regions Involved in Cancers." Proc Natl Acad Sci U S A **101**(9): 2999-3004.

Cam, J. A., C. V. Zerbinatti, J. M. Knisely, S. Hecimovic, Y. Li and G. Bu (2004). "The Low Density Lipoprotein Receptor-Related Protein 1b Retains Beta-Amyloid Precursor Protein at the Cell Surface and Reduces Amyloid-Beta Peptide Production." J Biol Chem **279**(28): 29639-46.

Carim-Todd, L., M. Escarceller, X. Estivill and L. Sumoy (2003). "Lrrn6a/Lern1 (Leucine-Rich Repeat Neuronal Protein 1), a Novel Gene with Enriched Expression in Limbic System and Neocortex." Eur J Neurosci **18**(12): 3167-82.

Carless, M. A. and L. R. Griffiths (2008). "Cytogenetics of Melanoma and Nonmelanoma Skin Cancer." Adv Exp Med Biol **624**: 227-40.

Casper, A. M., S. G. Durkin, M. F. Arlt and T. W. Glover (2004). "Chromosomal Instability at Common Fragile Sites in Seckel Syndrome." Am J Hum Genet **75**(4): 654-60.

Casper, A. M., P. Nghiem, M. F. Arlt and T. W. Glover (2002). "Atr Regulates Fragile Site Stability." Cell **111**(6): 779-89.

Chagnovich, D. and S. L. Cohn (1996). "Binding of a 40-Kda Protein to the N-Myc 3'-Untranslated Region Correlates with Enhanced N-Myc Expression in Human Neuroblastoma." J Biol Chem **271**(52): 33580-6.

Chagnovich, D., B. E. Fayos and S. L. Cohn (1996). "Differential Activity of Elav-Like Rna-Binding Proteins in Human Neuroblastoma." J Biol Chem **271**(52): 33587-91.

Chang, N. S., J. Doherty, A. Ensign, J. Lewis, J. Heath, L. Schultz, S. T. Chen and U. Oppermann (2003). "Molecular Mechanisms Underlying Wox1 Activation During Apoptotic and Stress Responses." Biochem Pharmacol **66**(8): 1347-54.

Chauvet, C., B. Bois-Joyeux, E. Berra, J. Pouyssegur and J. L. Danan (2004). "The Gene Encoding Human Retinoic Acid-Receptor-Related Orphan Receptor Alpha Is a Target for Hypoxia-Inducible Factor 1." Biochem J **384**(Pt 1): 79-85.

Chesi, M., P. L. Bergsagel, O. O. Shonukan, M. L. Martelli, L. A. Brents, T. Chen, E. Schrock, T. Ried and W. M. Kuehl (1998). "Frequent Dysregulation of the C-Maf Proto-Oncogene at 16q23 by Translocation to an Ig Locus in Multiple Myeloma." Blood **91**(12): 4457-63.

Chung, K. K., Y. Zhang, K. L. Lim, Y. Tanaka, H. Huang, J. Gao, C. A. Ross, V. L. Dawson and T. M. Dawson (2001). "Parkin Ubiquitinates the Alpha-Synuclein-Interacting Protein, Synphilin-1: Implications for Lewy-Body Formation in Parkinson Disease." Nat Med **7**(10): 1144-50.

Clark, L. N., N. Park, S. Kisselev, E. Rios, J. H. Lee and E. D. Louis "Replication of the Lingo1 Gene Association with Essential Tremor in a North American Population." Eur J Hum Genet **18**(7): 838-43.

Coquelle, A., E. Pipiras, F. Toledo, G. Buttin and M. Debatisse (1997). "Expression of Fragile Sites Triggers Intrachromosomal Mammalian Gene Amplification and Sets Boundaries to Early Amplicons." Cell **89**(2): 215-25.

Corbin, S., M. E. Neilly, R. Espinosa, 3rd, E. M. Davis, T. W. McKeithan and M. M. Le Beau (2002). "Identification of Unstable Sequences within the Common Fragile Site at 3p14.2: Implications for the Mechanism of Deletions within Fragile Histidine Triad Gene/Common Fragile Site at 3p14.2 in Tumors." Cancer Res **62**(12): 3477-84.

D'Assoro, A. B., W. L. Lingle and J. L. Salisbury (2002). "Centrosome Amplification and the Development of Cancer." Oncogene **21**(40): 6146-53.

De Braekeleer, M., C. Sreekantaiah and O. Haas (1992). "Herpes Simplex Virus and Human Papillomavirus Sites Correlate with Chromosomal Breakpoints in Human Cervical Carcinoma." Cancer Genet Cytogenet **59**(2): 135-7.

Debacker, K. and R. F. Kooy (2007). "Fragile Sites and Human Disease." Hum Mol Genet **16 Spec No. 2**: R150-8.

Dekaban, A. (1965). "Persisting Clone of Cells with an Abnormal Chromosome in a Woman Previously Irradiated." J Nucl Med **6**(10): 740-6.

Denison, S. R., F. Wang, N. A. Becker, B. Schule, N. Kock, L. A. Phillips, C. Klein and D. I. Smith (2003). "Alterations in the Common Fragile Site Gene Parkin in Ovarian and Other Cancers." Oncogene **22**(51): 8370-8.

Doughty, M. L., P. L. De Jager, S. J. Korsmeyer and N. Heintz (2000). "Neurodegeneration in Lurcher Mice Occurs Via Multiple Cell Death Pathways." J Neurosci **20**(10): 3687-94.

Drexler, H. G. (1998). "Review of Alterations of the Cyclin-Dependent Kinase Inhibitor Ink4 Family Genes P15, P16, P18 and P19 in Human Leukemia-Lymphoma Cells." Leukemia **12**(6): 845-59.

Driouch, K., H. Prydz, R. Monese, H. Johansen, R. Lidereau and E. Frengen (2002). "Alternative Transcripts of the Candidate Tumor Suppressor Gene, Wwox, Are Expressed at High Levels in Human Breast Tumors." Oncogene **21**(12): 1832-40.

Dronkert, M. L., H. B. Beverloo, R. D. Johnson, J. H. Hoeijmakers, M. Jasin and R. Kanaar (2000). "Mouse Rad54 Affects DNA Double-Strand Break Repair and Sister Chromatid Exchange." Mol Cell Biol **20**(9): 3147-56.

Druck, T., P. Hadaczek, T. B. Fu, M. Ohta, Z. Siprashvili, R. Baffa, M. Negrini, K. Kastury, M. L. Veronese, D. Rosen, J. Rothstein, P. McCue, M. G. Cotticelli, H. Inoue, C. M. Croce and K. Huebner (1997). "Structure and Expression of the Human Fhit Gene in Normal and Tumor Cells." Cancer Res **57**(3): 504-12.

Durkin, S. G., M. F. Arlt, N. G. Howlett and T. W. Glover (2006). "Depletion of Chk1, but Not Chk2, Induces Chromosomal Instability and Breaks at Common Fragile Sites." Oncogene **25**(32): 4381-8.

Durkin, S. G. and T. W. Glover (2007). "Chromosome Fragile Sites." Annu Rev Genet **41**: 169-92.

Dussault, I., D. Fawcett, A. Matthyssen, J. A. Bader and V. Giguere (1998). "Orphan Nuclear Receptor Ror Alpha-Deficient Mice Display the Cerebellar Defects of Staggerer." Mech Dev **70**(1-2): 147-53.

El Achkar, E., M. Gerbault-Seureau, M. Muleris, B. Dutrillaux and M. Debatisse (2005). "Premature Condensation Induces Breaks at the Interface of Early and Late Replicating Chromosome Bands Bearing Common Fragile Sites." Proc Natl Acad Sci U S A **102**(50): 18069-74.

Elder, F. F. and T. J. Robinson (1989). "Rodent Common Fragile Sites: Are They Conserved? Evidence from Mouse and Rat." Chromosoma **97**(6): 459-64.

Ellsworth, R. E., J. A. Hooke, B. Love, J. L. Kane, H. L. Patney, D. L. Ellsworth and C. D. Shriver (2008). "Correlation of Levels and Patterns of Genomic Instability with Histological Grading of Invasive Breast Tumors." Breast Cancer Res Treat **107**(2): 259-65.

Esquela-Kerscher, A. and F. J. Slack (2006). "Oncomirs - Micrornas with a Role in Cancer." Nat Rev Cancer **6**(4): 259-69.

Faienza, M. F., F. della Ragione, G. Basso, B. Coppola, E. Miraglia del Giudice, F. Schettini and A. Iolascon (1996). "P16ink4a Gene Homozygous Deletions in Human Acute Leukaemias with Alterations of Chromosome 9." Br J Haematol **93**(3): 632-6.

Farrell, W. E., D. J. Simpson, J. E. Bicknell, A. J. Talbot, A. S. Bates and R. N. Clayton (1997). "Chromosome 9p Deletions in Invasive and Noninvasive Nonfunctional Pituitary Adenomas: The Deleted Region Involves Markers Outside of the Mts1 and Mts2 Genes." Cancer Res **57**(13): 2703-9.

Fechter, A., I. Buettel, E. Kuehnel, M. Schwab and L. Savelyeva (2007). "Cloning of Genetically Tagged Chromosome Break Sequences Reveals New Fragile Sites at 6p21 and 13q22." Int J Cancer **120**(11): 2359-67.

Feichtinger, W. and M. Schmid (1989). "Increased Frequencies of Sister Chromatid Exchanges at Common Fragile Sites (1)(Q42) and (19)(Q13)." Hum Genet **83**(2): 145-7.

Ferber, M. J., P. Eilers, E. Schuuring, J. A. Fenton, G. J. Fleuren, G. Kenter, K. Szuhai, D. I. Smith, A. K. Raap and A. A. Brink (2004). "Positioning of Cervical Carcinoma and Burkitt Lymphoma Translocation Breakpoints with Respect to the Human Papillomavirus Integration Cluster in Fra8c at 8q24.13." Cancer Genet Cytogenet **154**(1): 1-9.

Finnis, M., S. Dayan, L. Hobson, G. Chenevix-Trench, K. Friend, K. Ried, D. Venter, E. Woollatt, E. Baker and R. I. Richards (2005). "Common Chromosomal Fragile Site Fra16d Mutation in Cancer Cells." Hum Mol Genet **14**(10): 1341-9.

Fong, K. M., E. J. Biesterveld, A. Virmani, I. Wistuba, Y. Sekido, S. A. Bader, M. Ahmadian, S. T. Ong, F. V. Rassool, P. V. Zimmerman, G. Giaccone, A. F. Gazdar and J. D. Minna (1997). "Fhit and Fra3b 3p14.2 Allele Loss Are Common in Lung Cancer and Preneoplastic Bronchial Lesions and Are Associated with Cancer-Related Fhit Cdna Splicing Aberrations." Cancer Res **57**(11): 2256-67.

Fong, L. Y., V. Fidanza, N. Zanesi, L. F. Lock, L. D. Siracusa, R. Mancini, Z. Siprashvili, M. Ottey, S. E. Martin, T. Druck, P. A. McCue, C. M. Croce and K. Huebner (2000). "Muir-Torre-Like Syndrome in Fhit-Deficient Mice." Proc Natl Acad Sci U S A **97**(9): 4742-7.

Fukamachi, K., Matsuoka, Y., Ohno, H., Hamaguchi, T., Tsuda, H., (2002). "Neuronal Leucine-Rich Repeat Protein-3 Amplifies Mapk Activation by Epidermal Growth Factor through a Carboxyl-Terminal Region Containing Endocytosis Motifs." J. Biol. Chem. **277**: 43539-43552.

Fukasawa, K. (2005). "Centrosome Amplification, Chromosome Instability and Cancer Development." Cancer Lett **230**(1): 6-19.

Fuller, L. F. and R. B. Painter (1988). "A Chinese Hamster Ovary Cell Line Hypersensitive to Ionizing Radiation and Deficient in Repair Replication." Mutat Res **193**(2): 109-21.

Gandhi, M., L. W. Dillon, S. Pramanik, Y. E. Nikiforov and Y. H. Wang (2010). "DNA Breaks at Fragile Sites Generate Oncogenic Ret/Ptc Rearrangements in Human Thyroid Cells." Oncogene.

Garcia-Castellano, J. M., A. Villanueva, J. H. Healey, R. Sowers, C. Cordon-Cardo, A. Huvos, J. R. Bertino, P. Meyers and R. Gorlick (2002). "Methylthioadenosine Phosphorylase Gene Deletions Are Common in Osteosarcoma." Clin Cancer Res **8**(3): 782-7.

Gellibolian, R., A. Bacolla and R. D. Wells (1997). "Triplet Repeat Instability and DNA Topology: An Expansion Model Based on Statistical Mechanics." J Biol Chem **272**(27): 16793-7.

Ghosh, A., S. Ghosh, G. P. Maiti, M. G. Sabbir, N. Alam, N. Sikdar, B. Roy, S. Roychoudhury and C. K. Panda (2009). "Sh3gl2 and Cdkn2a/2b Loci Are Independently Altered in Early Dysplastic Lesions of Head and Neck: Correlation with Hpv Infection and Tobacco Habit." J Pathol **217**(3): 408-19.

Giachino, C., E. Lantelme, L. Lanzetti, S. Saccone, G. Bella Valle and N. Migone (1997). "A Novel Sh3-Containing Human Gene Family Preferentially Expressed in the Central Nervous System." Genomics **41**(3): 427-34.

Giarnieri, E., N. Zanesi, A. Bottoni, M. Alderisio, A. Lukic, A. Vecchione, V. Ziparo, C. M. Croce and R. Mancini "Oncosuppressor Proteins of Fragile Sites Are Reduced in Cervical Cancer." Cancer Lett **289**(1): 40-5.

Giordani, L., A. Iolascon, V. Servedio, K. Mazzocco, L. Longo and G. P. Tonini (2002). "Two Regions of Deletion in 9p22- P24 in Neuroblastoma Are Frequently Observed in Favorable Tumors." Cancer Genet Cytogenet **135**(1): 42-7.

Glover, T. W. (1998). "Instability at Chromosomal Fragile Sites." Recent Results Cancer Res **154**: 185-99.

Glover, T. W., C. Berger, J. Coyle and B. Echo (1984). "DNA Polymerase Alpha Inhibition by Aphidicolin Induces Gaps and Breaks at Common Fragile Sites in Human Chromosomes." Hum Genet **67**(2): 136-42.

Glover, T. W., A. W. Hoge, D. E. Miller, J. E. Ascara-Wilke, A. N. Adam, S. L. Dagenais, C. M. Wilke, H. A. Dierick and D. G. Beer (1998). "The Murine Fhit Gene Is Highly Similar to Its Human Orthologue and Maps to a Common Fragile Site Region." Cancer Res **58**(15): 3409-14.

Glover, T. W. and C. K. Stein (1987). "Induction of Sister Chromatid Exchanges at Common Fragile Sites." Am J Hum Genet **41**(5): 882-90.

Glover, T. W. and C. K. Stein (1988). "Chromosome Breakage and Recombination at Fragile Sites." Am J Hum Genet **43**(3): 265-73.

Gokcumen, O. and C. Lee (2009). "Copy Number Variants (Cnvs) in Primate Species Using Array-Based Comparative Genomic Hybridization." Methods **49**(1): 18-25.

Gorgoulis, V. G., L. V. Vassiliou, P. Karakaidos, P. Zacharatos, A. Kotsinas, T. Liloglou, M. Venere, R. A. Ditullio, Jr., N. G. Kastrinakis, B. Levy, D. Kletsas, A. Yoneta, M. Herlyn, C. Kittas and T. D. Halazonetis (2005). "Activation of the DNA Damage Checkpoint and Genomic Instability in Human Precancerous Lesions." Nature **434**(7035): 907-13.

Grady, B., R. Goharderakhshan, J. Chang, L. A. Ribeiro-Filho, G. Perinchery, J. Franks, J. Presti, P. Carroll and R. Dahiya (2001). "Frequently Deleted Loci on Chromosome 9 May Harbor Several Tumor Suppressor Genes in Human Renal Cell Carcinoma." J Urol **166**(3): 1088-92.

Gratacos, M., M. Nadal, R. Martin-Santos, M. A. Pujana, J. Gago, B. Peral, L. Armengol, I. Ponsa, R. Miro, A. Bulbena and X. Estivill (2001). "A Polymorphic Genomic Duplication on Human Chromosome 15 Is a Susceptibility Factor for Panic and Phobic Disorders." Cell **106**(3): 367-79.

Haines, B. P., Gupta, R., Jones, C.M., Summerbell, D., Rigby, P.W.J. (2005). "The Nlrr Gene Family and Mouse Developement: Modified Differential Display Pcr Identifies Nlrr-1 as a Gene Expressed in Earlysomatic Myoblasts." Dev. Biol. **281**: 145-159.

Haines, B. P. and P. W. Rigby (2008). "Expression of the Lingo/Lern Gene Family During Mouse Embryogenesis." Gene Expr Patterns **8**(2): 79-86.

Haines, B. P., L. M. Wheldon, D. Summerbell, J. K. Heath and P. W. Rigby (2006). "Regulated Expression of Flrt Genes Implies a Functional Role in the Regulation of Fgf Signalling During Mouse Development." Dev Biol **297**(1): 14-25.

Halazonetis, T. D., V. G. Gorgoulis and J. Bartek (2008). "An Oncogene-Induced DNA Damage Model for Cancer Development." Science **319**(5868): 1352-5.

Hamada, K., T. Kohno, M. Takahashi, M. Yamazaki, H. Tashiro, C. Sugawara, S. Ohwada, Y. Sekido, J. D. Minna and J. Yokota (2000). "Two Regions of Homozygous Deletion Clusters at Chromosome Band 9p21 in Human Lung Cancer." Genes Chromosomes Cancer **27**(3): 308-18.

Handt, O., Sutherland, G.R., Richards, R.I. (2000). "Fragile Sites and Minisatellite Repeat Instability." Mol. Genet. Metab. **70**: 99-105.

Harris, C. P., X. Y. Lu, G. Narayan, B. Singh, V. V. Murty and P. H. Rao (2003). "Comprehensive Molecular Cytogenetic Characterization of Cervical Cancer Cell Lines." Genes Chromosomes Cancer **36**(3): 233-41.

Hassan, M. I., A. Naiyer and F. Ahmad (2010). "Fragile Histidine Triad Protein: Structure, Function, and Its Association with Tumorogenesis." J Cancer Res Clin Oncol **136**(3): 333-50.

Haubenberger, D., C. Hotzy, W. Pirker, R. Katzenschlager, T. Brucke, F. Zimprich, E. Auff and A. Zimprich (2009). "Role of Lingo1 Polymorphisms in Parkinson's Disease." Mov Disord **24**(16): 2404-7.

Haus, O. (2000). "The Genes of Interferons and Interferon-Related Factors: Localization and Relationships with Chromosome Aberrations in Cancer." Arch Immunol Ther Exp (Warsz) **48**(2): 95-100.

Hellman, A., A. Rahat, S. W. Scherer, A. Darvasi, L. C. Tsui and B. Kerem (2000). "Replication Delay Along Fra7h, a Common Fragile Site on Human Chromosome 7, Leads to Chromosomal Instability." Mol Cell Biol **20**(12): 4420-7.

Hellman, A., E. Zlotorynski, S. W. Scherer, J. Cheung, J. B. Vincent, D. I. Smith, L. Trakhtenbrot and B. Kerem (2002). "A Role for Common Fragile Site Induction in Amplification of Human Oncogenes." Cancer Cell **1**(1): 89-97.

Helmrich, A., K. Stout-Weider, A. Matthaei, K. Hermann, T. Heiden and E. Schrock (2007). "Identification of the Human/Mouse Syntenic Common Fragile Site Fra7k/Fra12c1--Relation of Fra7k and Other Human Common Fragile Sites on Chromosome 7 to Evolutionary Breakpoints." Int J Cancer **120**(1): 48-54.

Henegariu, O., P. Bray-Ward and D. C. Ward (2000). "Custom Fluorescent-Nucleotide Synthesis as an Alternative Method for Nucleic Acid Labeling." Nat Biotechnol **18**(3): 345-8.

Hewett, D. R., O. Handt, L. Hobson, M. Mangelsdorf, H. J. Eyre, E. Baker, G. R. Sutherland, S. Schuffenhauer, J. I. Mao and R. I. Richards (1998). "Fra10b Structure Reveals Common Elements in Repeat Expansion and Chromosomal Fragile Site Genesis." Mol Cell **1**(6): 773-81.

Hirsch, B. (1991). "Sister Chromatid Exchanges Are Preferentially Induced at Expressed and Nonexpressed Common Fragile Sites." Hum Genet **87**(3): 302-6.

Hormozian, F., J. G. Schmitt, E. Sagulenko, M. Schwab and L. Savelyeva (2007). "Fra1e Common Fragile Site Breaks Map within a 370kilobase Pair Region and Disrupt the Dihydropyrimidine Dehydrogenase Gene (Dpyd)." Cancer Lett **246**(1-2): 82-91.

Howlett, N. G., T. Taniguchi, S. G. Durkin, A. D. D'Andrea and T. W. Glover (2005). "The Fanconi Anemia Pathway Is Required for the DNA Replication Stress Response and for the Regulation of Common Fragile Site Stability." Hum Mol Genet **14**(5): 693-701.

Huang, H., C. Qian, R. B. Jenkins and D. I. Smith (1998). "Fish Mapping of Yac Clones at Human Chromosomal Band 7q31.2: Identification of Yacs Spanning Fra7g within the Common Region of Loh in Breast and Prostate Cancer." Genes Chromosomes Cancer **21**(2): 152-9.

Huebner, K. and C. M. Croce (2001). "Fra3b and Other Common Fragile Sites: The Weakest Links." Nat Rev Cancer **1**(3): 214-21.

Ikeda, Y., Y. Imai, H. Kumagai, T. Nosaka, Y. Morikawa, T. Hisaoka, I. Manabe, K. Maemura, T. Nakaoka, T. Imamura, K. Miyazono, I. Komuro, R. Nagai and T. Kitamura (2004). "Vasorin, a Transforming Growth Factor Beta-Binding Protein Expressed in Vascular Smooth Muscle Cells, Modulates the Arterial Response to Injury in Vivo." Proc Natl Acad Sci U S A **101**(29): 10732-7.

Ishii, N., A. Wanaka and M. Tohyama (1996). "Increased Expression of Nlrr-3 Mrna after Cortical Brain Injury in Mouse." Brain Res Mol Brain Res **40**(1): 148-52.

Ishwad, C. S., R. E. Ferrell, K. N. Rossie, B. N. Appel, J. T. Johnson, E. N. Myers, J. C. Law, S. Srivastava and S. M. Gollin (1996). "Loss of Heterozygosity of the Short Arm of Chromosomes 3 and 9 in Oral Cancer." Int J Cancer **69**(1): 1-4.

Jacobs, P. A., T. W. Glover, M. Mayer, P. Fox, J. W. Gerrard, H. G. Dunn and D. S. Herbst (1980). "X-Linked Mental Retardation: A Study of 7 Families." Am J Med Genet **7**(4): 471-89.

James, C. D., J. He, V. P. Collins, M. J. Allalunis-Turner and R. S. Day, 3rd (1993). "Localization of Chromosome 9p Homozygous Deletions in Glioma Cell Lines with Markers Constituting a Continuous Linkage Group." Cancer Res **53**(16): 3674-6.

Jin, Y., Y. Stewenius, D. Lindgren, A. Frigyesi, O. Calcagnile, T. Jonson, A. Edqvist, N. Larsson, L. M. Lundberg, G. Chebil, F. Liedberg, S. Gudjonsson, W. Mansson, M. Hoglund and D. Gisselsson (2007). "Distinct Mitotic Segregation Errors Mediate

Chromosomal Instability in Aggressive Urothelial Cancers." Clin Cancer Res **13**(6): 1703-12.

Jones, C., Penny, L., Mattina, T., Yu, S., Baker, E., Voullair, L., Langdon, WY., Sutherland, GR., Richards, RI., Tunnacliffe, A. (1995). "Association of a Chromosome Deletion Syndrome with a Fragile Site within the Proto-Oncogene Cbl2." Nature **376**(6536): 145-149.

Kamatani, N., W. A. Nelson-Rees and D. A. Carson (1981). "Selective Killing of Human Malignant Cell Lines Deficient in Methylthioadenosine Phosphorylase, a Purine Metabolic Enzyme." Proc Natl Acad Sci U S A **78**(2): 1219-23.

Kamath, A., H. Tara, B. Xiang, R. Bajaj, W. He and P. Li (2008). "Double-Minute Myc Amplification and Deletion of Mtap, Cdkn2a, Cdkn2b, and Elavl2 in an Acute Myeloid Leukemia Characterized by Oligonucleotide-Array Comparative Genomic Hybridization." Cancer Genet Cytogenet **183**(2): 117-20.

Kamb, A., N. A. Gruis, J. Weaver-Feldhaus, Q. Liu, K. Harshman, S. V. Tavtigian, E. Stockert, R. S. Day, 3rd, B. E. Johnson and M. H. Skolnick (1994). "A Cell Cycle Regulator Potentially Involved in Genesis of Many Tumor Types." Science **264**(5157): 436-40.

Kameoka, Y., H. Tagawa, S. Tsuzuki, S. Karnan, A. Ota, M. Suguro, R. Suzuki, M. Yamaguchi, Y. Morishima, S. Nakamura and M. Seto (2004). "Contig Array Cgh at 3p14.2 Points to the Fra3b/Fhit Common Fragile Region as the Target Gene in Diffuse Large B-Cell Lymphoma." Oncogene **23**(56): 9148-54.

Kisselev L.L., J. J., Wolfson A.D., Frolova L.Y. (1998). "Diadenosine Oligophosphates (Ap(N)a), a Novel Class of Signaling Molecules." Fed. Euro. Biochem. Soc. Lett. **427**: 157–163.

Kobayashi, H., H. Kajiwara, S. Kanayama, Y. Yamada, N. Furukawa, T. Noguchi, S. Haruta, S. Yoshida, M. Sakata, T. Sado and H. Oi (2009). "Molecular Pathogenesis of Endometriosis-Associated Clear Cell Carcinoma of the Ovary (Review)." Oncol Rep **22**(2): 233-40.

Koundrioukoff, S., S. Polo and G. Almouzni (2004). "Interplay between Chromatin and Cell Cycle Checkpoints in the Context of Atr/Atm-Dependent Checkpoints." DNA Repair (Amst) **3**(8-9): 969-78.

Krajewski, W. A. (1995). "Alterations in the Internucleosomal DNA Helical Twist in Chromatin of Human Erythroleukemia Cells in Vivo Influences the Chromatin Higher-Order Folding." FEBS Lett **361**(2-3): 149-52.

Krajewski, W. A. and J. Ausio (1997). "Relationship between Chromatin High-Order Folding and Nucleosomal Linker Twist in Nuclei of Human Hela S3 Cells." J Biomol Struct Dyn **14**(5): 641-9.

Krummel, K. A., S. R. Denison, E. Calhoun, L. A. Phillips and D. I. Smith (2002). "The Common Fragile Site Fra16d and Its Associated Gene Wwox Are Highly Conserved in the Mouse at Fra8e1." Genes Chromosomes Cancer **34**(2): 154-67.

Krummel, K. A., L. R. Roberts, M. Kawakami, T. W. Glover and D. I. Smith (2000). "The Characterization of the Common Fragile Site Fra16d and Its Involvement in Multiple Myeloma Translocations." Genomics **69**(1): 37-46.

Kuo, M. T., R. C. Vyas, L. X. Jiang and W. N. Hittelman (1994). "Chromosome Breakage at a Major Fragile Site Associated with P-Glycoprotein Gene Amplification in Multidrug-Resistant Cho Cells." Mol Cell Biol **14**(8): 5202-11.

Kuroki, T., F. Trapasso, T. Shiraishi, H. Alder, K. Mimori, M. Mori and C. M. Croce (2002). "Genetic Alterations of the Tumor Suppressor Gene Wwox in Esophageal Squamous Cell Carcinoma." Cancer Res **62**(8): 2258-60.

Kuroki, T., S. Yendamuri, F. Trapasso, A. Matsuyama, R. I. Aqeilan, H. Alder, S. Rattan, R. Cesari, M. L. Nolli, N. N. Williams, M. Mori, T. Kanematsu and C. M. Croce (2004). "The Tumor Suppressor Gene Wwox at Fra16d Is Involved in Pancreatic Carcinogenesis." Clin Cancer Res **10**(7): 2459-65.

Lambert, S. and B. S. Lopez (2001). "Role of Rad51 in Sister-Chromatid Exchanges in Mammalian Cells." Oncogene **20**(45): 6627-31.

Lauren, J., Airaksinen, M., Saarma, M., Timmusk, T.T., (2003). "A Novel Gene Family Encoding Leucine-Rich Repeat Transmembrane Proteins Differentially Expressed in the Nervous System." Genomics **81**: 411-421.

Le Beau, M. M., F. V. Rassool, M. E. Neilly, R. Espinosa, 3rd, T. W. Glover, D. I. Smith and T. W. McKeithan (1998). "Replication of a Common Fragile Site, Fra3b, Occurs Late in S Phase and Is Delayed Further Upon Induction: Implications for the Mechanism of Fragile Site Induction." Hum Mol Genet **7**(4): 755-61.

Le Beau, M. M., Rassool, F.V., Neilly, M.E., Espinosa III, R., Glover, T.W., Smith, D.I., McKeithan, T.W. (1998). "Replication of a Common Fragile Site, Fra3b, Occurs Late in S Phase and Is Delayed Further Upon Induction: Implications for the Mechanism of Fragile Site Induction." Hum. Mol. Genet. **7**: 755-761.

Lee, S. H., W. H. Kim, H. K. Kim, K. M. Woo, H. S. Nam, H. S. Kim, J. G. Kim and M. H. Cho (2001). "Altered Expression of the Fragile Histidine Triad Gene in Primary Gastric Adenocarcinomas." Biochem Biophys Res Commun **284**(3): 850-5.

Lewandowska, U., M. Zelazowski, K. Seta, M. Byczewska, E. Pluciennik and A. K. Bednarek (2009). "Wwox, the Tumour Suppressor Gene Affected in Multiple Cancers." J Physiol Pharmacol **60 Suppl 1**: 47-56.

Lim, G., J. Karaskova, B. Beheshti, B. Vukovic, J. Bayani, S. Selvarajah, S. K. Watson, W. L. Lam, M. Zielenska and J. A. Squire (2005). "An Integrated Mband and Submegabase Resolution Tiling Set (Smrt) Cgh Array Analysis of Focal Amplification, Microdeletions, and Ladder Structures Consistent with Breakage-Fusion-Bridge Cycle Events in Osteosarcoma." Genes Chromosomes Cancer **42**(4): 392-403.

Limongi, M. Z., F. Pelliccia and A. Rocchi (2003). "Characterization of the Human Common Fragile Site Fra2g." Genomics **81**(2): 93-7.

Lorenzetti, D., B. Antalffy, H. Vogel, J. Noveroske, D. Armstrong and M. Justice (2004). "The Neurological Mutant Quaking(Viable) Is Parkin Deficient." Mamm Genome **15**(3): 210-7.

Ludes-Meyers, J. H., H. Kil, J. Parker-Thornburg, D. F. Kusewitt, M. T. Bedford and C. M. Aldaz (2009). "Generation and Characterization of Mice Carrying a Conditional Allele of the Wwox Tumor Suppressor Gene." PLoS One **4**(11): e7775.

Lukusa, T. and J. P. Fryns (2008). "Human Chromosome Fragility." Biochim Biophys Acta **1779**(1): 3-16.

Lydiatt, W. M., B. J. Davidson, S. P. Schantz, S. Caruana and R. S. Chaganti (1998). "9p21 Deletion Correlates with Recurrence in Head and Neck Cancer." Head Neck **20**(2): 113-8.

Magenis, R. E., F. Hecht and E. W. Lovrien (1970). "Heritable Fragile Site on Chromosome 16: Probable Localization of Haptoglobin Locus in Man." Science **170**(953): 85-7.

Makino, K., K. Umeda, A. Uezu, Y. Hiragami, T. Sakamoto, H. Ihn and H. Nakanishi (2008). "Identification and Characterization of the Novel Centrosomal Protein Centlein." Biochem Biophys Res Commun **366**(4): 958-62.

Mangelsdorf, M., K. Ried, E. Woollatt, S. Dayan, H. Eyre, M. Finnis, L. Hobson, J. Nancarrow, D. Venter, E. Baker and R. I. Richards (2000). "Chromosomal Fragile Site Fra16d and DNA Instability in Cancer." Cancer Res **60**(6): 1683-9.

Mangelsdorf M., H. D., Hobson L,. Baker E., Eyre H.J., Lapsys N., Le Paslier D., Dogget N.A., Sutherland G.R., Richards R.I. (1997). "Human Chromosomal Fragile Site Fra16bis an Amplified at-Rich Minisatellite Repeat." Cell **88**: 367-374.

Mao, L., J. S. Lee, Y. H. Fan, J. Y. Ro, J. G. Batsakis, S. Lippman, W. Hittelman and W. K. Hong (1996). "Frequent Microsatellite Alterations at Chromosomes 9p21 and 3p14 in Oral Premalignant Lesions and Their Value in Cancer Risk Assessment." Nat Med **2**(6): 682-5.

Matsuyama, A., T. Shiraishi, F. Trapasso, T. Kuroki, H. Alder, M. Mori, K. Huebner and C. M. Croce (2003). "Fragile Site Orthologs Fhit/Fra3b and Fhit/Fra14a2: Evolutionarily Conserved but Highly Recombinogenic." Proc Natl Acad Sci U S A **100**(25): 14988-93.

Mc Clintock, B. (1951). "Chromosome Organization and Genic Expression." Cold Spring Harb Symp Quant Biol **16**: 13-47.

McAllister, B. F. and I. F. Greenbaum (1997). "How Common Are Common Fragile Sites: Variation of Aphidicolin-Induced Chromosomal Fragile Sites in a Population of the Deer Mouse (Peromyscus Maniculatus)." Hum Genet **100**(2): 182-8.

McDermott, K. M., J. Zhang, C. R. Holst, B. K. Kozakiewicz, V. Singla and T. D. Tlsty (2006). "P16(Ink4a) Prevents Centrosome Dysfunction and Genomic Instability in Primary Cells." PLoS Biol **4**(3): e51.

Michael, D., D. G. Beer, C. W. Wilke, D. E. Miller and T. W. Glover (1997). "Frequent Deletions of Fhit and Fra3b in Barrett's Metaplasia and Esophageal Adenocarcinomas." Oncogene **15**(14): 1653-9.

Mimori, K., T. Druck, H. Inoue, H. Alder, L. Berk, M. Mori, K. Huebner and C. M. Croce (1999). "Cancer-Specific Chromosome Alterations in the Constitutive Fragile Region Fra3b." Proc Natl Acad Sci U S A **96**(13): 7456-61.

Miro, R., I. C. Clemente, C. Fuster and J. Egozcue (1987). "Fragile Sites, Chromosome Evolution, and Human Neoplasia." Hum Genet **75**(4): 345-9.

Mishmar, D., A. Rahat, S. W. Scherer, G. Nyakatura, B. Hinzmann, Y. Kohwi, Y. Mandel-Gutfroind, J. R. Lee, B. Drescher, D. E. Sas, H. Margalit, M. Platzer, A. Weiss, L. C. Tsui, A. Rosenthal and B. Kerem (1998). "Molecular Characterization of a Common Fragile Site (Fra7h) on Human Chromosome 7 by the Cloning of a Simian Virus 40 Integration Site." Proc Natl Acad Sci U S A **95**(14): 8141-6.

Mora, J., M. Alaminos, C. de Torres, P. Illei, J. Qin, N. K. Cheung and W. L. Gerald (2004). "Comprehensive Analysis of the 9p21 Region in Neuroblastoma Suggests a Role for Genes Mapping to 9p21-23 in the Biology of Favourable Stage 4 Tumours." Br J Cancer **91**(6): 1112-8.

Musio, A., C. Montagna, T. Mariani, M. Tilenni, M. L. Focarelli, L. Brait, E. Indino, P. A. Benedetti, L. Chessa, A. Albertini, T. Ried and P. Vezzoni (2005). "Smc1 Involvement in Fragile Site Expression." Hum Mol Genet **14**(4): 525-33.

Nancarrow, J. K., K. Holman, M. Mangelsdorf, T. Hori, M. Denton, G. R. Sutherland and R. I. Richards (1995). "Molecular Basis of P(Ccg)N Repeat Instability at the Fra16a Fragile Site Locus." Hum Mol Genet **4**(3): 367-72.

Neville, E. M., M. Stewart, M. Myskow, R. J. Donnelly and J. K. Field (1995). "Loss of Heterozygosity at 9p23 Defines a Novel Locus in Non-Small Cell Lung Cancer." Oncogene **11**(3): 581-5.

Nobori, T., K. Miura, D. J. Wu, A. Lois, K. Takabayashi and D. A. Carson (1994). "Deletions of the Cyclin-Dependent Kinase-4 Inhibitor Gene in Multiple Human Cancers." Nature **368**(6473): 753-6.

O'Keefe, L. V. and R. I. Richards (2006). "Common Chromosomal Fragile Sites and Cancer: Focus on Fra16d." Cancer Lett **232**(1): 37-47.

Oberle, I., F. Rousseau, D. Heitz, C. Kretz, D. Devys, A. Hanauer, J. Boue, M. F. Bertheas and J. L. Mandel (1991). "Instability of a 550-Base Pair DNA Segment and Abnormal Methylation in Fragile X Syndrome." Science **252**(5010): 1097-102.

Ohnishi, H., M. Kawamura, K. Ida, X. M. Sheng, R. Hanada, T. Nobori, S. Yamamori and Y. Hayashi (1995). "Homozygous Deletions of P16/Mts1 Gene Are Frequent but Mutations Are Infrequent in Childhood T-Cell Acute Lymphoblastic Leukemia." Blood **86**(4): 1269-75.

Ohta, M., H. Inoue, M. G. Cotticelli, K. Kastury, R. Baffa, J. Palazzo, Z. Siprashvili, M. Mori, P. McCue, T. Druck, C. M. Croce and K. Huebner (1996). "The Fhit Gene, Spanning the Chromosome 3p14.2 Fragile Site and Renal Carcinoma-Associated T(3;8) Breakpoint, Is Abnormal in Digestive Tract Cancers." Cell **84**(4): 587-97.

Olopade, O. I., D. L. Buchhagen, K. Malik, J. Sherman, T. Nobori, S. Bader, M. M. Nau, A. F. Gazdar, J. D. Minna and M. O. Diaz (1993). "Homozygous Loss of the Interferon Genes Defines the Critical Region on 9p That Is Deleted in Lung Cancers." Cancer Res **53**(10 Suppl): 2410-5.

Ozeri-Galai, E., M. Schwartz, A. Rahat and B. Kerem (2008). "Interplay between Atm and Atr in the Regulation of Common Fragile Site Stability." Oncogene **27**(15): 2109-17.

Pack, S. D., L. X. Qin, E. Pak, Y. Wang, D. O. Ault, P. Mannan, S. Jaikumar, C. A. Stratakis, E. H. Oldfield, Z. Zhuang and R. J. Weil (2005). "Common Genetic Changes in Hereditary and Sporadic Pituitary Adenomas Detected by Comparative Genomic Hybridization." Genes Chromosomes Cancer **43**(1): 72-82.

Paige, A. J., K. J. Taylor, A. Stewart, J. G. Sgouros, H. Gabra, G. C. Sellar, J. F. Smyth, D. J. Porteous and J. E. Watson (2000). "A 700-Kb Physical Map of a Region of 16q23.2 Homozygously Deleted in Multiple Cancers and Spanning the Common Fragile Site Fra16d." Cancer Res **60**(6): 1690-7.

Paige, A. J., K. J. Taylor, C. Taylor, S. G. Hillier, S. Farrington, D. Scott, D. J. Porteous, J. F. Smyth, H. Gabra and J. E. Watson (2001). "Wwox: A Candidate Tumor Suppressor Gene Involved in Multiple Tumor Types." Proc Natl Acad Sci U S A **98**(20): 11417-22.

Palakodeti, A., Y. Han, Y. Jiang and M. M. Le Beau (2004). "The Role of Late/Slow Replication of the Fra16d in Common Fragile Site Induction." Genes Chromosomes Cancer **39**(1): 71-6.

Paradee, W., C. M. Wilke, L. Wang, R. Shridhar, C. M. Mullins, A. Hoge, T. W. Glover and D. I. Smith (1996). "A 350-Kb Cosmid Contig in 3p14.2 That Crosses the T(3;8) Hereditary Renal Cell Carcinoma Translocation Breakpoint and 17 Aphidicolin-Induced Fra3b Breakpoints." Genomics **35**(1): 87-93.

Park, Y. B., M. J. Park, K. Kimura, K. Shimizu, S. H. Lee and J. Yokota (2002). "Alterations in the Ink4a/Arf Locus and Their Effects on the Growth of Human Osteosarcoma Cell Lines." Cancer Genet Cytogenet **133**(2): 105-11.

Pearson, C. E. and R. R. Sinden (1998). "Trinucleotide Repeat DNA Structures: Dynamic Mutations from Dynamic DNA." Curr Opin Struct Biol **8**(3): 321-30.

Perinchery, G., N. Bukurov, K. Nakajima, J. Chang, L. C. Li and R. Dahiya (1999). "High Frequency of Deletion on Chromosome 9p21 May Harbor Several Tumor-Suppressor Genes in Human Prostate Cancer." Int J Cancer **83**(5): 610-4.

Perry, A., R. Banerjee, C. M. Lohse, B. K. Kleinschmidt-DeMasters and B. W. Scheithauer (2002). "A Role for Chromosome 9p21 Deletions in the Malignant Progression of Meningiomas and the Prognosis of Anaplastic Meningiomas." Brain Pathol **12**(2): 183-90.

Pomykala, H. M., S. K. Bohlander, P. L. Broeker, O. I. Olopade and M. O. Diaz (1994). "Breakpoint Junctions of Chromosome 9p Deletions in Two Human Glioma Cell Lines." Mol Cell Biol **14**(11): 7604-10.

Popescu, N. C. and J. A. DiPaolo (1989). "Preferential Sites for Viral Integration on Mammalian Genome." Cancer Genet Cytogenet **42**(2): 157-71.

Ragland, R. L., M. W. Glynn, M. F. Arlt and T. W. Glover (2008). "Stably Transfected Common Fragile Site Sequences Exhibit Instability at Ectopic Sites." Genes Chromosomes Cancer **47**(10): 860-72.

Rassool, F. V., T. W. McKeithan, M. E. Neilly, E. van Melle, R. Espinosa, 3rd and M. M. Le Beau (1991). "Preferential Integration of Marker DNA into the Chromosomal Fragile Site at 3p14: An Approach to Cloning Fragile Sites." Proc Natl Acad Sci U S A **88**(15): 6657-61.

Re, A., D. Cora, A. M. Puliti, M. Caselle and I. Sbrana (2006). "Correlated Fragile Site Expression Allows the Identification of Candidate Fragile Genes Involved in Immunity and Associated with Carcinogenesis." BMC Bioinformatics **7**: 413.

Richards, R. I. (2001). "Fragile and Unstable Chromosomes in Cancer: Causes and Consequences." Trends Genet **17**(6): 339-45.

Ried, K., M. Finnis, L. Hobson, M. Mangelsdorf, S. Dayan, J. K. Nancarrow, E. Woollatt, G. Kremmidiotis, A. Gardner, D. Venter, E. Baker and R. I. Richards (2000). "Common Chromosomal Fragile Site Fra16d Sequence: Identification of the for Gene Spanning Fra16d and Homozygous Deletions and Translocation Breakpoints in Cancer Cells." Hum Mol Genet **9**(11): 1651-63.

Robinson, M., Parsons Perez, M.C., Tebar, L., Palmer, J., Patel, A., Marks, D., Sheasby, A., DE Felipe, C., Coffin, R., Livesey, F., Hunt, S.P. (2004). "Flrt3 Is Expressed in Sensory Neurons after Peripheral Nerve Injury and Regulates Neurite Outgrowth." Mol. Cell Neurosci. **27**: 202-214.

Romano, R. A., H. Li, R. Tummala, R. Maul and S. Sinha (2004). "Identification of Basonuclin2, a DNA-Binding Zinc-Finger Protein Expressed in Germ Tissues and Skin Keratinocytes." Genomics **83**(5): 821-33.

Rozier, L., E. El-Achkar, F. Apiou and M. Debatisse (2004). "Characterization of a Conserved Aphidicolin-Sensitive Common Fragile Site at Human 4q22 and Mouse 6c1: Possible Association with an Inherited Disease and Cancer." Oncogene **23**(41): 6872-80.

Ruiz-Herrera, A., J. Castresana and T. J. Robinson (2006). "Is Mammalian Chromosomal Evolution Driven by Regions of Genome Fragility?" Genome Biol **7**(12): R115.

Ruiz-Herrera, A., F. Garcia, L. Fronicke, M. Ponsa, J. Egozcue, M. G. Caldes and R. Stanyon (2004). "Conservation of Aphidicolin-Induced Fragile Sites in Papionini (Primates) Species and Humans." Chromosome Res **12**(7): 683-90.

Ruiz-Herrera, A., F. Garcia, E. Giulotto, C. Attolini, J. Egozcue, M. Ponsa and M. Garcia (2005). "Evolutionary Breakpoints Are Co-Localized with Fragile Sites and Intrachromosomal Telomeric Sequences in Primates." Cytogenet Genome Res **108**(1-3): 234-47.

Salah Z, A. R., Huebner K (2010). "Wwox Gene and Gene Product: Tumor Suppression through Specific Protein Interactions." Future Oncol. **6**(2): 249-259.

Sanz-Casla, M. T., M. L. Maestro, V. del Barco, I. Zanna, J. Moreno, M. Vidaurreta, I. Almansa, C. Fernandez, J. Blanco, C. Maestro and L. Resel (2003). "Loss of Heterozygosity and Methylation of P16 in Renal Cell Carcinoma." Urol Res **31**(3): 159-62.

Sarafidou, T., C. Kahl, I. Martinez-Garay, M. Mangelsdorf, S. Gesk, E. Baker, M. Kokkinaki, P. Talley, E. L. Maltby, L. French, L. Harder, B. Hinzmann, C. Nobile, K. Richkind, M. Finnis, P. Deloukas, G. R. Sutherland, K. Kutsche, N. K. Moschonas, R. Siebert and J. Gecz (2004). "Folate-Sensitive Fragile Site Fra10a Is Due to an Expansion of a Cgg Repeat in a Novel Gene, Fra10ac1, Encoding a Nuclear Protein." Genomics **84**(1): 69-81.

Sasaki, M. S., M. Takata, E. Sonoda, A. Tachibana and S. Takeda (2004). "Recombination Repair Pathway in the Maintenance of Chromosomal Integrity against DNA Interstrand Crosslinks." Cytogenet Genome Res **104**(1-4): 28-34.

Sato, M., K. Takahashi, K. Nagayama, Y. Arai, N. Ito, M. Okada, J. D. Minna, J. Yokota and T. Kohno (2005). "Identification of Chromosome Arm 9p as the Most Frequent Target of Homozygous Deletions in Lung Cancer." Genes Chromosomes Cancer **44**(4): 405-14.

Savelyeva, L., A. Claas, H. An, R. G. Weber, P. Lichter and M. Schwab (1999). "Retention of Polysomy at 9p23-24 During Karyotypic Evolution in Human Breast Cancer Cell Line Colo 824." Genes Chromosomes Cancer **24**(1): 87-93.

Savelyeva, L., A. Claas, I. Matzner, P. Schlag, W. Hofmann, S. Scherneck, B. Weber and M. Schwab (2001). "Constitutional Genomic Instability with Inversions, Duplications, and Amplifications in 9p23-24 in Brca2 Mutation Carriers." Cancer Res **61**(13): 5179-85.

Savelyeva, L., E. Sagulenko, J. G. Schmitt and M. Schwab (2006). "The Neurobeachin Gene Spans the Common Fragile Site Fra13a." Hum Genet **118**(5): 551-8.

Sawada, M., N. Inase, M. Imai, Y. Ohtani, S. Miyake, H. Akamatsu and Y. Yoshizawa (2003). "Chromosome 9p Deletion in Squamous Metaplasia in Cystic Lesion of the Lung." Respirology **8**(2): 239-42.

Sawinska, M., J. G. Schmitt, E. Sagulenko, F. Westermann, M. Schwab and L. Savelyeva (2007). "Novel Aphidicolin-Inducible Common Fragile Site Fra9g Maps to 9p22.2, within the C9orf39 Gene." Genes Chromosomes Cancer **46**(11): 991-9.

Schmid, M., D. Malicki, T. Nobori, M. D. Rosenbach, K. Campbell, D. A. Carson and C. J. Carrera (1998). "Homozygous Deletions of Methylthioadenosine Phosphorylase (Mtap) Are More Frequent Than P16ink4a (Cdkn2) Homozygous Deletions in Primary Non-Small Cell Lung Cancers (Nsclc)." Oncogene **17**(20): 2669-75.

Schwartz, M., E. Zlotorynski and B. Kerem (2006). "The Molecular Basis of Common and Rare Fragile Sites." Cancer Lett **232**(1): 13-26.

Serrano, M., G. J. Hannon and D. Beach (1993). "A New Regulatory Motif in Cell-Cycle Control Causing Specific Inhibition of Cyclin D/Cdk4." Nature **366**(6456): 704-7.

Sevignani, C., G. A. Calin, L. D. Siracusa and C. M. Croce (2006). "Mammalian Micrornas: A Small World for Fine-Tuning Gene Expression." Mamm Genome **17**(3): 189-202.

Shang, C., W. N. Fu, Y. Guo, D. F. Huang and K. L. Sun (2007). "Study of the Sh3-Domain Grb2-Like 2 Gene Expression in Laryngeal Carcinoma." Chin Med J (Engl) **120**(5): 385-8.

Shao, J. Y., W. F. Zeng and Y. X. Zeng (2002). "[Molecular Genetic Progression on Nasopharyngeal Carcinoma]." Ai Zheng **21**(1): 1-10.

Sherr, C. J. (2000). "The Pezcoller Lecture: Cancer Cell Cycles Revisited." Cancer Res **60**(14): 3689-95.

Shibukawa, K., N. Miyokawa, Y. Tokusashi, T. Sasaki, S. Osanai and Y. Ohsaki (2009). "High Incidence of Chromosomal Abnormalities at 1p36 and 9p21 in Early-Stage Central Type Squamous Cell Carcinoma and Squamous Dysplasia of Bronchus Detected by Autofluorescence Bronchoscopy." Oncol Rep **22**(1): 81-7.

Shiraishi, T., T. Druck, K. Mimori, J. Flomenberg, L. Berk, H. Alder, W. Miller, K. Huebner and C. M. Croce (2001). "Sequence Conservation at Human and Mouse Orthologous Common Fragile Regions, Fra3b/Fhit and Fra14a2/Fhit." Proc Natl Acad Sci U S A **98**(10): 5722-7.

Simoneau, A. R., C. H. Spruck, 3rd, M. Gonzalez-Zulueta, M. L. Gonzalgo, M. F. Chan, Y. C. Tsai, M. Dean, K. Steven, T. Horn and P. A. Jones (1996). "Evidence for Two Tumor Suppressor Loci Associated with Proximal Chromosome 9p to Q and Distal Chromosome 9q in Bladder Cancer and the Initial Screening for Gas1 and Ptc Mutations." Cancer Res **56**(21): 5039-43.

Sinclair, P., C. J. Harrison, M. Jarosova and L. Foroni (2005). "Analysis of Balanced Rearrangements of Chromosome 6 in Acute Leukemia: Clustered Breakpoints in Q22-Q23 and Possible Involvement of C-Myb in a New Recurrent Translocation, T(6;7)(Q23;Q32 through 36)." Haematologica **90**(5): 602-11.

Sinha, S., N. Chunder, N. Mukherjee, N. Alam, A. Roy, S. Roychoudhury and C. Kumar Panda (2008). "Frequent Deletion and Methylation in Sh3gl2 and Cdkn2a Loci Are Associated with Early- and Late-Onset Breast Carcinoma." Ann Surg Oncol **15**(4): 1070-80.

Siprashvili, Z., G. Sozzi, L. D. Barnes, P. McCue, A. K. Robinson, V. Eryomin, L. Sard, E. Tagliabue, A. Greco, L. Fusetti, G. Schwartz, M. A. Pierotti, C. M. Croce and K. Huebner (1997). "Replacement of Fhit in Cancer Cells Suppresses Tumorigenicity." Proc Natl Acad Sci U S A **94**(25): 13771-6.

Smeets, D. F. and F. A. van de Klundert (1990). "Common Fragile Sites in Man and Three Closely Related Primate Species." Cytogenet Cell Genet **53**(1): 8-14.

Smeets, D. F. C. M., Scheres, J.M.J.C., Hustinx, T.W.J. (1986). "The Most Common Fragile Site in Man Is 3p14." Hum. Genet. **72**: 215-220.

Smith, D. I., S. McAvoy, Y. Zhu and D. S. Perez (2007). "Large Common Fragile Site Genes and Cancer." Semin Cancer Biol **17**(1): 31-41.

Smith DI, Z. Y., McAvoy S, Kuhn R (2006). "Common Fragile Sites, Extremely Large Genes, Neural Development and Cancer." Cancer Lett **232**(1): 48-57.

Smith, P. P., C. L. Friedman, E. M. Bryant and J. K. McDougall (1992). "Viral Integration and Fragile Sites in Human Papillomavirus-Immortalized Human Keratinocyte Cell Lines." Genes Chromosomes Cancer **5**(2): 150-7.

Song, H., S. J. Ramus, J. Tyrer, K. L. Bolton, A. Gentry-Maharaj, E. Wozniak, H. Anton-Culver, J. Chang-Claude, D. W. Cramer, R. DiCioccio, T. Dork, E. L. Goode, M. T. Goodman, J. M. Schildkraut, T. Sellers, L. Baglietto, M. W. Beckmann, J. Beesley, J. Blaakaer, M. E. Carney, S. Chanock, Z. Chen, J. M. Cunningham, E. Dicks, J. A. Doherty, M. Durst, A. B. Ekici, D. Fenstermacher, B. L. Fridley, G. Giles, M. E. Gore, I.

De Vivo, P. Hillemanns, C. Hogdall, E. Hogdall, E. S. Iversen, I. J. Jacobs, A. Jakubowska, D. Li, J. Lissowska, J. Lubinski, G. Lurie, V. McGuire, J. McLaughlin, K. Medrek, P. G. Moorman, K. Moysich, S. Narod, C. Phelan, C. Pye, H. Risch, I. B. Runnebaum, G. Severi, M. Southey, D. O. Stram, F. C. Thiel, K. L. Terry, Y. Y. Tsai, S. S. Tworoger, D. J. Van Den Berg, R. A. Vierkant, S. Wang-Gohrke, P. M. Webb, L. R. Wilkens, A. H. Wu, H. Yang, W. Brewster, A. Ziogas, R. Houlston, I. Tomlinson, A. S. Whittemore, M. A. Rossing, B. A. Ponder, C. L. Pearce, R. B. Ness, U. Menon, S. K. Kjaer, J. Gronwald, M. Garcia-Closas, P. A. Fasching, D. F. Easton, G. Chenevix-Trench, A. Berchuck, P. D. Pharoah and S. A. Gayther (2009). "A Genome-Wide Association Study Identifies a New Ovarian Cancer Susceptibility Locus on 9p22.2." Nat Genet **41**(9): 996-1000.

Soulie, J. and J. De Grouchy (1981). "A Cytogenetic Survey of 110 Baboons (Papio Cynocephalus)." Am J Phys Anthropol **56**(2): 107-13.

Sozzi, G., S. Tornielli, E. Tagliabue, L. Sard, F. Pezzella, U. Pastorino, F. Minoletti, S. Pilotti, C. Ratcliffe, M. L. Veronese, P. Goldstraw, K. Huebner, C. M. Croce and M. A. Pierotti (1997). "Absence of Fhit Protein in Primary Lung Tumors and Cell Lines with Fhit Gene Abnormalities." Cancer Res **57**(23): 5207-12.

Stark, J. M., P. Hu, A. J. Pierce, M. E. Moynahan, N. Ellis and M. Jasin (2002). "Atp Hydrolysis by Mammalian Rad51 Has a Key Role During Homology-Directed DNA Repair." J Biol Chem **277**(23): 20185-94.

Stone, D. M., P. B. Jacky and D. J. Prieur (1991). "Chromosomal Fragile Site Expression in Dogs: Ii. Expression in Boxer Dogs with Mast Cell Tumors." Am J Med Genet **40**(2): 223-9.

Stone, D. M., K. E. Stephens and J. Doles (1993). "Folate-Sensitive and Aphidicolin-Inducible Fragile Sites Are Expressed in the Genome of the Domestic Cat." Cancer Genet Cytogenet **65**(2): 130-4.

Sun, X. J., K. L. Sun, Z. H. Zheng, W. N. Fu, D. M. Hao, H. M. Xu and X. M. Li (2006). "Gene Expression Patterns in Gastric Cancer." Zhonghua Yi Xue Yi Chuan Xue Za Zhi **23**(2): 142-6.

Sunamura, M., M. Oonuma, F. Motoi, H. Abe, Y. Saitoh, T. Hoshida, S. Ottomo, A. Horii and S. Matsuno (2002). "Gene Therapy for Pancreatic Cancer Targeting the Genomic Alterations of Tumor Suppressor Genes Using Replication-Selective Oncolytic Adenovirus." Hum Cell **15**(3): 138-50.

Sutherland, G. R. (1979). "Heritable Fragile Sites on Human Chromosomes I. Factors Affecting Expression in Lymphocyte Culture." Am J Hum Genet **31**(2): 125-35.

Sutherland, G. R. (2003). "Rare Fragile Sites." Cytogenet Genome Res **100**(1-4): 77-84.

Sutherland, G. R., E. Baker and R. S. Seshadri (1980). "Heritable Fragile Sites on Human Chromosomes. V. A New Class of Fragile Site Requiring Brdu for Expression." Am J Hum Genet **32**(4): 542-8.

Sutherland, G. R., P. B. Jacky and E. G. Baker (1984). "Heritable Fragile Sites on Human Chromosomes. Xi. Factors Affecting Expression of Fragile Sites at 10q25, 16q22, and 17p12." Am J Hum Genet **36**(1): 110-22.

Sutherland, G. R. and R. I. Richards (1995). "The Molecular Basis of Fragile Sites in Human Chromosomes." Curr Opin Genet Dev **5**(3): 323-7.

Takata, M., M. S. Sasaki, S. Tachiiri, T. Fukushima, E. Sonoda, D. Schild, L. H. Thompson and S. Takeda (2001). "Chromosome Instability and Defective Recombinational Repair in Knockout Mutants of the Five Rad51 Paralogs." Mol Cell Biol **21**(8): 2858-66.

Takita, J., Y. Hayashi, T. Kohno, N. Yamaguchi, R. Hanada, K. Yamamoto and J. Yokota (1997). "Deletion Map of Chromosome 9 and P16 (Cdkn2a) Gene Alterations in Neuroblastoma." Cancer Res **57**(5): 907-12.

Tanaka, H., Y. Shimada, M. Imamura, I. Shibagaki and K. Ishizaki (1997). "Multiple Types of Aberrations in the P16 (Ink4a) and the P15(Ink4b) Genes in 30 Esophageal Squamous-Cell-Carcinoma Cell Lines." Int J Cancer **70**(4): 437-42.

Thorland EC, M. S., Persing DH, Sarkar G, McGovern RM, Gostout BS, Smith D (2000). "Human Papillomavirus Type 16 Integrations in Cervical Tumours Frequently Occur in Common Fragile Sites." Cancer Res. **60**(21): 5916-21.

Thorland, E. C., S. L. Myers, B. S. Gostout and D. I. Smith (2003). "Common Fragile Sites Are Preferential Targets for Hpv16 Integrations in Cervical Tumors." Oncogene **22**(8): 1225-37.

Toledo, F., D. Le Roscouet, G. Buttin and M. Debatisse (1992). "Co-Amplified Markers Alternate in Megabase Long Chromosomal Inverted Repeats and Cluster Independently in Interphase Nuclei at Early Steps of Mammalian Gene Amplification." EMBO J **11**(7): 2665-73.

Tucker, J. D., N. J. Jones, N. A. Allen, J. L. Minkler, L. H. Thompson and A. V. Carrano (1991). "Cytogenetic Characterization of the Ionizing Radiation-Sensitive Chinese Hamster Mutant Irs1." Mutat Res **254**(2): 143-52.

Unger, K., E. Malisch, G. Thomas, H. Braselmann, A. Walch, G. Jackl, P. Lewis, E. Lengfelder, T. Bogdanova, J. Wienberg and H. Zitzelsberger (2008). "Array Cgh Demonstrates Characteristic Aberration Signatures in Human Papillary Thyroid Carcinomas Governed by Ret/Ptc." Oncogene **27**(33): 4592-602.

Usdin, K. and K. J. Woodford (1995). "Cgg Repeats Associated with DNA Instability and Chromosome Fragility Form Structures That Block DNA Synthesis in Vitro." Nucleic Acids Res **23**(20): 4202-9.

Usvasalo, A., S. Ninomiya, R. Raty, J. Hollmen, U. M. Saarinen-Pihkala, E. Elonen and S. Knuutila "Focal 9p Instability in Hematologic Neoplasias Revealed by Comparative Genomic Hybridization and Single-Nucleotide Polymorphism Microarray Analyses." Genes Chromosomes Cancer **49**(4): 309-18.

Vanhoutteghem, A. and P. Djian (2006). "Basonuclins 1 and 2, Whose Genes Share a Common Origin, Are Proteins with Widely Different Properties and Functions." Proc Natl Acad Sci U S A **103**(33): 12423-8.

Verkerk, A. J., C. A. Mathews, M. Joosse, B. H. Eussen, P. Heutink and B. A. Oostra (2003). "Cntnap2 Is Disrupted in a Family with Gilles De La Tourette Syndrome and Obsessive Compulsive Disorder." Genomics **82**(1): 1-9.

Verri, C., L. Roz, D. Conte, T. Liloglou, A. Livio, A. Vesin, A. Fabbri, F. Andriani, C. Brambilla, L. Tavecchio, G. Calarco, E. Calabro, A. Mancini, D. Tosi, P. Bossi, J. K. Field, E. Brambilla and G. Sozzi (2009). "Fragile Histidine Triad Gene Inactivation in Lung Cancer: The European Early Lung Cancer Project." Am J Respir Crit Care Med **179**(5): 396-401.

Vilarino-Guell, C., C. Wider, O. A. Ross, B. Jasinska-Myga, J. Kachergus, S. A. Cobb, A. I. Soto-Ortolaza, B. Behrouz, M. G. Heckman, N. N. Diehl, C. M. Testa, Z. K. Wszolek, R. J. Uitti, J. Jankovic, E. D. Louis, L. N. Clark, A. Rajput and M. J. Farrer "Lingo1 and Lingo2 Variants Are Associated with Essential Tremor and Parkinson Disease." Neurogenetics **11**(4): 401-8.

Virgilio, L., M. Shuster, S. M. Gollin, M. L. Veronese, M. Ohta, K. Huebner and C. M. Croce (1996). "Fhit Gene Alterations in Head and Neck Squamous Cell Carcinomas." Proc Natl Acad Sci U S A **93**(18): 9770-5.

Wang, F., S. Denison, J. P. Lai, L. A. Philips, D. Montoya, N. Kock, B. Schule, C. Klein, V. Shridhar, L. R. Roberts and D. I. Smith (2004). "Parkin Gene Alterations in Hepatocellular Carcinoma." Genes Chromosomes Cancer **40**(2): 85-96.

Wang, L., W. Paradee, C. Mullins, R. Shridhar, R. Rosati, C. M. Wilke, T. W. Glover and D. I. Smith (1997). "Aphidicolin-Induced Fra3b Breakpoints Cluster in Two Distinct Regions." Genomics **41**(3): 485-8.

Wang, Y.-H., Gellibolian, R., Shimizu, M., Wells, R.D., Griffith, J. (1996). "Long Ccg Triplet Repeat Blocks Exclude Nucleosomes: A Possible Mechanism for the Nature of Fragile Sites in Chromosomes." J Mol Biol **263**(4): 511-516.

Wang, Y. H. (2006). "Chromatin Structure of Human Chromosomal Fragile Sites." Cancer Lett **232**(1): 70-8.

Wilke, C. M., S. W. Guo, B. K. Hall, F. Boldog, R. M. Gemmill, S. C. Chandrasekharappa, C. L. Barcroft, H. A. Drabkin and T. W. Glover (1994). "Multicolor Fish Mapping of Yac Clones in 3p14 and Identification of a Yac Spanning Both Fra3b and the T(3;8) Associated with Hereditary Renal Cell Carcinoma." Genomics **22**(2): 319-26.

Wilke, C. M., B. K. Hall, A. Hoge, W. Paradee, D. I. Smith and T. W. Glover (1996). "Fra3b Extends over a Broad Region and Contains a Spontaneous Hpv16 Integration Site: Direct Evidence for the Coincidence of Viral Integration Sites and Fragile Sites." Hum Mol Genet **5**(2): 187-95.

Winnepenninckx, B., K. Debacker, J. Ramsay, D. Smeets, A. Smits, D. R. FitzPatrick and R. F. Kooy (2007). "Cgg-Repeat Expansion in the Dip2b Gene Is Associated with the Fragile Site Fra12a on Chromosome 12q13.1." Am J Hum Genet **80**(2): 221-31.

Wistuba, II, F. D. Montellano, S. Milchgrub, A. K. Virmani, C. Behrens, H. Chen, M. Ahmadian, J. A. Nowak, C. Muller, J. D. Minna and A. F. Gazdar (1997). "Deletions of Chromosome 3p Are Frequent and Early Events in the Pathogenesis of Uterine Cervical Carcinoma." Cancer Res **57**(15): 3154-8.

Yang, M. Y. and S. E. Long (1993). "Folate Sensitive Common Fragile Sites in Chromosomes of the Domestic Pig (Sus Scrofa)." Res Vet Sci **55**(2): 231-5.

Yang, Q., M. Nakamura, Y. Nakamura, G. Yoshimura, T. Suzuma, T. Umemura, Y. Shimizu, I. Mori, T. Sakurai and K. Kakudo (2002). "Two-Hit Inactivation of Fhit by Loss of Heterozygosity and Hypermethylation in Breast Cancer." Clin Cancer Res **8**(9): 2890-3.

Yendamuri, S., T. Kuroki, F. Trapasso, A. C. Henry, K. R. Dumon, K. Huebner, N. N. Williams, L. R. Kaiser and C. M. Croce (2003). "Ww Domain Containing Oxidoreductase Gene Expression Is Altered in Non-Small Cell Lung Cancer." Cancer Res **63**(4): 878-81.

Yu, S., M. Mangelsdorf, D. Hewett, L. Hobson, E. Baker, H. J. Eyre, N. Lapsys, D. Le Paslier, N. A. Doggett, G. R. Sutherland and R. I. Richards (1997). "Human Chromosomal Fragile Site Fra16b Is an Amplified at-Rich Minisatellite Repeat." Cell **88**(3): 367-74.

Yunis, J. J. and A. L. Soreng (1984). "Constitutive Fragile Sites and Cancer." Science **226**(4679): 1199-204.

Zanesi, N., V. Fidanza, L. Y. Fong, R. Mancini, T. Druck, M. Valtieri, T. Rudiger, P. A. McCue, C. M. Croce and K. Huebner (2001). "The Tumor Spectrum in Fhit-Deficient Mice." Proc Natl Acad Sci U S A **98**(18): 10250-5.

Zhang, H., Z. H. Chen and T. M. Savarese (1996). "Codeletion of the Genes for P16ink4, Methylthioadenosine Phosphorylase, Interferon-Alpha1, Interferon-Beta1, and Other 9p21 Markers in Human Malignant Cell Lines." Cancer Genet Cytogenet **86**(1): 22-8.

Zhang, H., Freindenreich, C. H. (2007). "An at-Rich Sequence in Human Common Fragile Site Fra16d Causes Fork Stalling and Chromosome Breakage in S. Cerevisiae." Mol. Cell **27**(3): 367-379.

Zhang, Y. H., B. L. Huang, K. K. Niakan, L. L. McCabe, E. R. McCabe and K. M. Dipple (2004). "Il1rapl1 Is Associated with Mental Retardation in Patients with Complex Glycerol Kinase Deficiency Who Have Deletions Extending Telomeric of Dax1." Hum Mutat **24**(3): 273.

Zimonjic, D. B., M. E. Durkin, C. L. Keck-Waggoner, S. W. Park, S. S. Thorgeirsson and N. C. Popescu (2003). "Smad5 Gene Expression, Rearrangements, Copy Number, and Amplification at Fragile Site Fra5c in Human Hepatocellular Carcinoma." Neoplasia **5**(5): 390-6.

Zlotorynski, E., A. Rahat, J. Skaug, N. Ben-Porat, E. Ozeri, R. Hershberg, A. Levi, S. W. Scherer, H. Margalit and B. Kerem (2003). "Molecular Basis for Expression of Common and Rare Fragile Sites." Mol Cell Biol **23**(20): 7143-51.